UNIVERSITY OF CALIFORNIA
RIVERSIDE

Mass Spectrometric Study of Genetic and Epigenetic DNA Modifications

A Dissertation submitted in partial satisfaction
of the requirements for the degree of

Doctor of Philosophy

in

Chemistry

by

Hongxia Wang

December 2010

Dissertation Committee:
Dr. Yinsheng Wang, Chairperson
Dr. Ryan Julian
Dr. Wenwan Zhong

The Dissertation of Hongxia Wang is approved:

_____

_____

_____

Committee Chairperson

University of California, Riverside

ACKNOWLEDGEMENTS

This thesis would not have been possible unless the supports from many persons. First and foremost, I am heartily thankful to my supervisor, Professor Yinsheng Wang, whose patience, encouragement, guidance and support from the initial to the final level enabled me to have the opportunity to participate in many bioanalytical fields and complete this work. His enthusiasm and dedication to science are contagious and motivational for me, even during tough times in the Ph.D. pursuit. I appreciate all his contributions of time, ideas and help on both my professional and personal growth.

I would like to show my gratitude to the rest of my committee members, Professor Ryan Julian and Professor Wenwan Zhong for their suggestions and discussion with my research. I truly appreciate your concerns, generous help and accessibility over the past five years. I also thank other members of my doctoral committee: Professor Yadong Yin and Professor Jiankuang Zhu for their constructive commons during my graduate study.

I am grateful for the technical supports from staffs at UC Riverside. I thank Dr. Dan Borchardt and Mr. Yi Meng in Analytical Chemistry Instrumentation at UCR for their helps with NMR measurements and data processing. Thank Mr. Ron New and Dr. Richard Kondrat's training of using MALDI-MS and TOF-MS. In addition, I would like thank our collaborators, Professor Chuan-Ming Hao at Vanderbilt University for providing mouse tissue samples and Professor Mike Kimzey at University of Arizona offering the human buffy coat blood samples.

The members of the Wang group have contributed greatly to my personal and professional time at UC Riverside that became part of my life. The group has been a source of friendships as well as good advice and collaboration. I express my sincere thanks to the original group members Dr. Chunang Gu, Dr. Huachuan Cao, Dr. Yuan Gao, and Dr. Yong Jiang for their helps on the training of utilization of instruments, organinc syntheis and biological experiments. Especially thank Jianshuang Wang and Mario Vargas's discussion and helps on NMR experiment and interpretation of data, which benefits me a lot. I would also like to thank Dr. Haibo Qiu and Dr. Bifeng Yuan's helps on cell culture and biological issues; Lei Xiong, Dr. Xiaoli Dong, Fan Zhang and Yongsheng Xiao for their valuable discussion and help in my research. My thanks also go to other previous and current group members, Renee Willams, Nisana Anderson, Candace Guerrero, Dr. Jin Zhang, Dr. Jin Wang, Dr. Changjun You, Lijuan Fu, Asheley Swanson, Qian Cai, Xueyun Zheng, Jiang Wu for your friendship and assistance. Additional thanks Jianshuang, Dong, Yu, Lei and Qingyu for your wonderful friendship. It is my great pleasure to know and work with all these good friends.

Lastly, I am indebted to my parents and sister for their endless love, continuous encouragement and support; my husband, Yanfei for his love, understanding and sharing with my joy and frustration. Furthermore, I offer my regards and blessings to all of those who supported me in any respect during the completion of the project.

COPYRIGHT ACKNOWLEDGEMENTS

The text and figures in Chapter 2, in part or in full, are a reprint of the material as it appears in *Chem. Res. Toxicol*., **2010**, 23 (1), pp. 74-81. The coauthor (Dr. Yinsheng Wang) listed in that publication directed and supervised the research which forms the basis of this chapter. The co-author (Dr. Huachuan Cao) listed in that publication helped resolving technical problems during the research.

The text and figures in Chapter 3, in part or in full, are a reprint of the material as it appears in *Biochemistry*, **2009**, 48 (10), pp. 2290-2299. The coauthor (Dr. Yinsheng Wang) listed in that publication directed and supervised the research which forms the basis of this chapter.

The text and figures in Chapter 4, in part or in full, are a reprint of the material as it appears in *Anal. Chem*., **2010**, 82 (13), pp. 5797-5803. The coauthor (Dr. Yinsheng Wang) listed in that publication directed and supervised the research which forms the basis of this chapter.

ABSTRACT OF THE DISSERTATION

Mass Spectrometric Study of Genetic and Epigenetic DNA Modifications

by

Hongxia Wang

Doctor of Philosophy, Graduate Program in Chemistry
University of California, Riverside, December 2010
Dr. Yinsheng Wang, Chairperson

In this dissertation, I focus on the development of novel MS-based strategies to identify and quantify DNA lesions formed in isolated DNA and in cells to monitor the progression of enzymatic reactions *in vitro* and glyoxal or methylglyoxal exposure *in vivo*. In addition, a combined SILAC, one-step affinity purification and LC-MS/MS approach was employed for identifying systematically cellular proteins capable of binding to 6-thioguanine-containing duplex DNA.

In Chapter 2, a stable isotope dilution coupled with LC-MS/MS/MS method was developed to quantify accurately DNA advance glycation end products (AGEs) including N^2-carboxymethyl-2'-deoxyguanosine (N^2-CMdG), and two diastereomers of N^2-(1-carboxyethyl)-2'-deoxyguanosine (N^2-CEdG) induced by hyperglycemia in calf thymus DNA, cellular DNA, rat and mouse tissues and human blood samples. The results showed that N^2-CMdG and N^2-CEdG were stable and the level of N^2-CMdG and two diastereomers of N^2-CEdG were higher in the liver tissues of diabetic mice than those of

the healthy control. This work shows that N^2-CMdG and N^2-CEdG might serve as molecular biomarkers for monitoring glyoxal and methylglyoxal exposure.

In Chapter 3, I established a novel restriction enzyme digestion coupled with LC-MS/MS method to investigate the effect of 6-thioguanine on the *Hpa*II- and DNMT1-mediated methylation of cytosine in synthetic duplex DNA. Moreover, the level of global cytosine methylation in different leukemia cell lines upon 6-thioguanine treatment was evaluated by an offline HPLC method. These results provided important new knowledge about the antileukemic effects of 6-thioguanine.

In Chapter 4, 6-thioguanine and its metabolite, S^6-methylthio-2'-deoxyguanosine in genomic DNA of five different cancer cell lines were accurately quantified by using LC-MS/MS. The data support our hypothesis that, after being incorporated into DNA, 6-thioguanine instead of S^6-methylthio-2'-deoxyguanosine plays the major role to exert the cytotoxic effects of thiopurines. In addition, another nucleotide metabolite, 6-thioguanosine triphosphate was extracted and quantified by LC-MS/MS.

In Chapter 5, a strategy, including SILAC, affinity purification and LC-MS/MS, was employed to identify nuclear proteins that are capable of binding to 6-thioguanine-containing duplex DNA. The outcome of the study will facilitate the exploration of other mechanisms involved in the cytotoxicity of the thiopurine drugs.

TABLE OF CONTENTS

Chapter 3. Investigating the Effect of 6-Thioguanine on the Cytosine Methylation *In-Vitro* and *In-Vivo*

Chapter 4. Identification and Quantification of 6-Thioguanine and Its Metabolites in Human Cancer Cells upon 6-Thioguanine Treatment

LIST OF FIGURES

(b) and (c) are the MS/MS for the $[M + 2H]^{2+}$ ions of EGDVLTLLESER and EGDVLTLLESER*, respectively.

LIST OF SCHEMES

LIST OF TABLES

CHAPTER 1

General Overview

1.1 Genomic Instability

Genomic instability is a hallmark of cancer cells, and is thought to be involved in the process of carcinogenesis (*1*). As genetic material, DNA has to maintain its integrity. However, DNA is constantly challenged by destabilizing factors including normal DNA replication and cell division, as well as a host of intracellular and extracellular environmental stresses. For example, its nucleobases can be oxidized or alkylated during normal metabolic processes and its *N*-glycosidic linkage can be spontaneously hydrolyzed (*2*). In addition, UV light, ionizing radiation and various chemical agents can modify DNA directly or after metabolic activation. Although a certain level of genomic instability may be necessary for fostering genetic diversity, the damaged genome can lead to an enhanced rate of mutagenesis, resulting in compromised cellular function and tumor formation (*2*).

1.1.1 DNA Modifications Induced by Glyoxal and Methylglyoxal

Humans are exposed to glyoxal and methylglyoxal from both endogenous and exogenous sources. Glyoxal and methylglyoxal (see Figure 1.1) are widely distributed in the environment and found in foods, beverages, and cigarette smoke (*3-5*). Glyoxal arises endogenously from a multitude of pathways, which encompass the oxidation of lipids and carbohydrates (*6-9*). Methylglyoxal can be produced in all cells of all organisms from the nonenzymatic fragmentation of triose phosphate, which include

glyceraldehyde-3-phosphate and dihydroxyacetone phosphate that are produced as metabolites of the highly conserved glycolysis pathways (*10-12*). As major degradation products of glucose under physiological conditions, glyoxal and methylglyoxal were observed to be present at elevated levels in blood of patients with diabetes (*13*), peritoneal dialysis, uremia (*14-16*) and in the kidney, lens, and blood of streptozotocin-induced diabetic rats (*17*).

As highly reactive electrophiles, glyoxal and methylglyoxal react readily with nucleophilic moieties in proteins, lipids and DNA to produce covalent adducts known as advanced glycation end products (AGEs) (*18, 19*). The accumulation of AGEs in tissues plays an important role in the pathogenesis of diabetic nephropathy, chronic renal failure, atherosclerosis, cataract, Alzheimer's disease, and rheumatoid arthritis (*20-23*). Protein AGEs have been well characterized and were demonstrated to correlate with human diseases. Among them, hemoglobin HbA_{1c} adduct has been a commonly used biomarker for the diagnosis and monitoring the treatment of diabetes (*15, 16, 24*). More recently, it was shown that nucleosides and DNA react with sugars and sugar degradation products *in vitro* in a similar way as proteins (*25-27*), leading to the formation of so called DNA-bound AGEs. DNA-bound AGEs have potential as biomarkers because all nucleated cells contain the same DNA content and should reflect the relative level of glycation status in particular target tissues, while choosing an appropriate protein-AGE biomarker is complicated by unequal protein-AGE distributions across different tissues and varying adduct stabilities (*19*).

It has been demonstrated that the exocyclic amino group of 2'-deoxyguanosine (dG) is particularly prone to glycation reactions (*28-31*). Previous studies on the reactions of glyoxal with 2'-deoxyribonucleosides showed that, under physiological conditions, glyoxal reacts preferentially with dG to form 3-(2'-deoxy-β-D-*erythro*-pentofuranosyl)-5,6,7-trihydro-6,7-dihydroxyimidazo[1,2-*a*]purine-9-one (1,N^2-glyoxal-dG) in DNA; this adduct can further couple with dA, dC and dG to render dA-glyoxal-dG, dC-glyoxal-dG and dG-glyoxal-dG cross-links (*32, 33*). The latter crosslinks were recently quantified in calf thymus and human placental DNA by using capillary liquid chromatography nano-electrospray ionization tandem mass spectrometry (*34*). In addition to the known 1,N^2-glyoxal-dG adduct, two new adducts, 5-carboxymethyl-3-(2'-deoxy-β-D-*erythro*-pentofuranosyl)-5,6,7-trihydro-6,7-dihydroxyimidazo[1,2-*a*]purine-9-one (Gx_2-dG) and N^2-carboxymethyl-2'-deoxyguanosine (N^2-CMdG) were found to be produced in the reactions of glyoxal with dG and calf thymus DNA under physiological conditions (*35*). Methylglyoxal adducts of DNA have also been investigated and not surprisingly guanine is again the predominant nucleobase being modified when calf thymus DNA was used as a substrate. An earlier study showed that cyclic adduct 1,N^2-(1,2-dihydroxy-2-methyl)ethano-2'-deoxyguanosine (cMG-dGuo) was the major product when guanine reacted with MG at 65 °C for 18 h (*36*) and it was detected in isolated DNA as well as genomic DNA in lymphocyte and human bucal epithelial cells that were exposed to MG (*37, 38*). Schneider *et al.* (*39*) identified a bis adduct of dG and MG, N^2,7-bis(1-hydroxy-2-oxopropyl)-dGuo, as the main product when dG was incubated with MG at 37 °C for 48 h. Among the above-described DNA adducts,

N^2-(1-carboxyethyl)-2'-deoxyguanosine (N^2-CEdG) and N^2-CMdG (see Figure 1.1) were identified as the major stable DNA adducts formed in calf thymus DNA, upon prolonged exposure to physiologically relevant concentrations of methylglyoxal and glyoxal, respectively (*35, 40*).

N^2-CMdG has been quantified in calf thymus DNA exposed with D-glucose and glyoxal as well as in human kidney epithelial cells. The formation of N^2-CMdG was correlated with the concentration of glyoxal and glucose (*41*). N^2-CEdG was detected in WM-266-4 human melanoma cells and treatment of these cells with methylglyoxal or glucose led to a dose-responsive increase in adduct formation (*42*). N^2-CEdG has also been measured in urine samples from healthy human subjects using immunoaffinity chromatography with a polyclonal antibody raised against N^2-CEdG (*43*). The result revealed that the level of the lesion was enhanced in the kidney and aorta of patients with diabetic nephropathy and uremic atherosclerosis, respectively (*44*). This implies that carboxyalkylated dG adducts might serve as reliable biomarkers for monitoring the progression of diabetes, which is manifested by a higher level of glucose in the blood.

It is well established that reactive carbonyl compounds, such as glyoxal and methylglyoxal induce mutations in bacteria and mammalian cells (*45, 46*). Furthermore, DNA-AGEs could perturb DNA structure and function. Glycation of DNA destabilized the *N*-glycosidic bond, leading to depurination (*47*) and the formation of single strand breaks (*48*). These can give rise to mutations including insertions, deletions (*49*) and single-base substitutions (*50*). Therefore, these DNA-AGEs could contribute to the loss of genomic instability that occurs during aging and aging-related complications.

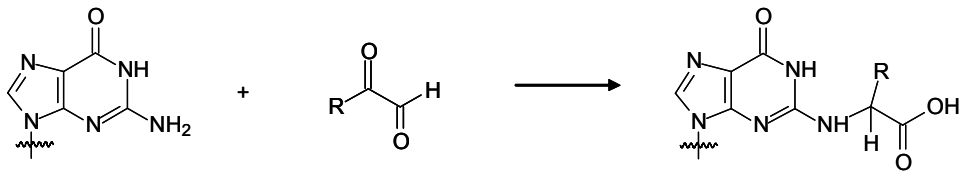

Figure 1.1 Formation of N^2-CMdG and N^2-CEdG.

1.1.2 DNA Alterations Induced by Exogenous Drug Treatment

1.1.2.1 Thiopurines and Their Metabolic Transformation

Nucleoside analogs are widely used for treating a range of human diseases including cancer, HIV infection, chronic inflammation, etc. (*51*). Thiopurine drugs, which include 6-thioguanine (^{S}G) and 6-mercaptopurine (6-MP) (Figure 1.2), are commonly used for the treatment of acute lymphoblastic leukemia, inflammatory bowel disease, autoimmune hepatitis, and other pathological conditions (*52, 53*). Azathioprine (Figure 1.2), which is converted to 6-mercaptopurine *in vivo*, is a standard immunosuppressant prescribed to prevent graft rejection in organ transplant patients (*52*). 6-MP and azathioprine were approved by FDA for the treatment of ALL in children in 1953 (*54*) and for the prolongation of renal allograft survival in 1963 (*55*), respectively.

Thiopurines are inactive prodrugs and, to exert their cytotoxic effect, these prodrugs need to be metabolically activated (i.e., to thioguanine nucleotides) and incorporated into DNA (Figure 1.2) (*52*). During metabolism, ^{S}G is converted to its corresponding nucleoside monophosphate (^{S}GMP) in a single-step reaction catalyzed by hypoxanthine phosphoribosyltransferase (HPRT), whereas three enzymatic steps are required to convert 6-MP and azathioprine to ^{S}GMP. ^{S}GMP is then phosphorylated by kinases to give ^{S}GDP and ^{S}GTP, and ^{S}GDP can be converted to ^{S}dGTP through the sequential actions of ribonucleotide reductase and kinase (*56*). The incorporation of thioguanine nucleotides into DNA or RNA is considered to be crucial steps for thiopurines to exert their therapeutic effects (*57*), which is consistent with the delayed cytotoxic effect of the thiopurine drugs (*58, 59*).

1.1.2.2 The Implications of 6-Thioguanine Metabolites in Cytotoxic Effects of Thiopurine Drugs

The primary activation pathway of thiopurines is through the formation of 6-thioguanine nucleotides (TGN) and their subsequent incorporation into nucleic acids (*57*). Thiopurine methyltransferase (TPMT), which exhibits genetic polymorphism, catalyzes the *S*-methylation of thiopurines. Clinical studies revealed that TPMT-deficient patients accumulated excessive ^{S}G nucleotides in erythrocytes and are susceptible to develop severe hematopoietic toxicity or even death from neutropenic sepsis (*60-62*). In addition, S^{6}-methylthioinosine-5′-monophosphate is a potent inhibitor for *de novo* purine synthesis, which may constitute an alternative mechanism for the cytotoxicity of 6-MP (*63*).

1.1.2.3 Biological Significance of 6-Thioguanine and Its Metabolites

Despite their success in treating a variety of pathological conditions, the exact mechanisms underlying the cytotoxic effects of the thiopurine drugs remain elusive (*64, 65*). Compared to guanine, the increased chemical reactivity of 6-thioguanine may contribute to the cytotoxic effects of the thiopurine drugs. NMR structural data and thermodynamic studies suggested that the replacement of a guanine with ^{S}G perturbs slightly double helical structure of DNA (*66-68*), where the sulfur atom in ^{S}G exists in keto form and assumes weakened Watson-Crick hydrogen bonding with the opposing cytosine. The presence of ^{S}G in DNA leads to the formation of DNA strand breaks (*69*), DNA-protein cross-links (*70*), and results in sister chromatid exchange (*71*), and large-scale chromosomal damage (*72*).

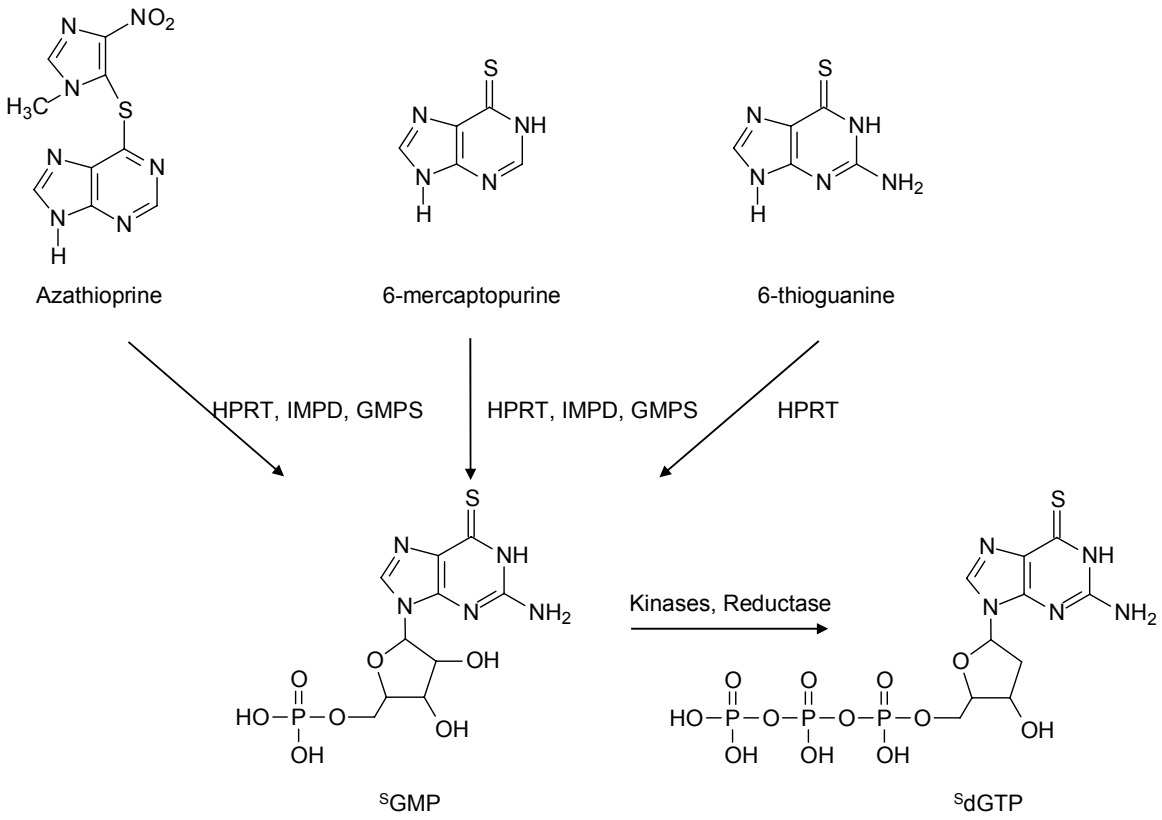

Figure 1.2 Thiopurines and their metabolic activation to render 6-thioguanine nucleotide.

After being incorporated into DNA, ^{S}G can be methylated spontaneously to S^6-methylthioguanine (S^6mG) in the presence of *S*-adenosyl-L-methionine (*S*-AdoMet) (*73*) or oxidized to guanine-S^6-sulfonic acid (^{SO3H}G) upon exposure to UVA light (*74*). Both S^6mG and ^{SO3H}G exhibit considerable miscoding properties (*73-76*). A recent study showed that in *Escherichia coli* (*E. coli*) cells, these two modified nucleosides could lead to G →A transition at frequencies of 94% and 77%, respectively (*77*). Furthermore, recent *in-vivo* replication studies carried out in this group revealed that ^{S}G and S^6mG are also mutagenic in human cells, which gave rise to G→A mutation at frequencies of 10% and 40%, respectively (*78*). The coding property of S^6mG directs the misincorporation of thymidine to give S^6mG:T base pair during DNA replication, which is recognized by the post-replicative mismatch repair (MMR) machinery. As a result, futile cycles of repair synthesis may give rise to cell death (*73*). This could account for the cytotoxicity of the thiopurine drugs.

The relatively high mutagenic potential of ^{S}G in bacterial and human cells also raises the possibility that the replication-produced ^{S}G:T mispair may trigger directly the post-replicative mismatch repair pathway thereby inducing cytotoxic effect.

1.1.2.4 Cytosine Methylation and Implications in Cancer Development

Epigenetic gene regulation refers to different states of phenotypic expression caused by differential effects of chromosome or chromatin packaging rather than by differences in DNA sequence (*79, 80*). Chromatin structure is formed from the packaging of genomic DNA through association with histone proteins (*81*). The majority of

nucleosomes, the basic repeating unit of chromatin, are composed of the same four types of core histones, H2A, H2B, H3, and H4 (*82*). Tremendous diversity in the histone/nucleosome structures is generated by a variety of post-translational modifications (PTMs) of histone proteins, such as acetylation, phosphorylation, methylation, and ubiquitination. These PTMs of histone proteins can alter chromatin conformation and play direct regulatory roles in gene expression (*83*). In addition to chromatin changes, DNA methylation is another crucial epigenetic modification of the genome that is involved in regulating many cellular processes. These include embryonic development, transcription, chromatin structure, X chromosome inactivation, genomic imprinting and chromosome stability (*84*). DNA methylation is found in the genomes of diverse organisms including both prokaryotes and eukaryotes. In prokaryotes, DNA methylation occurs on both cytosine and adenine bases and is an integrated part of the host restriction system (*85*). In multi-cellular eukaryotes, DNA methylation refers to the cytosine methylation at CpG dinucleotide sites in the promoter and initial exons of genes (*86*). In this respect, all proteins revealed by biochemical experiments to be involved in the establishment, maintenance, or interpretation of genomic methylation pattern in mammals are encoded by essential genes, underscoring the biological importance of CpG methylation (*87*).

Mammalian DNA methylation machinery is comprised of two components, the DNA methyltransferases (DNMTs) and the methyl-CpG binding proteins (MBDs). DNA methyltransferase enzymes fall into two general classes based on their preferred DNA substrates. The *de novo* methyltransferases DNMT3a and DNMT3b are mainly

responsible for introducing cytosine methylation at previously unmethylated CpG sites, whereas the maintenance methyltransferase DNMT1 copies pre-existing methylation patterns onto nascent DNA strand during DNA replication (*88*). Another DNA methyltransferase, DNMT2, has little involvement in establishing DNA methylation patterns (*89*). DNMT3L is a DNMT-related protein that does not contain intrinsic DNA methyltransferase activity, but physically associates with DNMT3a and DNMT3b and modulates their catalytic activity (*90*).

Aside from the installation of cytosine methylation marks by DNMTs, cells are also equipped with protein machineries which can specifically recognize the 5-methylcytosine-containing DNA. Upon binding to methylated DNA, these methyl-CpG binding proteins may further recruit histone-modifying enzymes to promote chromatin condensation and gene silencing (*88*). Properly established and maintained DNA methylation patterns are essential for mammalian development and normal function of the adult organism. It has been demonstrated that the covalent modifications of nucleobases at the CpG dinucleotide site could perturb cytosine methylation by DNA methyltransferases (*91-95*).

A growing number of human diseases have been found to be associated with aberrant DNA methylation (*96-98*). The first link between DNA methylation and cancer was reported in 1983, where the genomes of cancer cells were found to be hypomethylated relative to those of normal cells (*99*). The hypomethylation in cancer cells is primarily due to the loss of methylation from repetitive regions of genome, which leads to the genomic instability and becomes the hallmark of cancer cells. Loss of

genomic methylation is a frequent and early event in cancer, and correlates with disease severity and metastatic potential in many tumor types (*100*). Aberrant cytosine methylation in cancer usually occurs at CpG islands and the resulting changes in chromatin structure results in transcription suppression.

As successful chemotherapeutic reagents, 6-mercaptopurine and 6-thioguanine have been widely employed to treat childhood acute lymphoblastic leukemia (*54, 101, 102*). However, long-term thiopurine treatment leads to high occurrence of secondary cancer development (*53, 103*). On the hand, high cancer incidence is frequently observed in organ transplant recipients who take azathioprine as an immunosuppressant (*104, 105*). Therefore, the cytotoxic effect of thiopurines might be related to the altered DNA cytosine methylation in the cells treated with 6-thioguanine.

1.2 The Application of Mass Spectrometry for the Analysis of DNA adducts

Since the 1960s it has been known that DNA was a macromolecular target for chemical carcinogens, which covalently bind to DNA to form DNA adducts (*106*). The analyses of DNA adducts are often complicated by their low formation frequency *in vivo*. Several techniques, including the use of radiolabeled mutagens or carcinogens, immunoassay, fluorescence, and ^{32}P-postlabelling have been developed to analyze DNA adducts (*107*). Although all previous methods are highly sensitive, they do not allow the determination of the molecular structure of the detected adducts, which brings the uncertainty with regard to the nature and type of carcinogen exposure. With the fast development in instrumentation in the last several decades, mass spectrometry has now

become a powerful tool for studying DNA modifications due to its advantage to offer structure information.

Prior to the advent of LC-MS, GC-MS utilizing electron impact ionization or chemical ionization was the major MS method for analyzing DNA adducts (*108, 109*). However, the main limitation of GC-MS lies in that only non-polar volatile compounds can be analyzed. For non-volatile or polar DNA adducts, derivatization at high temperature is often needed prior to the analysis (*110*), which may give rise to artificial generation of DNA lesions (*111, 112*). GC-MS analysis of complex nucleosides containing more polar modifications has not been successful (*113*).

The introduction of electrospray ionization (ESI) and atmospheric pressure chemical ionization (APCI) interfaced with liquid chromatography-mass spectrometry (LC-MS) allows for the analysis of non-volatile and thermally labile compounds without derivatization. In addition to single-stage mass spectrometry, tandem mass spectrometry (MS/MS) or MS^n has become a particularly important analytical tool in the structure elucidation of unknown DNA adducts. Along this line, high-resolution hybrid-type tandem mass spectrometers have been developed recently. These instruments, including quadrupole time-of-flight (Q-TOF), linear ion trap-orbitrap (LTQ-orbitrap), TOF-TOF and quadrupole ion trap Fourier-transform ion cyclotron resonance (QIT-FTICR), bear the dual capabilities of providing the exact mass measurement and tandem mass spectrum in high sensitivity, which yield structure information for DNA lesions (*110*).

The accurate and reproducible quantification of DNA adducts has been achieved by LC-MS coupled with stable isotope dilution technique. The isotope-labeled standards

allow for the confirmation of structure identity of product ions formed by collision induced dissociation (CID) of unlabeled DNA adduct of interest (*41*, *114*, *115*). Among the various types of mass analyzers, triple quadrupole is the most commonly used for DNA adduct analysis, which is followed by ion-trap, particularly in recent years the linear ion trap mass spectrometer. The typical detection limits of LC-ESI-MS for various DNA adducts range from 0.5-5 adducts per 10^8 unmodified DNA bases when 10-100 μg of DNA is used (*110*, *114*, *116*). The recent introduction of nano or capillary LC coupled with nanoelectrospray ionization MS has proven to significantly increase detection limits and sensitivity, endowing LC-MS/MS with a level of sensitivity that is comparable to ^{32}P-postlabelling for DNA adduct analysis. Accelerator MS is by far the most sensitive analytical method available for detecting DNA adducts with a detection limit of 1 adduct per 10^{12} unmodified DNA bases; this method, however, requires the use of radiolabeled ^{14}C (*117*).

Another function of mass spectrometry is to sequence oligodeoxyribonucleotides (ODNs) and to locate the modification sites in ODNs. In MS/MS, the major fragmentation of ODNs occurs at *N*-glycoside bond and 3' C-O bond to afford the formation of [a_n-base] and w_n ions (Figure 1.3) (*118*). The sequence of ODNs can be determined by comparing the mass difference between neighboring w_n or [a_n-base] ions, which allows for the identification of the sandwiched nucleotide.

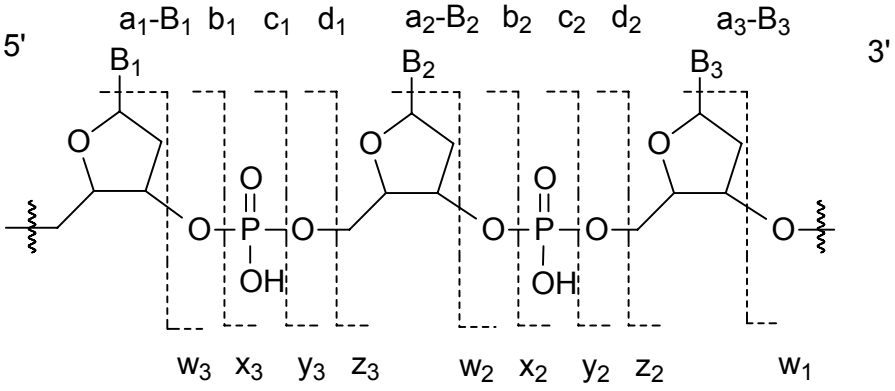

Figure 1.3 The nomenclature of fragment ions observed for oligodeoxynucleotides.

1.3 Mass Spectrometry-Based Quantitative Proteomics

Proteomics in general deals with the large-scale determination of gene and cellular function directly at the protein level (*119*). Proteomics has been successfully applied to determine protein composition of organelles, systematic elucidation of protein-protein interactions and the large-scale mapping of protein PTMs in cells in response to a variety of stimuli (*120*). As one of the most powerful techniques in analytical sciences, mass spectrometry, coupled with sample preparation and separation techniques, has played an essential role on the rise of proteomics (*119*). However, the wide dynamic range of protein expression in complex biological samples, i.e. tissues, sera and body fluids, brings challenge to MS-based proteomics method for identifying and quantifying low-abundance proteins for biomarkers and drug targets. In addition, most changes resulting from a targeted perturbation of a biological system are only detectable if some quantification information is obtained (*120*). In recent years many stable isotope-labeling techniques for quantitative proteomic analysis have been developed to address these issues and have been proven to solve successfully a wide range of biological problems. Quantitative proteomics methods focus on assessing the changes of protein abundance to reflect synthesis, degradation and modifications. Three major techniques for stable isotope incorporation are widely employed for MS-based quantitative proteomics.

1.3.1 Stable Isotope Labeling for MS-Based Quantitation

Stable isotope labeling techniques have become the gold standard of MS-based quantitative proteomics due to highly accurate results obtained from these measurements

(*121*). In early 1990s, Desiderio *et. al*. (*122*) extended the well-established stable isotope dilution technique to the quantification of small molecules to neuropeptides. Along this line, stable isotope-labeled peptides were chemically synthesized and known quantities were subsequently spiked into sample as internal standards during or after protein digestion. This approach is applicable for protein biomarker quantification in clinical samples. However, it is difficult to correct for any prior variations during sample processing steps before the addition of internal standards. In addition, this approach is usually limited to a small number of proteins due to the lack of suitable internal standards.

Proteolytic ^{18}O labeling serves as an alternative strategy for the incorporation of stable isotopes into peptides. The introduction of labels is catalyzed by members of the serine protease family, which include trypsin, Glu-C, Lys-C and chymotrypsin (*123*). The enzymatic digestion performed in $H_2{}^{18}O$ water allows for the addition of ^{18}O on the carboxyl terminus of the peptide. Even though this method facilitates the labeling of every peptide with the only exception of the original C-terminus of the protein, one or two carboxyl oxygens may be exchanged, leading to inaccurate quantification (*124*). Another significant limitation is due to oxygen "back-exchange" where ^{18}O is replaced with ^{16}O after labeling through a residual trypsin-catalyzed reaction when the sample is placed into a buffer containing ^{16}O water (*125*). This makes it problematic to accurately quantify the relative abundance differences between the ^{18}O- and ^{16}O-labeled samples. Therefore, ^{18}O labeling has not been widely applied in quantitative proteomics.

1.3.2 Chemical Tagging Approaches for Quantitative Proteomics

This approach is based on the use of stable isotope-coded chemical reagents to label differentially proteins or peptides and to compare the relative abundances of the proteins or peptides in different samples (*126*). Isotope-coded affinity tag (ICAT), developed by Aebersold and co-workers (*127*), and isobaric tags for relative and absolute quantitation (iTRAQ), developed by Pappin and colleagues (*128*), are among the most successful chemical labeling approaches used in quantitative proteomic studies.

1.3.2.1 Isotope-Coded Affinity Tag

ICAT reagent consists of three components: A biotin-labeled affinity tag, used to isolate and enrich ICAT-labeled peptides; a linker that contains light (hydrogen) or heavy (deuterium) stable isotopes; and a reactive group (iodoacetyl) with the specificity to the thiol group in cysteine residues of proteins (Figure 1.4a). The strategy of ICAT to quantify differential protein expression is shown in Figure 1.4b. Disulfide bonds in two protein mixtures representing two different cell states are reduced first to release free thiol groups on cysteine, which are then derivatized with the isotopically labeled light or heavy ICAT regents. Equal amounts of the two populations of proteins are subsequently combined and enzymatically cleaved to generate peptide fragments. The ICAT-labeled peptides are enriched by avidin affinity chromatography, separated and analyzed by LC-MS/MS.

The development of ICAT reagents allows for quantitation through isotopic labeling and simultaneously achieves a reduction in sample complexity (*129*). However,

several shortcomings were identified for this reagent. Hydrogen- and deuterium-labeled peptides did not coelute during separation using reverse-phase chromatography (*130*) and a 8-Da mass difference for the heavy ICAT reagent produced potential isobaric ambiguity between peptides containing two ICAT-labeled cysteine residues (ΔM =16.100 Da) and the common oxidation of methionine residues (ΔM =15.995 Da). Furthermore, fragmentations of the bulky biotin tag occur more readily than the cleavages of the peptide backbone, which sometimes compromises protein identification (*131*). The development of solid-phase ICAT reagents with a photocleavable linker significantly improved the sensitivity but still suffered from the chromatographic separation of light- and heavy-modified species (*132*), which was then solved by the introduction of an acid-cleavable linker group with ^{13}C isotopic labeling between the biotin moiety and the sulfhydryl reactive isotope tag (*133, 134*).

1.3.2.2 Isobaric Tags for Relative and Absolute Quantitation

iTRAQ was developed with the advantage of facilitating the quantitative comparison of proteins from multiple states. Compared to ICAT, iTRAQ is more amenable to the identification of post-translational modifications (PTM) on peptides due to the fact that the isobaric mass labels are placed at the N-termini and amino group on the side chain of lysine residue in peptides (*128*). iTRAQ reagent includes a reporter group with *m/z* ranging from 114 to 117, a mass balance group (carbonyl group), and an amine-specific peptide reactive group (NHS ester) (Figure 1.5a). For iTRAQ strategy, reagents are differentially isotopically labeled so that all derivatized forms of the same

(a)

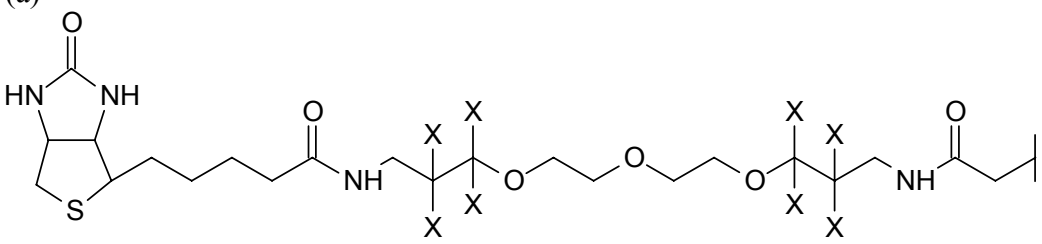

Biotin tag

Isotope labeled linker
Heavy: d_8-ICAT (X=D)
Light: d_0-ICAT (X=H)

Thiol-specific reactive group

(b)

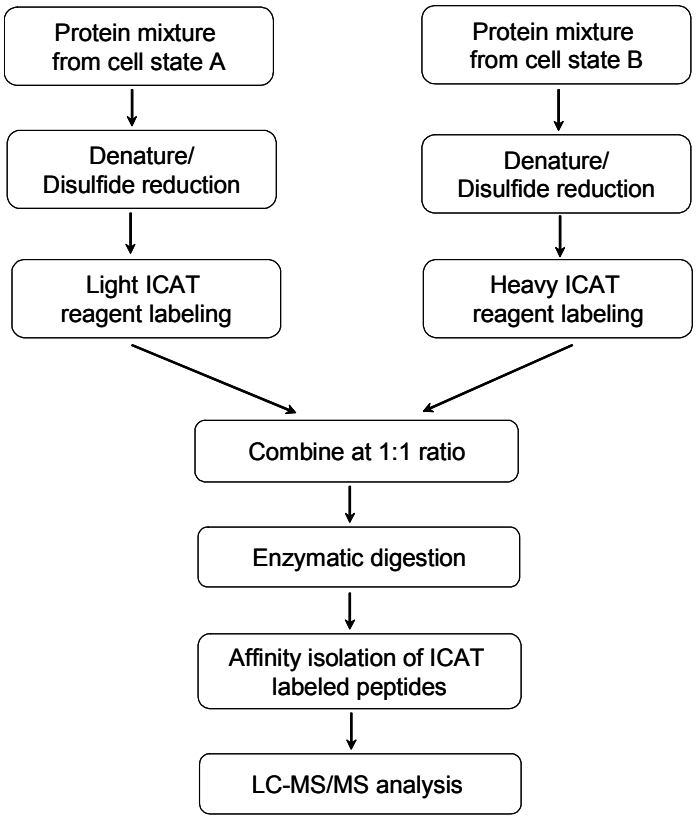

Figure 1.4 (a) Structure of ICAT reagent. (b) Procedures of using ICAT for quantitative proteomics.

peptides from different states are isobaric in the chromatogram of LC-MS, but they produce different reporter ions (Figure 1.5b) in the MS/MS. By comparing the relative abundances of the corresponding reporter ions, we can quantify the relative abundances of proteins from different states.

1.3.3 Metabolic Labeling

Metabolic labeling for quantitation was first introduced in proteomics by the Langen group (*135*) in 1998 and subsequently used for quantitation by the Chait group (*136*). Among the many currently used isotope-labeling strategies for quantitative proteomics, stable isotope labeling with amino acid in cell culture (SILAC) has emerged as a simple and powerful approach for metabolic labeling (*137*). Compared to chemical labeling strategy, the advantage of metabolic labeling lies in that it allows for mixing of labeled and unlabeled cells prior to sample fractionation, purification and digestion, which can eliminate the variations introduced from two separate sample processing procedures thereby affording accurate quantitation. The shortcoming of this approach is that current metabolic labeling cannot be extended to clinical studies. More recently, Oda *et al.* (*138*) developed the culture-derived isotope tags (CDIT) method, which uses SILAC-labeled cells as the bridging internal standard between two tissue samples.

In SILAC experiment, two populations of cells are cultured. One portion of cells are grown in light medium with normal amino acid and the other in heavy medium containing stable isotope (i.e. ^{13}C , ^{15}N, ^{2}H) labels on certain amino acids (e.g. lysine and/or arginine). After 5 cell doublings, the normal amino acids in the protein with heavy

medium will be completely replaced by the stable-isotope-labeled heavy amino acids, which leads to a known mass shift for the quantitation but no other chemical changes. Proteins from two states will be extracted, quantified separately and combined at 1:1 ratio. Protein mixture is further purified or fractionated and enzymatically digested to peptides. The light- and heavy-labeled peptides are analyzed by LC-MS/MS. Proteins are identified by searching *m/z* files of peptides against the database and quantified by comparing the relative peak intensities between unlabeled and labeled peptides. The quantification result can be used to evaluate the effects of specific treatment on a large number of proteins in a single experiment.

As an efficient, reproducible and accurate quantitative approach, SILAC allows for the comparative studies of protein expression and relative quantification of small changes in protein expression in different cell populations. The *in-vivo* incorporation of stable isotopes in living cells enables SILAC to remove false-positives in protein-interaction studies, reveals large-scale kinetics of proteomes, and uncovers important points in the cell signaling pathways (*139*).

SILAC is not only applicable for the quantitative comparison of proteomes, but has also been extended to an unbiased proteome-wide screening for the identification and quantification of specific binding proteins to baits by using peptides (*140*), proteins (*141*), DNA (*142*) and RNA (*143*). Traditional methods for the unbiased identification of sequence-specific nucleic acid-binding proteins employ a combination of several steps of classical chromatography followed by a final affinity purification step that uses their cognate recognition sequence as a ligand (*144*), which is labor-intensive and thus

impractical on a proteomic scale. Routine high-throughput identification of sequence-specific DNA-binding factors is mainly hampered by their low abundance, the degradation of their binding sites, and the non-specific binding of positively charged nuclear proteins to the negatively charged phosphate backbone of DNA (*142*).

SILAC combined with one-step affinity purification and highly sensitive LC-MS/MS analysis has been successfully employed to overcome above-mentioned obstacles. In this new strategy, proteins are first extracted from light and heavy isotope-labeled cells, and equal amounts of proteins from two different cultures are incubated with control and modified DNA baits, respectively. Following an one-step affinity purification, proteins bound to DNA baits are combined, eluted and digested to peptides, which are identified and quantified by LC-MS/MS. For background proteins occurring equally in control and bait elutes, the SILAC peptide pairs in the MS spectrum show a 1:1 intensity ratio. By contrast, proteins with specific binding to the bait exhibits heavy/light ratio substantially greater than 1.

Because metabolic labeling of cells with heavy derivatives of lysine and arginine leads to the complete labeling of tryptic peptides representing the total cellular proteome, this approach has the potential to quantify almost all peptides (*145*). Furthermore, it is completely unbiased with respect to both the DNA sequence and potential binding proteins and does not require the knowledge of DNA binding specificity of the proteins involved (*142*).

(a)

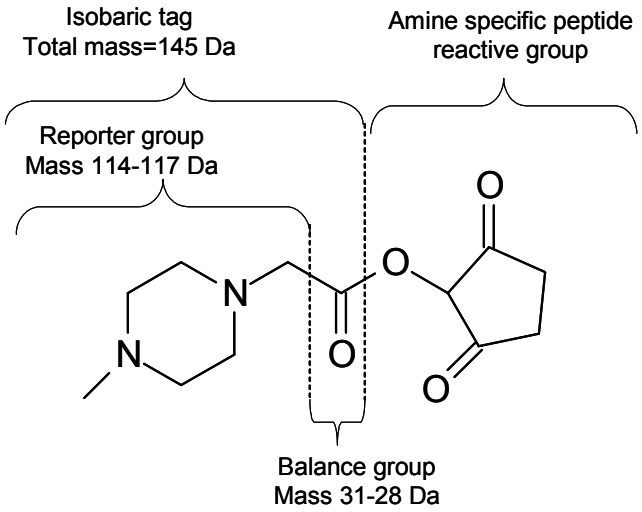

(b)

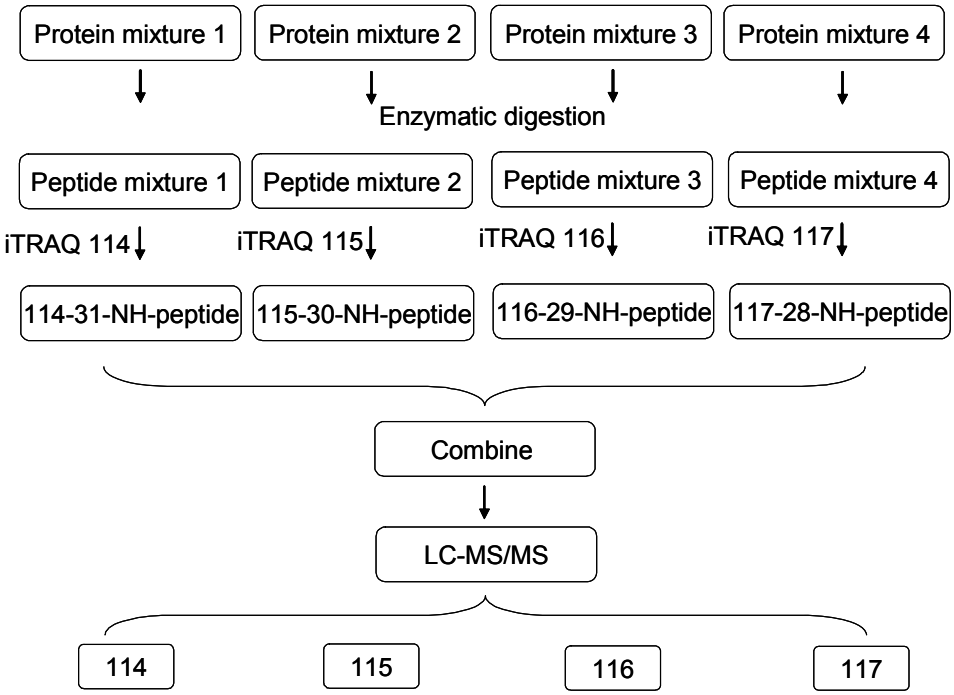

Figure 1.5 (a) The structure of the iTRAQ reagent. (b) Procedures of using iTRAQ for quantitative proteomics.

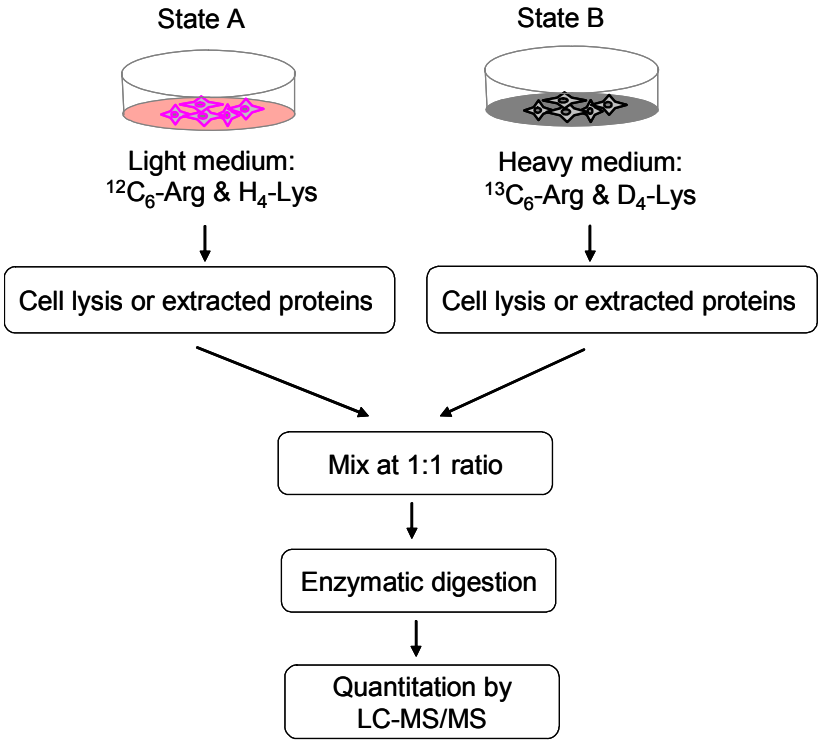

Figure 1.6 Procedures for using SILAC strategy in quantitative proteomics.

1.4 Scope of This Dissertation

Mass spectrometry has become a very powerful tool for bioanalysis. The combination of MS with other techniques extends its application from the structure elucidation of small molecules, qualitative studies and sequencing of oligodeoxynucleotides and peptides to quantitative analysis. In this thesis, I focus on the development of novel MS-based strategies to identify and quantify DNA lesions formed in isolated DNA and in cells to monitor the progression of enzymatic reactions *in vitro* and diabetes *in vivo*. In addition, the systematic identification of proteins capable of binding to 6-thioguanine-containing duplex DNA will be described.

In Chapter 2, a stable isotope dilution coupled with LC-MS/MS/MS method was developed to quantify accurately DNA-AGEs including N^2-CMdG, cyclic-CMdG, and N^2-CEdG induced by hyperglycemia in calf thymus DNA, cellular DNA, rat and mouse tissues and human blood samples to establish novel DNA biomarker for monitoring the progression of diabetes. In Chapter 3, a novel restriction enzyme digestion coupled with LC-MS/MS method has been established to investigate the effect of 6-thioguanine on the DNMT1-mediated methylation of cytosine in synthetic duplex DNA. Moreover, the global cytosine methylation level in different leukemia cell lines upon 6-thioguanine treatment was evaluated by an offline HPLC method. These results provide us important insights about the relationship between aberrant cytosine methylation and cancer development. In Chapter 4, 6-thioguanine and its metabolite, S^6-methylthioguanine in genomic DNA of five different cancer cell lines were accurately quantified. The data support our hypothesis that, after being incorporated into DNA, 6-thioguanine instead of

S^6-methylthioguanine plays the major role to exert the cytotoxic effects of thiopurines. In addition, another nucleotide metabolite, 6-thioguanosine triphosphate was extracted and quantified by LC-MS/MS. This novel method is applicable to other nucleotide analysis. In Chapter 5, a strategy, including SILAC, affinity purification and LC-MS/MS, was employed to identify proteins that are capable of binding to 6-thioguanine-containing duplex DNA in Jurkat T acute lymphoblastic leukemia cells. The outcome of the study will facilitate the exploration of other mechanisms involved in the cytotoxicity of the thiopurine drugs.

References

(1) Little, J. B. (2003) Genomic instability and radiation. *J. Radiol. Prot. 23*, 173-181.

(2) Lindahl, T. (1993) Instability and decay of the primary structure of DNA. *Nature 362*, 709-715.

(3) Muratakamiya, N., Kamiya, H., Iwamoto, N. and Kasai, H. (1995) Formation of a mutagen, glyoxal, from DNA treated with oxygen-free radicals. *Carcinogenesis 16*, 2251-2253.

(4) Nagao, M., Fujita, Y., Wakabayashi, K., Nukaya, H., Kosuge, T. and Sugimura, T. (1986) Mutagens in coffee and other beverages. *Environ. Health Perspect. 67*, 89-91.

(5) Moree-Testa, P. and Saint-Jalm, Y. (1981) Determination of [alpha]-dicarbonyl compounds in cigarette smoke. *J. Chromatogr. A 217*, 197.

(6) Frankel, E. N. (1983) Volatile lipid oxidation-products. *Prog. Lipid Res. 22*, 1-33.

(7) Loidlstahlhofen, A. and Spiteller, G. (1994) Alpha-hydroxyaldehydes, products of lipid-peroxidation. *Biochim. Biophys. Acta. Lipids Lipid Metabol. 1211*, 156-160.

(8) Mizutari, K., Ono, T., Ikeda, K., Kayashima, K. and Horiuchi, S. (1997) Photo-enhanced modification of human skin elastin in actinic elastosis by N-epsilon-(carboxymethyl)lysine, one of the glycoxidation products of the Maillard reaction. *J. Invest. Dermatol. 108*, 797-802.

(9) Thornalley, P. J., Langborg, A. and Minhas, H. S. (1999) Formation of glyoxal, methylglyoxal and 3-deoxyglucosone in the glycation of proteins by glucose. *Biochem. J. 344*, 109-116.

(10) Thornalley, P. J. (1990) The glyoxalase system - new developments towards functional-characterization of a metabolic pathway fundamental to biological life. *Biochem. J. 269*, 1-11.

(11) Fothergillgilmore, L. A. and Michels, P. A. M. (1993) Evolution of glycolysis. *Prog. Biophys. Molec. Biol. 59*, 105-235.

(12) Thornalley, P. J. (1996) Pharmacology of methylglyoxal: formation, modification of proteins and nucleic acids, and enzymatic detoxification-A role in pathogenesis and antiproliferative chemotherapy. *Gen. Pharmacol. 27*, 565-573.

(13) Phillips, S. A., Mirrlees, D. and Thornalley, P. J. (1993) Modification of the glyoxalase system in streptozotocin-induced diabetic rats - effect of the aldose reductase inhibitor statil. *Biochem. Pharmacol. 46*, 805-811.

(14) Lapolla, A., Flamini, R., Vedova, A. D., Senesi, A., Reitano, R., Fedele, D., Basso, E., Seraglia, R. and Traldi, P. (2003) Glyoxal and methylglyoxal levels in diabetic patients: quantitative determination by a new GC/MS method. *Clin. Chem. Lab. Med. 41*, 1166-1173.

(15) Ueda, Y., Miyata, T., Goffin, E., Yoshino, A., Inagi, R., Ishibashi, Y., Izuhara, Y., Saito, A., Kurokawa, K. and de Strihou, C. V. (2000) Effect of dwell time on carbonyl stress using icodextrin and amino acid peritoneal dialysis fluids. *Kidney Int. 58*, 2518-2524.

(16) Raj, D. S. C., Choudhury, D., Welbourne, T. C. and Levi, M. (2000) Advanced glycation end products: A nephrologist's perspective. *Am. J. Kidney Dis. 35*, 365-380.

(17) McLellan, A. C., Thornalley, P. J., Benn, J. and Sonksen, P. H. (1994) Glyoxalase system in clinical diabetes-mellitus and correlation with diabetic complications. *Clin. Sci. 87*, 21-29.

(18) Lo, T. W. C., Selwood, T. and Thornalley, P. J. (1994) The reaction of methylglyoxal with aminoguanidine under physiological conditions and prevention of methylglyoxal binding to plasma-proteins. *Biochem. Pharmacol. 48*, 1865-1870.

(19) Ahmed, N. and Thornalley, P. J. (2003) Quantitative screening of protein biomarkers of early glycation, advanced glycation, oxidation and nitrosation in cellular and extracellular proteins by tandem mass spectrometry multiple reaction monitoring. *Biochem. Soc. Trans. 31*, 1417-1422.

(20) Reddy, V. P., Obrenovich, M. E. and Atwood, C. S. (2002) Involvement of Millard reactions in Alzheimer disease. *Neurotox. Res. 4*, 191-209.

(21) Franke, S., Dawczynski, J., Strobel, J., Niwa, T., Stahl, P. and Stein, G. (2003) Increased levels of advanced glycation end products in human cataractous lenses. *J. Cataract Refract. Surg. 29*, 998-1004.

(22) Forbes, J. M., Cooper, M. E., Oldfield, M. D. and Thomas, M. C. (2003) Role of advanced glycation end products in diabetic nephropathy. *J. Am. Soc. Nephrol. 14*, S254-S258.

(23) Newkirk, M. M., Lepage, K., Niwa, T. and Rubin, L. (1998) Advanced glycation endproducts (AGE) on IgG, a target for circulating antibodies in North American Indians with rheumatoid arthritis (RA). *Cell. Mol. Biol. 44*, 1129-1138.

(24) Thornalley, P. J. (1998) Glutathione-dependent detoxification of [alpha]-oxoaldehydes by the glyoxalase system: involvement in disease mechanisms and antiproliferative activity of glyoxalase I inhibitors. *Chem. Biol. Interact. 137*, 111-112.

(25) Ochs, S. and Severin, T. (1994) Reaction of 2'-deoxyguanosine with glyceraldehyde. *Liebigs Ann. Chem. 8*, 851-853.

(26) Knerr, T. and Severin, T. (1993) Reaction of glucose with guanosine. *Tetrahedron Lett. 34*, 7389-7390.

(27) Lee, A. T. and Cerami, A. (1987) The formation of reactive intermediate(s) of glucose-6-phosphate and lysine capable of rapidly reacting with DNA. *Mutat. Res. 179*, 151-158.

(28) Shapiro, R. and Hachmann, H. (1966) Reaction of guanine derivatives with 1,2-dicarbonyl compounds. *Biochemistry 5*, 2799-2807.

(29) Staehelin, M. (1959) Inactivation of virus nucleic acid with glyoxal derivatives. *Biochim. Biophys. Acta 31*, 448-454.

(30) Olsen, R., Molander, P., Ovrebo, S., Ellingsen, D. G., Thorud, S., Thomassen, Y., Lundanes, E., Greibrokk, T., Backman, J., Sjoholm, R. and Kronberg, L. (2005) Reaction of glyoxal with 2 '-deoxyguanosine, 2 '-deoxyadenosine, 2 '-deoxycytidine, cytidine, thymidine, and calf thymus DNA: Identification of DNA adducts. *Chem. Res. Toxicol. 18*, 730-739.

(31) Li, Y. Y., Cohenford, M. A., Dutta, U. and Dain, J. A. (2008) The structural modification of DNA nucleosides by nonenzymatic glycation: an in vitro study

based on the reactions of glyoxal and methylglyoxal with 2 '-deoxyguanosine. *Anal. Bioanal. Chem. 390*, 679-688.

(32) Kasai, H., Iwamoto-Tanaka, N. and Fukada, S. (1998) DNA modifications by the mutagen glyoxal: adduction to G and C, deamination of C and GC and GA cross-linking. *Carcinogenesis 19*, 1459-1465.

(33) Brock, A. K., Kozekov, I. D., Rizzo, C. J. and Harris, T. M. (2004) Coupling products of nucleosides with the glyoxal adduct of deoxyguanosine. *Chem. Res. Toxicol. 17*, 1047-1056.

(34) Chen, H. J. C. and Chen, Y. C. (2009) Analysis of glyoxal-induced DNA cross-links by capillary liquid chromatography nanospray ionization tandem mass spectrometry. *Chem. Res. Toxicol. 22*, 1334-1341.

(35) Pluskota-Karwatka, D., Pawlowicz, A. J., Tomas, M. and Kronberg, L. (2008) Formation of adducts in the reaction of glyoxal with 2 '-deoxyguanosine and with calf thymus DNA. *Bioorg. Chem. 36*, 57-64.

(36) Shapiro, R., Cohen, B. I., Shiuey, S. J. and Maurer, H. (1969) On reaction of guanine with glyoxal pyruvaldehyde and kethoxal and structure of acylguanines. A new synthesis of N2-alkylguanines. *Biochemistry 8*, 238-&.

(37) Vaca, C. E., Nilsson, J. A., Fang, J. L. and Grafstrom, R. C. (1998) Formation of DNA adducts in human buccal epithelial cells exposed to acetaldehyde and methylglyoxal in vitro. *Chem.-Biol. Interact. 108*, 197-208.

(38) Vaca, C. E., Fang, J. L., Conradi, M. and Hou, S. M. (1994) Development of a P-32 postlabeling method for the analysis of

2'-deoxyguanosine-3'-monophosphate and DNA-adducts of methylglyoxal. *Carcinogenesis 15*, 1887-1894.

(39) Schneider, M., Quistad, G. B. and Casida, J. E. (1998) N-2,7-bis(1-hydroxy-2-oxopropyl)-2 '-deoxyguanosine: Identical noncyclic adducts with 1,3-dichloropropene epoxides and methylglyoxal. *Chem. Res. Toxicol. 11*, 1536-1542.

(40) Frischmann, M., Bidmon, C., Angerer, J. and Pischetsrieder, M. (2005) Identification of DNA adducts of methylglyoxal. *Chem. Res. Toxicol. 18*, 1586-1592.

(41) Wang, H. X., Cao, H. C. and Wang, Y. S. (2010) Quantification of N-2-carboxymethyl-2 '-deoxyguanosine in calf thymus DNA and cultured human kidney epithelial cells by capillary high-performance liquid chromatography-tandem mass spectrometry coupled with stable isotope dilution method. *Chem. Res. Toxicol. 23*, 74-81.

(42) Yuan, B. F., Cao, H. C., Jiang, Y., Hong, H. Z. and Wang, Y. S. (2008) Efficient and accurate bypass of N-2-(1-carboxyethyl)-2 '-deoxyguanosine by DinB DNA polyrnerase in vitro and in vivo. *Proc. Natl. Acad. Sci. USA 105*, 8679-8684.

(43) Schneider, M., Thoss, G., Hubner-Parajsz, C., Kientsch-Engel, R., Stahl, P. and Pischetsrieder, M. (2004) Determination of glycated nucleobases in human urine by a new monoclonal antibody specific for N-2-carboxyethyl-2 '-deoxyguanosine. *Chem. Res. Toxicol. 17*, 1385-1390.

(44) Li, H., Nakamura, S., Miyazaki, S., Morita, T., Suzuki, M., Pischetsrieder, M. and Niwa, T. (2006) N-2-carboxyethyl-2 '-deoxyguanosine, a DNA glycation marker, in kidneys and aortas of diabetic and uremic patients. *Kidney Int. 69*, 388-392.

(45) MurataKamiya, N., Kamiya, H., Kaji, H. and Kasai, H. (1997) Mutational specificity of glyoxal, a product of DNA oxidation, in the lacI gene of wild-type Escherichia coli W3110. *Mutat. Res. 377*, 255-262.

(46) Hou, S. M., Nori, P., Fang, J. L. and Vaca, C. E. (1995) Methylglyoxal induces hprt mutation and DNA adducts in human T-Lymphocytes in vitro. *Environ. Mol. Mutagen. 26*, 286-291.

(47) Seidel, W. and Pischetsrieder, M. (1998) DNA-glycation leads to depurination by the loss of N2-carboxyethylguanine in vitro. *Cell. Mol. Biol. 44*, 1165-1170.

(48) Pischetsrieder, M., Seidel, W., Munch, G. and Schinzel, R. (1999) N-2-(1-carboxyethyl)deoxyguanosine, a nonenzymatic glycation adduct of DNA, induces single-strand breaks and increases mutation frequencies. *Biochem. Biophys. Res. Commun. 264*, 544-549.

(49) Bucala, R., Model, P., Russel, M. and Cerami, A. (1985) Modification of DNA by glucose-6-phosphate induces DNA rearrangements in an Escherichia-coli plasmid. *Proc. Natl. Acad. Sci. USA 82*, 8439-8442.

(50) Bucala, R., Lee, A. T., Rourke, L. and Cerami, A. (1993) Transposition of an alu-containing element induced by DNA-advanced glycosylation endproducts. *Proc. Natl. Acad. Sci. USA 90*, 2666-2670.

(51) Balzarini, J. (1994) Metabolism and mechanism of antiretroviral action of purine and pyrimidine-derivatives. *Pharm. World Sci. 16*, 113-126.

(52) Elion, G. B. (1989) The purine path to chemotherapy. *Science 244*, 41-47.

(53) Pui, C. H. and Evans, W. E. (1998) Acute lymphoblastic leukemia. *N. Engl. J. Med. 339*, 605-615.

(54) Burchenal, J. H., Murphy, M. L., Ellison, R. R., Sykes, M. P., Tan, T. C., Leone, L. A., Karnofsky, D. A., Craver, L. F., Dargeon, H. W. and Rhoads, C. P. (1953) Clinical evaluation of a new antimetabolite, 6-mercaptopurine, in the treatment of leukemia and allied diseases. *Blood 8*, 965-999.

(55) Murray, J. E., Harrison, J. H., Dammin, G. J., Wilson, R. E. and Merrill, J. P. (1963) Prolonged survival of human-kidney homografts by immunosuppressive drug therapy. *N. Engl. J. Med. 268*, 1315-&.

(56) McLeod, H. L., Krynetski, E. Y., Relling, M. V. and Evans, W. E. (2000) Genetic polymorphism of thiopurine methyltransferase and its clinical relevance for childhood acute lymphoblastic leukemia. *Leukemia 14*, 567-572.

(57) Krynetskaia, N. F., Krynetski, E. Y. and Evans, W. E. (1999) Human RNase H-mediated RNA cleavage from DNA-RNA duplexes is inhibited by 6-deoxythioguanosine incorporation into DNA. *Mol. Pharmacol. 56*, 841-848.

(58) Christie, N. T., Drake, S., Meyn, R. E. and Nelson, J. A. (1984) 6-thioguanine-induced DNA damage as a determinant of cyto-toxicity in cultured Chinese-hamster ovary cells. *Cancer Res. 44*, 3665-3671.

(59) Lee, S. H. and Sartorelli, A. C. (1981) The effects of inhibitors of DNA biosynthesis on the cytotoxicity of 6-thioguanine. *Cancer Biochem. Biophys. 5*, 189-194.

(60) Schutz, E., Gummert, J., Mohr, F. and Oellerich, M. (1993) Azathioprine-induced myelosuppression in thiopurine methyltransferase deficient heart-transplant recipient. *Lancet 341*, 436-436.

(61) Evans, W. E., Horner, M., Chu, Y. Q., Kalwinsky, D. and Roberts, W. M. (1991) Altered mercaptopurine metabolism, toxic effects, and dosage requirement in a thiopurine methyltransferase-deficient child with acute lymphocytic-leukemia. *J. Pediatr. 119*, 985-989.

(62) McLeod, H. L., Miller, D. R. and Evans, W. E. (1993) Azathioprine-induced myelosuppression in thiopurine methyltransferase deficient heart-transplant recipient. *Lancet 341*, 1151-1151.

(63) Krynetski, E. Y., Tai, H. L., Yates, C. R., Fessing, M. Y., Loennechen, T., Schuetz, J. D., Relling, M. V. and Evans, W. E. (1996) Genetic polymorphism of thiopurine S-methyltransferase: Clinical importance and molecular mechanisms. *Pharmacogenetics 6*, 279-290.

(64) Gunnarsdottir, S. and Elfarra, A. A. (2003) Distinct tissue distribution of metabolites of the novel glutathione-activated thiopurine prodrugs cis-6-(2-acetylvinylthio)purine and trans-6-(2-acetylvinylthio)guanine and 6-thioguanine in the mouse. *Drug Metab. Dispos. 31*, 718-726.

(65) Duley, J. A. and Florin, T. H. J. (2005) Thiopurine therapies - problems, complexities, and progress with monitoring thioguanine nucleotides. *Ther. Drug Monit. 27*, 647-654.

(66) Somerville, L., Krynetski, E. Y., Krynetskaia, N. F., Beger, R. D., Zhang, W. X., Marhefka, C. A., Evans, W. E. and Kriwacki, R. W. (2003) Structure and dynamics of thioguanine-modified duplex DNA. *J. Biol. Chem. 278*, 1005-1011.

(67) Bohon, J. and de los Santos, C. R. (2003) Structural effect of the anticancer agent 6-thioguanine on duplex DNA. *Nucleic Acids Res. 31*, 1331-1338.

(68) Bohon, J. and de los Santos, C. R. (2005) Effect of 6-thioguanine on the stability of duplex DNA. *Nucleic Acids Res. 33*, 2880-2886.

(69) Fairchild, C. R., Maybaum, J. and Kennedy, K. A. (1986) Concurrent unilateral chromatid damage and DNA strand breakage in response to 6-thioguanine treatment. *Biochem. Pharmacol. 35*, 3533-3541.

(70) Covey, J. M., Dincalci, M. and Kohn, K. W. (1986) Production of DNA-protein cross-links (DPC) by 6-thioguanine (TG) and 2'-deoxy-6-thioguanosine (TGdR) In L1210 cells-Invitro. *Proc. Am. Assoc. Cancer Res. 27*, 17-17.

(71) Maybaum, J. and Mandel, H. G. (1983) Unilateral chromatid damage - a new basis for 6-thioguanine cyto-toxicity. *Cancer Res. 43*, 3852-3856.

(72) Pan, B. F. and Nelson, J. A. (1990) Characterization of the DNA damage in 6-thioguanine-treated cells. *Biochem. Pharmacol. 40*, 1063-1069.

(73) Swann, P. F., Waters, T. R., Moulton, D. C., Xu, Y. Z., Zheng, Q. G., Edwards, M. and Mace, R. (1996) Role of postreplicative DNA mismatch repair in the cytotoxic action of thioguanine. *Science 273*, 1109-1111.

(74) O'Donovan, P., Perrett, C. M., Zhang, X. H., Montaner, B., Xu, Y. Z., Harwood, C. A., McGregor, J. M., Walker, S. L., Hanaoka, F. and Karran, P. (2005) Azathioprine and UVA light generate mutagenic oxidative DNA damage. *Science 309*, 1871-1874.

(75) Gu, C. N. and Wang, Y. S. (2007) In vitro replication and thermodynamic studies of methylation and oxidation modifications of 6-thioguanine. *Nucleic Acids Res. 35*, 3693-3704.

(76) Zhang, X. H., Jeffs, G., Ren, X. L., O'Donovan, P., Montaner, B., Perrett, C. M., Karran, P. and Xu, Y. Z. (2007) Novel DNA lesions generated by the interaction between therapeutic thiopurines and UVA light. *DNA Repair 6*, 344-354.

(77) Yuan, B. F. and Wang, Y. S. (2008) Mutagenic and cytotoxic properties of 6-thioguanine, S-6-methylthioguanine, and guanine-S-6-sulfonic acid. *J. Biol. Chem. 283*, 23665-23670.

(78) Yuan, B. F., O'Conner, T. R. and Wang, Y. S. (2010) 6-Thioguanine and S-6-methylthioguanine are mutagenic in human cells. *Chem. Biol.*, revision pending.

(79) Holliday, R. (1987) The inheritance of epigenetic defects. *Science 238*, 163-170.

(80) Hendrich, B. D. and Willard, H. F. (1995) Epigenetic regulation of gene-expression - The effect of altered chromatin structure from yeast to mammals. *Hum. Mol. Genet. 4*, 1765-1777.

(81) Cheung, P. and Lau, P. (2005) Epigenetic regulation by histone methylation and histone variants. *Mol. Endocrinol. 19*, 563-573.

(82) Kornberg, R. D. and Lorch, Y. L. (1999) Twenty-five years of the nucleosome, fundamental particle of the eukaryote chromosome. *Cell 98*, 285-294.

(83) Felsenfeld, G. and Groudine, M. (2003) Controlling the double helix. *Nature 421*, 448-453.

(84) Robertson, K. D. (2005) DNA methylation and human disease. *Nat. Rev. Genet. 6*, 597-610.

(85) Wilson, G. G. and Murray, N. E. (1991) Restriction and modification systems. *Annu. Rev. Genet. 25*, 585-627.

(86) Bird, A. P. and Wolffe, A. P. (1999) Methylation-induced repression - Belts, braces, and chromatin. *Cell 99*, 451-454.

(87) Bestor, T. H. (2000) The DNA methyltransferases of mammals. *Hum. Mol. Genet. 9*, 2395-2402.

(88) Klose, R. J. and Bird, A. P. (2006) Genomic DNA methylation: the mark and its mediators. *Trends Biochem. Sci. 31*, 89-97.

(89) Okano, M., Xie, S. P. and Li, E. (1998) DNMT2 is not required for de novo and maintenance methylation of viral DNA in embryonic stem cells. *Nucleic Acids Res. 26*, 2536-2540.

(90) Suetake, I., Shinozaki, F., Miyagawa, J., Takeshima, H. and Tajima, S. (2004) DNMT3L stimulates the DNA methylation activity of DNMT3a and DNMT3b through a direct interaction. *J. Biol. Chem. 279*, 27816-27823.

(91) Wang, H. X. and Wang, Y. S. (2009) 6-Thioguanine perturbs cytosine methylation at the CpG dinucleotide site by DNA methyltransferases in vitro and acts as a DNA demethylating agent in Vivo. *Biochemistry 48*, 2290-2299.

(92) Turk, P. W., Laayoun, A., Steven, S. S. and Weitzman, S. A. (1995) DNA adduct 8-hydroxyl-2'-deoxyguanosine (8-hydroxyguanine) affects function of human DNA methyltransferase. *Carcinogenesis 16*, 1253-1255.

(93) Tan, N. W. and Li, B. F. L. (1990) Interaction of oligonucleotides containing 6-O-methylguanine with human DNA (cytosine-5-)-methyltransferase. *Biochemistry 29*, 9234-9240.

(94) Subach, O. M., Maltseva, D. V., Shastry, A., Kolbanovskiy, A., Klimasauskas, S., Geacintov, N. E. and Gromova, E. S. (2007) The stereochemistry of benzo[a]pyrene-2 '-deoxyguanosine adducts affects DNA methylation by SssI and HhaI DNA methyltransferases. *FEBS J. 274*, 2121-2134.

(95) Valinluck, V. and Sowers, L. C. (2007) Endogenous cytosine damage products alter the site selectivity of human DNA maintenance methyltransferase DNMT1. *Cancer Res. 67*, 946-950.

(96) Gopalakrishnan, S., Van Emburgh, B. O. and Robertson, K. D. (2008) DNA methylation in development and human disease. *Mutat. Res. 647*, 30-38.

(97) Laird, P. W. Principles and challenges of genome-wide DNA methylation analysis. *Nat. Rev. Genet. 11*, 191-203.

(98) Wilson, A. S., Power, B. E. and Molloy, P. L. (2007) DNA hypomethylation and human diseases. *Biochim. Biophys. Acta 1775*, 138-162.

(99) Feinberg, A. P. and Tycko, B. (2004) Timeline - The history of cancer epigenetics. *Nat. Rev. Cancer 4*, 143-153.

(100) Widschwendter, M., Jiang, G. C., Woods, C., Muller, H. M., Fiegl, H., Goebel, G., Marth, C., Muller-Holzner, E., Zeimet, A. G., Laird, P. W. and Ehrlich, M. (2004) DNA hypomethylation and ovarian cancer biology. *Cancer Res. 64*, 4472-4480.

(101) Estlin, E. J. (2001) Continuing therapy for childhood acute lymphoblastic leukaemia: clinical and cellular pharmacology of methotrexate, 6-mercaptopurine and 6-thioguanine. *Cancer Treat. Rev. 27*, 351-363.

(102) Evans, W. E. and Relling, M. V. (1994) Mercaptopurine vs thioguanine for the treatment of acute lymphoblastic-leukemia. *Leuk. Res. 18*, 811-814.

(103) Schmiegelow, K., Bjork, O., Glomstein, A., Gustafsson, G., Keiding, N., Kristinsson, J., Makipernaa, A., Rosthoj, S., Szumlanski, C., Sorensen, T. M. and Weinshilboum, R. (2003) Intensification of mercaptopurine/methotrexate maintenance chemotherapy may increase the risk of relapse for some children with acute lymphoblastic leukemia. *J. Clin. Oncol. 21*, 1332-1339.

(104) Veness, M. J., Quinn, D. I., Ong, C. S., Keogh, A. M., Macdonald, P. S., Cooper, S. G. and Morgan, G. W. (1999) Aggressive cutaneous malignancies following cardiothoracic transplantation - The Australian experience. *Cancer 85*, 1758-1764.

(105) Sheil, A. G. R., Disney, A. P. S., Mathew, T. H., Amiss, N. and Excell, L. (1991) Cancer development in cadaveric donor renal-allograft recipients treated with zzathioprine (Aza) or cyclosporine (Cya) or Aza/Cya. *Transplant. Proc. 23*, 1111-1112.

(106) Banoub, J. H., Newton, R. P., Esmans, E., Ewing, D. F. and Mackenzie, G. (2005) Recent developments in mass spectrometry for the characterization of nucleosides, nucleotides, oligonucleotides, and nucleic acids. *Chem. Rev. 105*, 1869-1915.

(107) Randerath, K., Reddy, M. V. and Gupta, R. C. (1981) P-32-labeling test for DNA damage. *Proc. Natl. Acad. Sci. USA 78*, 6126-6129.

(108) Shuker, D. E. G., Bailey, E., Gorf, S. M., Lamb, J. and Farmer, P. B. (1984) Determination of N-7-[H-2(3)]methyl guanine in rat urine by gas-chromatography mass-spectrometry following administration of trideuteromethylating agents or precursors. *Anal. Biochem. 140*, 270-275.

(109) Stillwell, W. G., Xu, H. X., Adkins, J. A., Wishnok, J. S. and Tannenbaum, S. R. (1989) Analysis of methylated and oxidized purines in urine by capillary gas-chromatography mass-spectrometry. *Chem. Res. Toxicol. 2*, 94-99.

(110) Singh, R. and Farmer, P. B. (2006) Liquid chromatography-electrospray ionization-mass spectrometry: the future of DNA adduct detection. *Carcinogenesis 27*, 178-196.

(111) Collins, A. R., Cadet, J., Moller, L., Poulsen, H. E. and Vina, J. (2004) Are we sure we know how to measure 8-oxo-7,8-dihydroguanine in DNA from human cells? *Arch. Biochem. Biophys. 423*, 57-65.

(112) Cadet, J., Douki, T. and Ravanat, J. L. (2008) Oxidatively generated damage to the guanine moiety of DNA: Mechanistic aspects and formation in cells. *Acc. Chem. Res. 41*, 1075-1083.

(113) Esmans, E. L., Broes, D., Hoes, I., Lemiere, F. and Vanhoutte, K. (1998) Liquid chromatography mass spectrometry in nucleoside, nucleotide and modified nucleotide characterization. *J. Chromatogr. A 794*, 109-127.

(114) Singh, R., Kaur, B. and Farmer, P. B. (2005) Detection of DNA damage derived from a direct acting ethylating agent present in cigarette smoke by use of liquid chromatography-tandem mass spectrometry. *Chem. Res. Toxicol. 18*, 249-256.

(115) Wang, H. X. and Wang, Y. S. (2010) LC-MS/MS coupled with stable isotope dilution method for the quantification of 6-thioguanine and S-6-methylthioguanine in genomic DNA of human cancer cells treated with 6-thioguanine. *Anal. Chem. 82*, 5797-5803.

(116) da Costa, G. G., Churchwell, M. I., Hamilton, L. P., Von Tungeln, L. S., Beland, F. A., Marques, A. M. and Doerge, D. R. (2003) DNA adduct formation from acrylamide via conversion to glycidamide in adult and neonatal mice. *Chem. Res. Toxicol. 16*, 1328-1337.

(117) Turteltaub, K. W. and Dingley, K. H. (1998) Application of accelerated mass spectrometry (AMS) in DNA adduct quantification and identification. *Toxicol. Lett. 103*, 435-439.

(118) McLuckey, S. A., Vanberkel, G. J. and Glish, G. L. (1992) Tandem mass-spectrometry of small, multiply charged oligonucleotides. *J. Am. Soc. Mass Spectrom. 3*, 60-70.

(119) Aebersold, R. and Mann, M. (2003) Mass spectrometry-based proteomics. *Nature 422*, 198-207.

(120) Ong, S. E. and Mann, M. (2005) Mass spectrometry-based proteomics turns quantitative. *Nat. Chem. Biol. 1*, 252-262.

(121) Deleenheer, A. P. and Thienpont, L. M. (1992) Applications of isotope-dilution mass-spectrometry in clinical-chemistry, pharmacokinetics, and toxicology. *Mass Spectrom. Rev. 11*, 249-307.

(122) Kusmierz, J. J., Sumrada, R. and Desiderio, D. M. (1990) Fast-atom-bombardment mass-spectrometric quantitative-analysis of methionine-enkephalin in human pituitary tissues. *Anal. Chem. 62*, 2395-2400.

(123) Fenselau, C. (2007) A review of quantitative methods for proteomic studies. *J. Chromatogr. B 855*, 14-20.

(124) Miyagi, M. and Rao, K. C. S. (2007) Proteolytic O-18-labeling strategies for quantitative proteomics. *Mass Spectrom. Rev. 26*, 121-136.

(125) Petritis, B. O., Qian, W. J., Camp, D. G. and Smith, R. D. (2009) A simple pocedure for effective quenching of trypsin activity and prevention of O-18-labeling back-exchange. *J. Proteome Res. 8*, 2157-2163.

(126) Leitner, A. and Lindner, W. (2006) Chemistry meets proteomics: The use of chemical tagging reactions for MS-based proteomics. *Proteomics 6*, 5418-5434.

(127) Gygi, S. P., Rist, B., Gerber, S. A., Turecek, F., Gelb, M. H. and Aebersold, R. (1999) Quantitative analysis of complex protein mixtures using isotope-coded affinity tags. *Nat. Biotechnol. 17*, 994-999.

(128) Ross, P. L., Huang, Y. L. N., Marchese, J. N., Williamson, B., Parker, K., Hattan, S., Khainovski, N., Pillai, S., Dey, S., Daniels, S., Purkayastha, S., Juhasz, P., Martin, S., Bartlet-Jones, M., He, F., Jacobson, A. and Pappin, D. J. (2004) Multiplexed protein quantitation in Saccharomyces cerevisiae using amine-reactive isobaric tagging reagents. *Mol. Cell. Proteomics 3*, 1154-1169.

(129) Gygi, S. P., Han, D. K. M., Gingras, A. C., Sonenberg, N. and Aebersold, R. (1999) Protein analysis by mass spectrometry and sequence database searching: Tools for cancer research in the post-genomic era. *Electrophoresis 20*, 310-319.

(130) Zhang, R. J., Sioma, C. S., Wang, S. H. and Regnier, F. E. (2001) Fractionation of isotopically labeled peptides in quantitative proteomics. *Anal. Chem. 73*, 5142-5149.

(131) Borisov, O. V., Goshe, M. B., Conrads, T. P., Rakov, V. S., Veenstra, T. D. and Smith, R. D. (2002) Low-energy collision-induced dissociation fragmentation analysis of cysteinyl-modified peptides. *Anal. Chem. 74*, 2284-2292.

(132) Zhou, H. L., Ranish, J. A., Watts, J. D. and Aebersold, R. (2002) Quantitative proteome analysis by solid-phase isotope tagging and mass spectrometry. *Nat. Biotechnol. 20*, 512-515.

(133) Hansen, K. C., Schmitt-Ulms, G., Chalkley, R. J., Hirsch, J., Baldwin, M. A. and Burlingame, A. L. (2003) Mass spectrometric analysis of protein mixtures at low

levels using cleavable C-13-isotope-coded affinity tag and multidimensional chromatography. *Mol. Cell. Proteomics 2*, 299-314.

(134) Li, J. X., Steen, H. and Gygi, S. P. (2003) Protein profiling with cleavable isotope-coded affinity tag (cICAT) reagents - The yeast salinity stress response. *Mol. Cell. Proteomics 2*, 1198-1204.

(135) Lahm, H. W. and Langen, H. (2000) Mass spectrometry: A tool for the identification of proteins separated by gels. *Electrophoresis 21*, 2105-2114.

(136) Oda, Y., Huang, K., Cross, F. R., Cowburn, D. and Chait, B. T. (1999) Accurate quantitation of protein expression and site-specific phosphorylation. *Proc. Natl. Acad. Sci. USA 96*, 6591-6596.

(137) Ong, S. E., Blagoev, B., Kratchmarova, I., Kristensen, D. B., Steen, H., Pandey, A. and Mann, M. (2002) Stable isotope labeling by amino acids in cell culture, SILAC, as a simple and accurate approach to expression proteomics. *Mol. Cell. Proteomics 1*, 376-386.

(138) Ishihama, Y., Sato, T., Tabata, T., Miyamoto, N., Sagane, K., Nagasu, T. and Oda, Y. (2005) Quantitative mouse brain proteomics using culture-derived isotope tags as internal standards. *Nat. Biotechnol. 23*, 617-621.

(139) Mann, M. (2006) Functional and quantitative proteomics using SILAC. *Nat. Rev. Mol. Cell Biol. 7*, 952-958.

(140) Schulze, W. X. and Mann, M. (2004) A novel proteomic screen for peptide-protein interactions. *J. Biol. Chem. 279*, 10756-10764.

(141) Vermeulen, M., Hubner, N. C. and Mann, M. (2008) High confidence determination of specific protein-protein interactions using quantitative mass spectrometry. *Curr. Opin. Biotechnol. 19*, 331-337.

(142) Mittler, G., Butter, F. and Mann, M. (2009) A SILAC-based DNA protein interaction screen that identifies candidate binding proteins to functional DNA elements. *Genome Res. 19*, 284-293.

(143) Butter, F., Scheibe, M., Morl, M. and Mann, M. (2009) Unbiased RNA-protein interaction screen by quantitative proteomics. *Proc. Natl. Acad. Sci. USA 106*, 10626-10631.

(144) Kadonaga, J. T. (2004) Regulation of RNA polymerase II transcription by sequence-specific DNA binding factors. *Cell 116*, 247-257.

(145) Schulze, W. X., Deng, L. and Mann, M. (2005) Phosphotyrosine interactome of the ErbB-receptor kinase family. *Mol. Syst. Biol. 1*, E1-13.

CHAPTER 2

Quantification of DNA Advanced Glycation End Products: N^2-CMdG, 1,N^2-glyoxal-dG and N^2-CEdG Induced by Hyperglycemia in Biological Samples

Introduction

Humans are exposed to glyoxal (Gly) and methylglyoxal (MG) from both endogenous and exogenous sources. General exogenous sources of Gly and MG include cigarette smoke, food, and beverages (*3-5*). On the other hand, the fragmentation of triose phosphate during glycolysis, metabolism of acetone, and catabolism of aminoacetone all contribute to the endogenous formation of methylglyoxal (*13, 146*). And Gly can arise endogenously from a multitude of pathways, which encompass the oxidation of lipids, unsaturated fatty acids, and carbohydrates (*6, 7, 9*). As metabolites of the highly conserved glycolysis, Gly and MG were observed to be present at elevated levels in blood of patients with diabetes(*13, 147*), peritoneal dialysis, uremia (*14-16*) and in the kidney, lens, and blood of streptozotocin-induced diabetic rats (*17*).

Being reactive dicarbonyl compounds, Gly and MG are involved in numerous pathological process *in vivo* by binding irreversibly to proteins (*148-150*), DNA and other substrates to from AGEs (*40, 41*). The reactions of Gly and MG with 2'-deoxyribonucleosides and DNA have been studied (*28-31*), and guanine is the predominant modification site. Under physiological conditions, Gly reacts with 2'-deoxyguanosine (dG) and calf thymus DNA to form 3-(2'-deoxy-β-D-*erythro*-pentofuranosyl)-5,6,7-trihydro-6,7-dihydroxyimidazo[1,2-*a*]puri

ne-9-one (1,N^2-glyoxal-dG) (*31, 151*),

5-carboxymethyl-3-(2'-deoxy-β-D-*erythro*-pentofuranosyl)-5,6,7-trihydro-6,7-dihydroxyimidazo[1,2-*a*]purine-9-one (Gx_2-dG) and N^2-carboxymethyl-2'-deoxyguanosine (N^2-CMdG, Figure 1.1) in DNA (*35*). In above studies, 1,N^2-glyoxal-dG and Gx_2-dG were found to be unstable and transformed partially to N^2-CMdG. The same transformation was also observed in single-stranded DNA after prolonged incubation. Therefore, N^2-CMdG is the only stable adduct formed in calf thymus DNA upon treatment with Gly. Olsen and co-workers (*151*) quantified 1,N^2-glyoxal-dG adduct in calf thymus DNA and mouse hepatoma cells upon treatment with high concentrations of glyoxal by using column switching capillary LC-ESI-MS method. However, 1,N^2-glyoxal-dG adduct was only detected in mouse hepatoma cells exposed to 5 and 7 mM of glyoxal for 48 h, and the adduct was not detectable in cells treated with 1 or 3 mM of glyoxal (*151*).

MG adducts of DNA have also been investigated and two diastereomers of N^2-carboxyethyl-2'-deoxyguanosine (N^2-CEdG) (Figure 1.1) were identified as major stable DNA-AGEs adducts formed in calf thymus DNA upon prolonged exposure to MG at physiological concentration and temperature, respectively (*40*). N^2-CEdG was detected in urine samples from healthy human subjects (*43*) and WM-266-4 human melanoma cells (*152*). The treatment of the WM-266-4 cells with MG or glucose led to a dose-responsive increase in the formation of N^2-CEdG (*152*). In addition, the level of N^2-CEdG was enhanced in the kidney and aorta of patients with diabetic nephropathy and uremic atherosclerosis, respectively (*44*).

We reason that, as the only stable adduct formed from the reactions of Gly with dG or DNA, N^2-CMdG as well as N^2-CEdG may serve as reliable biomarkers for Gly and MG exposure. At this point of view, we developed a sensitive capillary LC-ESI-MS^3 coupled with stable isotope-dilution technique and quantified the formation of N^2-CMdG in calf thymus DNA exposed to D-glucose and glyoxal as well as in human kidney epithelial cells treated with glyoxal. Furthermore, the quantification of N^2-CMdG and N^2-CEdG has been extended to human blood cells $CD34^-$, buffy coat samples, healthy rat tissues and diabetic mouse livers as well.

Experimental Procedures

Regents and Methods

All reagents, unless otherwise specified, were from Sigma-Aldrich (St. Louis, MO). [U-$^{15}N_5$]-2'-deoxyguanosine was purchased from Cambridge Isotope Laboratories (Andover, MA). Proteinase K was obtained from New England Biolabs (Ipswich, WA). Fetal bovine serum, 293T human kidney cells, penicillin, and streptomycin were purchased from ATCC (Manassas, VA, USA). Electrospray ionization-mass spectrometry (ESI-MS) and tandem MS (MS/MS) experiments were carried out on an LCQ Deca XP ion-trap mass spectrometer (Thermo Fisher Scientific, San Jose, CA). A mixture of acetonitrile and water (50:50, v/v) was used as solvent for electrospray. The spray voltage was 3.0 kV, and the temperature for the ion transport tube was maintained at 275 °C. High-resolution mass spectra (HRMS) were acquired on an Agilent 6510 Q-TOF LC/MS instrument (Agilent Technologies, Santa Clara, CA) coupled with an electrospray

ionization (ESI) source and an Agilent HPLC-Chip Cube MS interface. ^{1}H NMR spectra were recorded at 500 MHz on a Varian Inova 500 NMR spectrometer (Varian Inc. Palo Alto, CA).

Synthesis and Characterization of [U-$^{15}N_5$]-N^2-CMdG (*153*)

To a closed vial were added 7.5-μL glyoxal solution (4%), 300 μg [U-$^{15}N_5$]-2'-deoxyguanosine and 0.5 mL of 1 M sodium phosphate buffer. The reaction mixture was heated at 100°C for 16 h. The desired [U-$^{15}N_5$]-N^2-CMdG was purified by HPLC on a Beckman system with pump module 125 and a UV detector (module 126). A 4.6×50 mm Luna C18 column (5 μm in particle size and 100 Å in pore size, Phenomenex Inc., Torrance, CA) was used. A solution of 10 mM ammonium formate (pH 6.3, solution A) and a mixture of 10 mM ammonium formate and acetonitrile (70:30, v/v, solution B) were employed as mobile phases. The flow rate was 0.30 mL/min, and a gradient of 5 min 0-4% B, 45 min 4-13% B and 2 min 13-100% B was used. After purification, the identity of [U-$^{15}N_5$]-N^2-CMdG was confirmed by both high-resolution ESI-QTOF MS and ion trap LC-MS/MS analyses (see Results).

Synthesis and Characterization of [U-$^{15}N_5$]-1,N^2-glyoxal-dG

[U-$^{15}N_5$]-1,N^2-glyoxal-dG was synthesized following a previously described method (*30*). Briefly, a mixture of 544 μg of [U-$^{15}N_5$]-2'-deoxyguanosine and 4.54-μL glyoxal solution (40% in water) at a molar ratio of 1:20 was incubated in 0.5 mL of 50 mM sodium phosphate buffer (pH 7.4) at 37 °C for 2 h. The desired

[U-$^{15}N_5$]-1,N^2-glyoxal-dG was purified by the above-described HPLC method. The structure of [U-$^{15}N_5$]-1,N^2-glyoxal-dG was confirmed by both high-resolution ESI-QTOF MS and ion trap LC-MS/MS analyses (see Results).

Measurement of Extinction Coefficients for N^2-CMdG and 1,N^2-glyoxal-dG

Unlabeled N^2-CMdG and 1,N^2-glyoxal-dG were synthesized and purified following the same methods as described above except that unlabeled 2'-deoxyguanosine was employed for the reaction. The extinction coefficients of N^2-CMdG and 1,N^2-glyoxal-dG at 260 nm were determined to be 1.03×10^4 and 1.07×10^4 $L\cdot mol^{-1}\cdot cm^{-1}$, respectively, by using a previously reported ^1H NMR method (*154*).

Stability Studies of N^2-CMdG and 1,N^2-glyoxal-dG

A 50 μM solution of N^2-CMdG in 1 mL phosphate-buffered saline (PBS, pH 7.4) was incubated at 37°C, and aliquots (200 μL each) were taken out at 0, 1, 2, 4, and 7 days. Similarly, a 100-μM solution of 1,N^2-glyoxal-dG was incubated under the same conditions and aliquots (100 μL each) were removed at 0, 2, 4, 8, and 16 hrs as well as at 1, 2, 3, 6 and 8 days. The aliquots were immediately stored in a -20°C freezer prior to being analyzed with HPLC. The HPLC analysis was carried out by using a 4.6×250 mm Apollo C18 column (5 μm in particle size and 300 Å in pore size, Grace Inc., Deerfield, IL) on an Agilent 1100 capillary pump (Agilent Technologies) with a UV detector monitoring at 260 nm and a Peak Simple Chromatography Data System (SRI Instruments Inc., Las Vegas, NV, USA). A solution of 10 mM ammonium formate (pH 6.3, solution A)

and a mixture of 10 mM ammonium formate and acetonitrile (70:30, v/v, solution B) were used as mobile phases. A gradient of 5 min 0-12% B, 40 min 10-35% B and 5 min 30-100% B was employed and the flow rate was 0.80 mL/min.

Glyoxal and Glucose Treatment of Calf Thymus DNA

Calf thymus DNA was incubated separately with 0, 10, 25, 50, 100, 250 and 500 μM of glyoxal or 0, 2, 5, 10, 25 and 50 mM of D-glucose in a 1.0-mL phosphate buffer (0.1 M, pH 7.4) at 37°C for 48 hrs. DNA was subsequently precipitated from the reaction mixture by the addition of 0.1 mL of 10 M ammonium acetate and 2.2 mL of cold ethanol and cooled at –20°C. The mixture was centrifuged at 5000 g for 15 min and the supernatant was removed. The recovered DNA was washed with 0.5 mL of cold 70% ethanol, centrifuged as described above, and the supernatant was removed. The same washing step was repeated. The DNA was then dried under vacuum, dissolved in doubly distilled water and quantified by UV spectrophotometry at 260 nm.

Cell Culture, Glyoxal Treatment and DNA Isolation

The 293T human kidney epithelial cells were cultured at 37°C in 5% CO_2 atmosphere and in a custom-prepared medium with the same ingredients as Dulbecco's Modified Eagle's Medium except that the glucose concentration was 5 mM. The medium was supplemented with 10% fetal bovine serum (Invitrogen, Carlsbad, CA), 100 IU/mL penicillin, and 100 μg/mL streptomycin. After growing to 80% confluence, cells were detached by trypsin-EDTA treatment and harvested by centrifugation to remove the

medium. The cell pellets were subsequently washed twice with PBS and resuspended in 20 mL of PBS buffer (at a density of 10^6 cells/mL) containing 0, 10, 50, 250 or 1250 μM of glyoxal and incubated at room temperature for 3 hrs with occasional shaking.

After treatment, cells (~ 2×10^7 cells) were harvested by centrifugation, and the cell pellets were resuspended in a lysis buffer containing 10 mM Tris-HCl (pH 8.0), 0.1 M EDTA, and 0.5% SDS. The cell lysates were then treated with 20 μg/mL of RNase A at 37°C for 1 hr and subsequently with 100 μg/mL of proteinase K at 50°C for 3 hrs. Genomic DNA was isolated by extraction with phenol/chloroform/isoamyl alcohol (25:24:1, v/v) and desalted by ethanol precipitation. The DNA pellet was redissolved in water and its concentration was measured by UV absorbance at 260 nm.

DNA Extraction from Human Buffy Coat Samples

Buffy coat samples (MB13, G81 and HS35) were washed with 1×PBS buffer and centrifuged at 7,000 rpm for 5 min. After the removal of supernatant, buffy coat pellets with white blood cells were collected and dissolved first in 1×TE buffer and then resuspended in a lysis buffer containing 10 mM Tris-HCl (pH 8.0), 10 mM EDTA, and 50 mM NaCl. The lysates were then treated with 20 μg/mL of RNase A at 37°C for 1 h and subsequently with 100 μg/mL of proteinase K at 50°C for 3 h. Genomic DNA was isolated by extraction with phenol/chloroform/isoamyl alcohol (75:24:1, v/v) and desalted by ethanol precipitation. The DNA pellet was redissolved in water and its concentration was measured by UV absorbance at 260 nm.

DNA Extraction from Animal Tissues

Tissue samples were first cut into small pieces, frozen and grinded into fine powders in a mortar prechilled with liquid nitrogen. Tissue powders were transferred into 50 mL tube with appropriate amount of lysis buffer (20 mM Tris-HCl, 20 mM EDTA, 400 mM NaCl and 1% SDS) and digested with proteinase K at a final concentration of 0.1 mg/mL at 50°C overnight. Saturated NaCl solution (1/2 volume) was subsequently added to the mixture, which was vortexed for 1 min, and then incubated at 50°C for 15 min. The mixture was centrifuged at 16,000g for 30 min and the supernatant was collected in a new tube. Nuclei acids in the supernatant were precipitated using 2 volumes of cold ethanol, washed with 70% ethanol and dissolved in TE buffer. RNA was removed by the treatment with RNase A (50 μg/mL) and RNase T1 (50 U/mL) at 37°C for 30 min. Genomic DNA was isolated by extraction with an equal volume of chloroform/isoamyl alcohol (24:1, v/v) and desalted by ethanol precipitation. The DNA pellet was redissolved in water and its concentration was measured by UV absorbance at 260 nm.

Enzymatic Digestion and HPLC Enrichment

For the enzymatic digestion of DNA, nuclease P1 (4 units) was added to a mixture containing 100 μg genomic DNA, 200 fmol [U-$^{15}N_5$]-N^2-CMdG, 200 fmol [U-$^{15}N_5$]-1,N^2-glyoxal-dG, 100 fmol D-N^2-CEdG and 100fmol L-N^2-CEdG, 30 mM sodium acetate (pH 5.5) and 1 mM zinc acetate, and the mixture was incubated at 37 °C for 4 hrs. Nuclease P1 is a single-stranded endonuclease; genomic DNA obtained by the

above phenol/chloroform extraction and ethanol precipitation procedures might be partially denatured, rendering it to be cleaved by nuclease P1. To the digestion mixture were then added 30 units of alkaline phosphatase in a 50 mM Tris-HCl buffer (pH 8.6), the digestion was continued at 37°C for 2.5 hrs, and the enzymes were removed by chloroform extraction. The aqueous DNA layer was dried by using a Speed-vac and the dried residues were reconstituted in water. The amount of nucleosides in the mixture was quantified by UV absorbance measurements.

A previous study indicated that the addition of carbonyl scavengers could minimize the artificial formation of N^2-CEdG from the involved methylglyoxal during DNA extraction and hydrolysis (*155*). We carried out the DNA extraction and enzymatic digestion with or without the addition of a carbonyl scavenger, D-penicillamine. The quantification results revealed that, when the enzymatic digestion was performed at 37°C, the addition of D-penicillamine did not influence appreciably the yield of N^2-CMdG. Thus, D-penicillamine was not added in subsequent experiments.

The HPLC removal of unmodified nucleosides from the digestion mixture of isolated or cellular DNA was carried out using the same HPLC system as employed for the stability studies. A solution of 10 mM ammonium formate (pH 6.3, solution A) and a mixture of 10 mM ammonium formate and acetonitrile (70:30, v/v, solution B) were used as mobile phases. A gradient of 5 min 0-8% B, 40 min 10-30% B and 5 min 30-100% B was employed and the flow rate was 0.80 mL/min. The fraction containing N^2-CMdG, and two isomers of N^2-CEdG was collected, dried in a Speedvac, reconstituted in distilled water and subjected to LC-MS/MS analysis.

LC-MS/MS Analysis

Quantitative analysis of N^2-CMdG and N^2-CEdG in the above DNA hydrolysates was performed by online capillary HPLC-ESI-MS/MS using an Agilent 1200 capillary HPLC pump (Agilent Technologies) interfaced with an LTQ linear ion trap mass spectrometer (Thermo Fisher Scientific, San Jose, CA). A 0.5×150 mm Zorbax SB-C18 column (5 μm in particle size, Agilent Technologies) was used for the separation of the DNA hydrolysis mixture and the flow rate was 6.0 μL/min. A gradient of 0-20% methanol (in 5-min) followed by 20-45% methanol (in 35-min) in water with 0.1% formic acid was employed. The effluent from the LC column was directed to MS/MS/MS analysis, where the LTQ mass spectrometer was set up for monitoring the further fragmentation of the protonated nucleobase portions of unlabeled and labeled N^2-CMdG and N^2-CEdG.

Results

Synthesis and Characterization of Isotope-labeled N^2-CMdG and 1,N^2-glyoxal-dG

[U-$^{15}N_5$]-N^2-CMdG was synthesized from the reaction of [U-$^{15}N_5$]-dG and glyoxal at 100 °C and purified from the reaction mixture (Figure 2.1 shows the HPLC trace for the separation of the reaction mixture). The formation of [U-$^{15}N_5$]-N^2-CMdG increases the mass of [U-$^{15}N_5$]-dG by 58 Da, which gives the $[M+H]^+$ ion at *m/z* 331. Collision-induced dissociation of the ion of *m/z* 331 led to the formation of fragment ions of *m/z* 215 and 313, which are attributed to the elimination of a 2-deoxyribose moiety and a H_2O molecule, respectively (Figure 2.2a). Further fragmentation of the *m/z*-215 ion

gave the most abundant product ion of *m/z* 169, which originated from the loss of a neutral HCOOH molecule and another product ion of *m/z* 197 for the loss of a H_2O molecule from the [U-$^{15}N_5$]-N^2-carboxymethylguanine (Figure 2.2b). High-resolution ESI MS gives *m/z* 331.0958 for the $[M+H]^+$ ion of [U-$^{15}N_5$]-N^2-CMdG, which is consistent with the calculated *m/z* of 331.0947 with a deviation of 3.4 ppm.

[U-$^{15}N_5$]-1,N^2-glyoxal-dG was synthesized by reacting [U-$^{15}N_5$]-dG with glyoxal at 37 °C for 2 h and purified from the reaction mixture by HPLC (*30*). High-resolution ESI MS gives *m/z* 331.0953 for the $[M+H]^+$ ion of [U-$^{15}N_5$]-1,N^2-glyoxal-dG, which is consistent with the calculated *m/z* of 331.0947 with a deviation of 1.9 ppm. Tandem MS analysis of the ion of *m/z* 331 shows the predominant fragment ion of *m/z* 215, which again arises from the loss of a 2-deoxyribose moiety (Figure 2.3a). Further fragmentation of the *m/z*-215 ion gives the most abundant product ion of *m/z* 197, which is attributed to the loss of a H_2O molecule and another product ion of *m/z* 169 for the loss of a HCOOH molecule from the [U-$^{15}N_5$]-1,N^2-glyoxal-dG (Figure 2.3b). In addition, we observed the protonated ion of guanine (*m/z* 157, Figure 2.3b), which was not observed in the corresponding spectrum of [U-$^{15}N_5$]-N^2-CMdG (Figure 2.2b) of *m/z* 215.0 observed in MS/MS of synthetic [U-$^{15}N_5$]-N^2-CMdG.

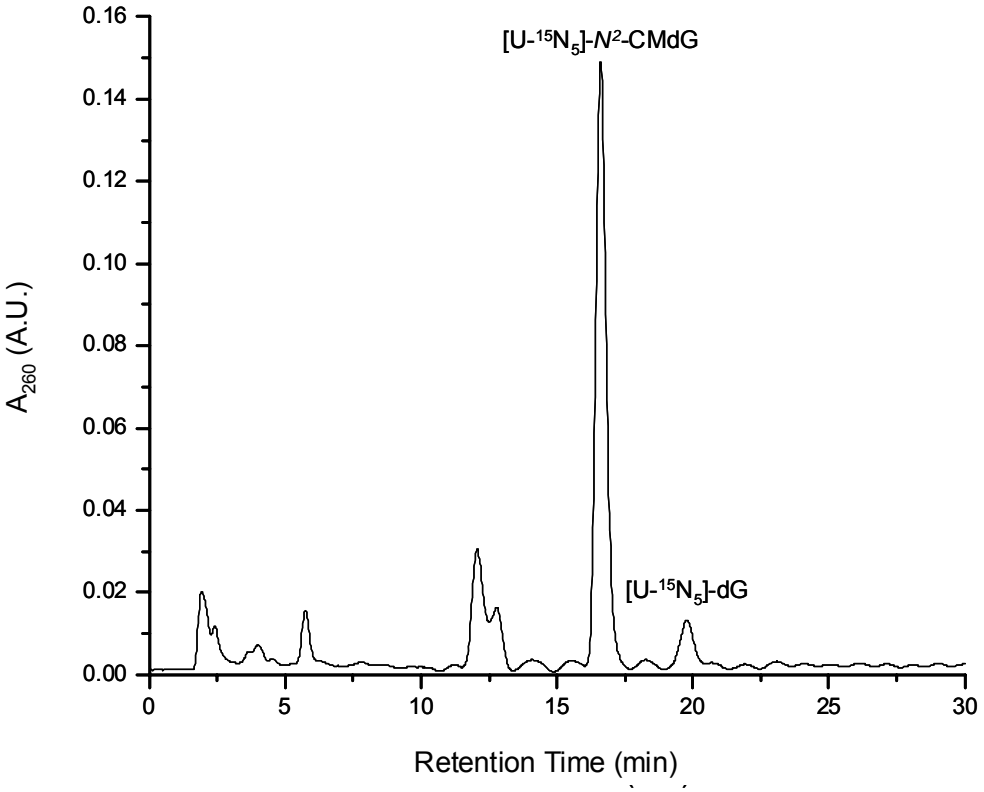

Figure 2.1 HPLC trace for the separation of the reaction mixture of the [U-$^{15}N_5$]-dG with glyoxal.

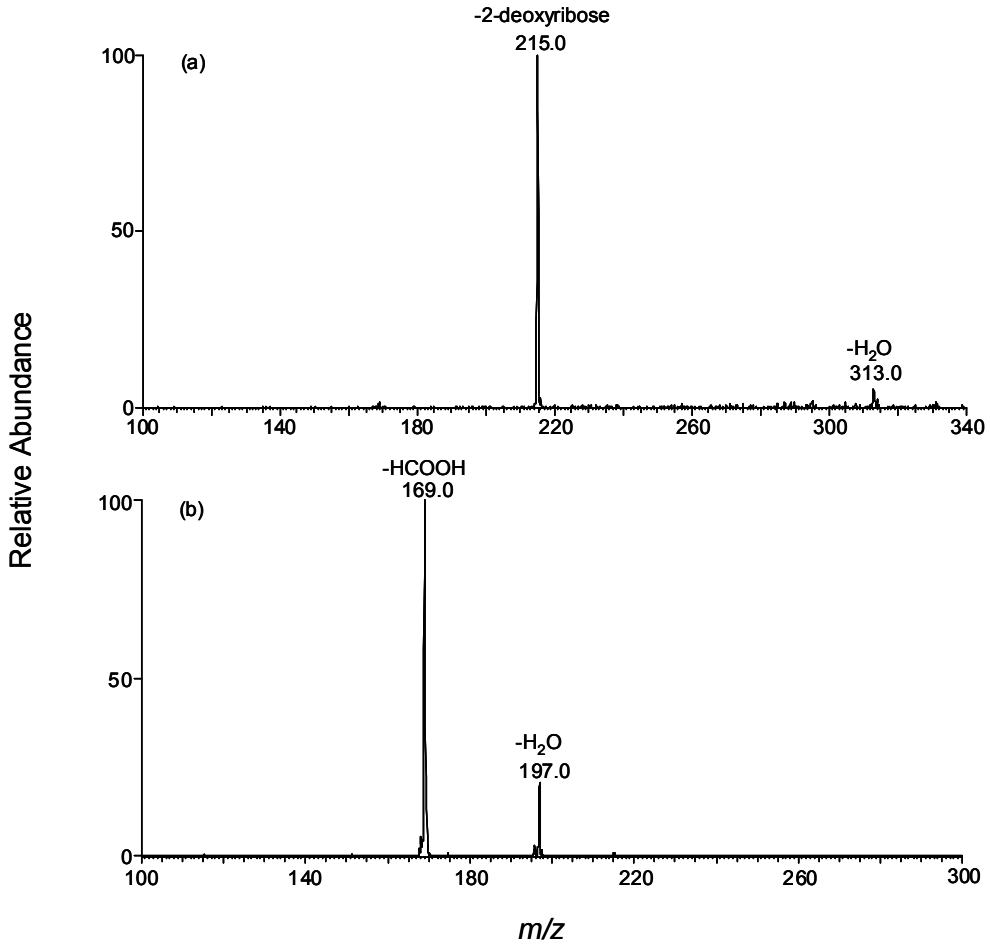

Figure 2.2 ESI-MS/MS (a) spectrum of the $[M+H]^+$ ion and MS^3 (b) spectrum of the ion.

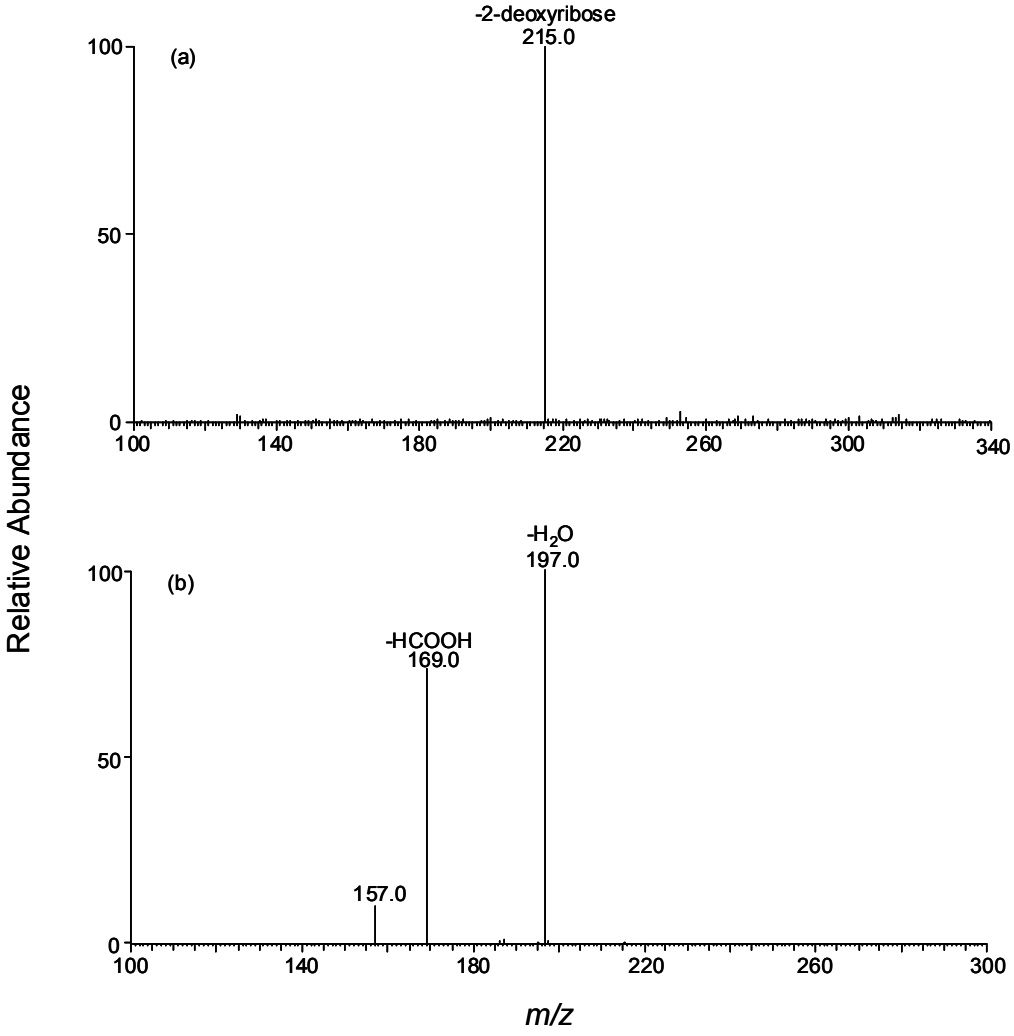

Figure 2.3 ESI-MS/MS of the $[M+H]^+$ ion of [U-$^{15}N_5$]-1,N^2-glyoxal-dG (a), and shown in (b) is the MS^3 of the ion of *m/z* 215.0 found in (a).

Stability Studies of N^2-CMdG and 1,N^2-glyoxal-dG

Prior to assessing quantitatively the formation of N^2-CMdG and 1,N^2-glyoxal-dG, we first examined the chemical stabilities of these two modified nucleosides. To this end, we synthesized the unlabeled N^2-CMdG and 1,N^2-glyoxal-dG (^{1}H-NMR spectra shown in Figures 2.4 and 2.5), which were incubated separately under physiological conditions (PBS buffer, pH 7.4 at 37 °C). Aliquots were removed at different time points and analyzed by HPLC. The HPLC analysis revealed that N^2-CMdG was a stable product with less than 0.5 % being decomposed to dG after a 7-day incubation and no other degradation products could be found (Figure 2.6a & 2.7). In contrast, 1,N^2-glyoxal-dG was found to be very unstable; approximately 70% of 1,N^2-glyoxal-dG was decomposed to dG during the first day of incubation (Figure 2.6b & 2.8). It is worth noting that, under the above conditions, the conversion from 1,N^2-glyoxal-dG to N^2-CMdG was too subtle to be detected.

LC-MS Quantification of N^2-CMdG in Calf Thymus DNA

LC-MS/MS with the isotope dilution method constitutes a reliable quantification method. In this study, we added isotope-labeled [U-$^{15}N_5$]-N^2-CMdG and [U-$^{15}N_5$]-1,N^2-glyoxal-dG to the samples prior to the enzymatic hydrolysis of genomic DNA, which corrected for the potential analyte loss during various stages of sample preparation process. Owing to the presence of the carboxylic moiety in N^2-CMdG and a better sensitivity afforded by the positive- than the negative-ion mode, we quantified this adduct by LC-MS in the positive-ion mode where 0.1% formic acid was added to the

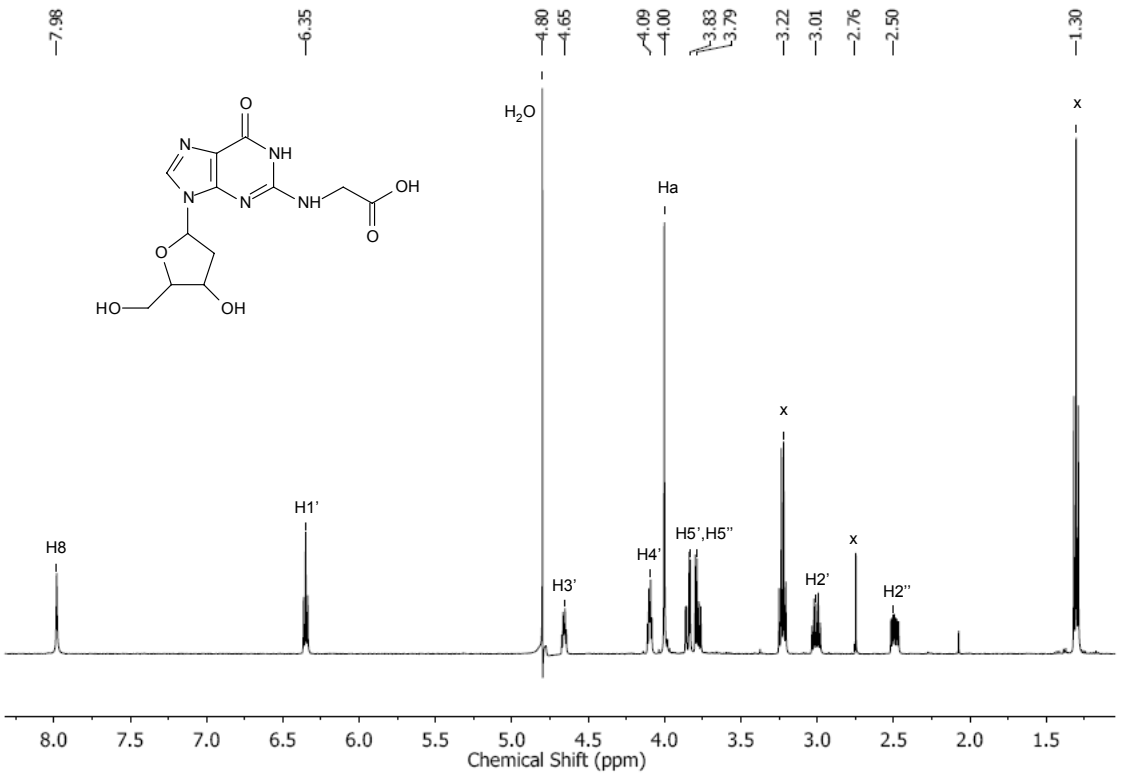

Figure 2.4 ^{1}H-NMR spectrum of standard N^2-CMdG (500 MHz, D_2O, 25 °C): δ 7.98 (s, 1H, H-8), 6.35 (t, 1H, H-1'), 4.65 (m, 1H, H-3'), 4.09 (m, 1H, H-4'), 4.00 (s, 2H, CH_2), 3.83 (m, 1H, H-5'), 3.79 (m, 1H, H-5''), 3.01 (m, 1H, H-2'), 2.50 (m, 1H, H-2''). "H-a" represents the carboxymethyl proton, and peaks marked with 'x' are from impurities.

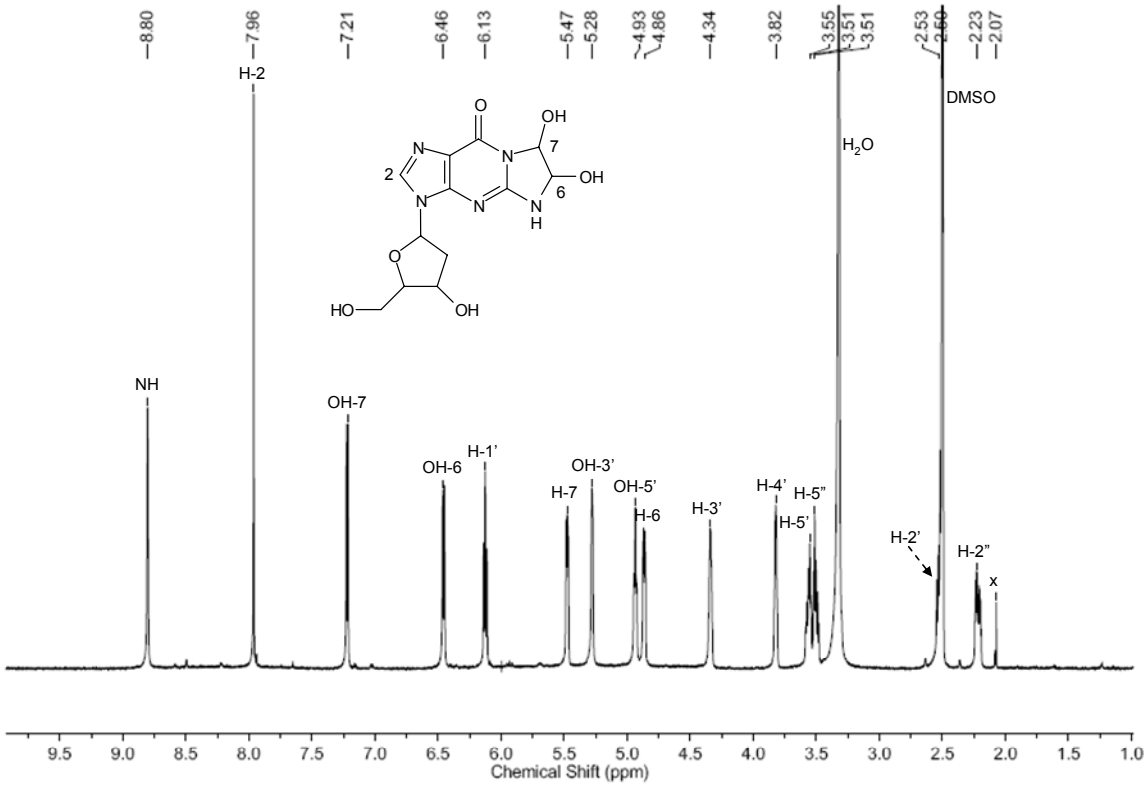

Figure 2.5 ^{1}H-NMR spectrum of standard 1,N^2-glyoxal-dG (600 MHz, DMSO, 25 °C): δ 8.80 (s, 1H, NH), 7.96 (s, 1H, H-2), 7.21 (d, 1H, OH-7), 6.46 (d, 1H, OH-6), 6.13 (m, 1H H-1'), 5.47 (m, 1H, H-7), 5.28 (d, 1H, OH-3'), 4.93 (t, 1H, OH-5'), 4.86 (m, 1H, H-6), 4.34 (m, 1H, H-3'), 3.82 (m, 1H, H-4'), 3.55 (m, 1H, H-5'), 3.51 (m, 1H, H-5"), 2.53 (m, 1H, H-2'), 2.23(m, 1H, H-2"). The peak marked with 'x' is from impurities.

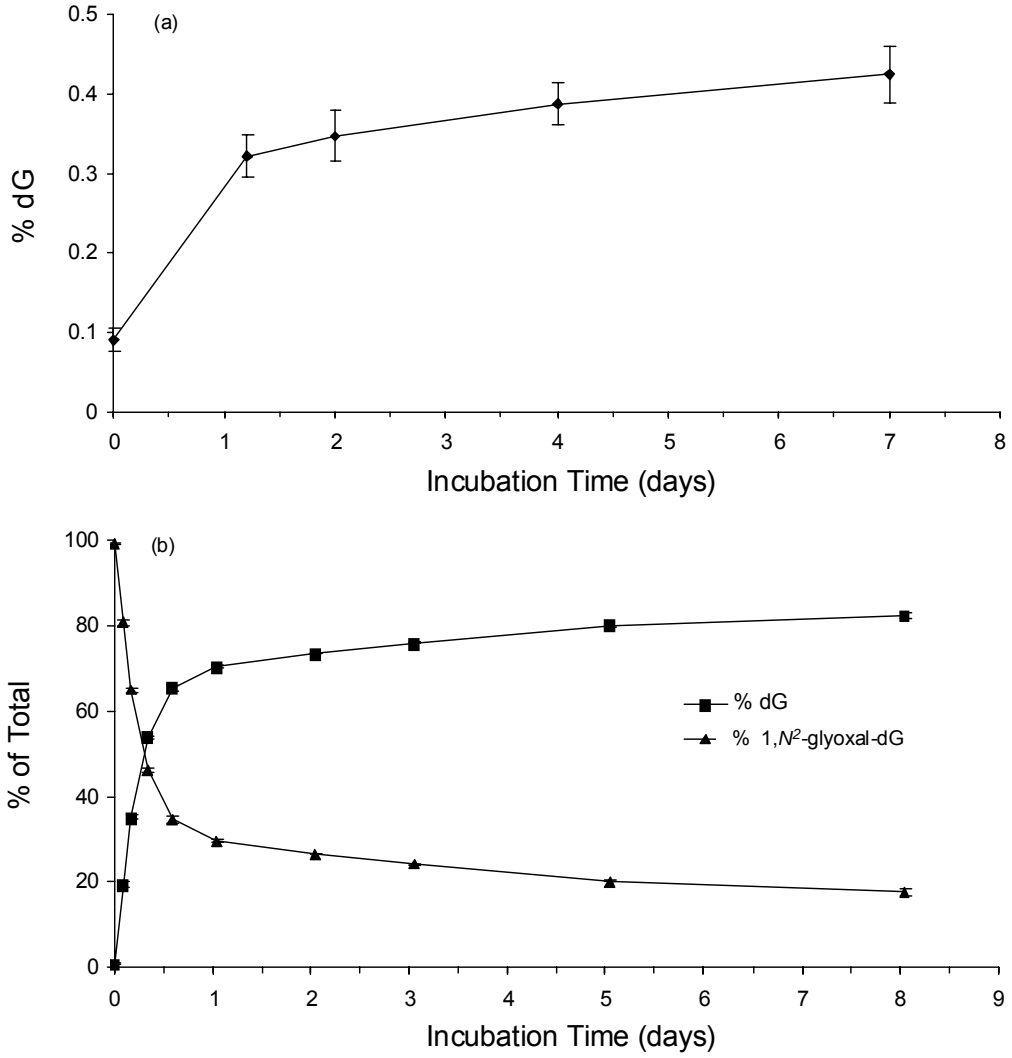

Figure 2.6 Time-dependant decomposition of N^2-CMdG (a) and 1,N^2-glyoxal-dG (b) in PBS buffer (pH 7.4) at 37°C. The data were obtained from HPLC analyses of the aliquots removed from the N^2-CMdG and 1,N^2-glyoxal-dG solutions after incubation in PBS buffer for the indicated periods of time. The quantification was based on peak areas observed in the chromatograms with the consideration of the extinction coefficients of dG, N^2-CMdG (1.03×10^4 L·mol^{-1}·cm^{-1}) and 1,N^2-glyoxal-dG (1.07×10^4 L·mol^{-1}·cm^{-1}) at 260 nm.

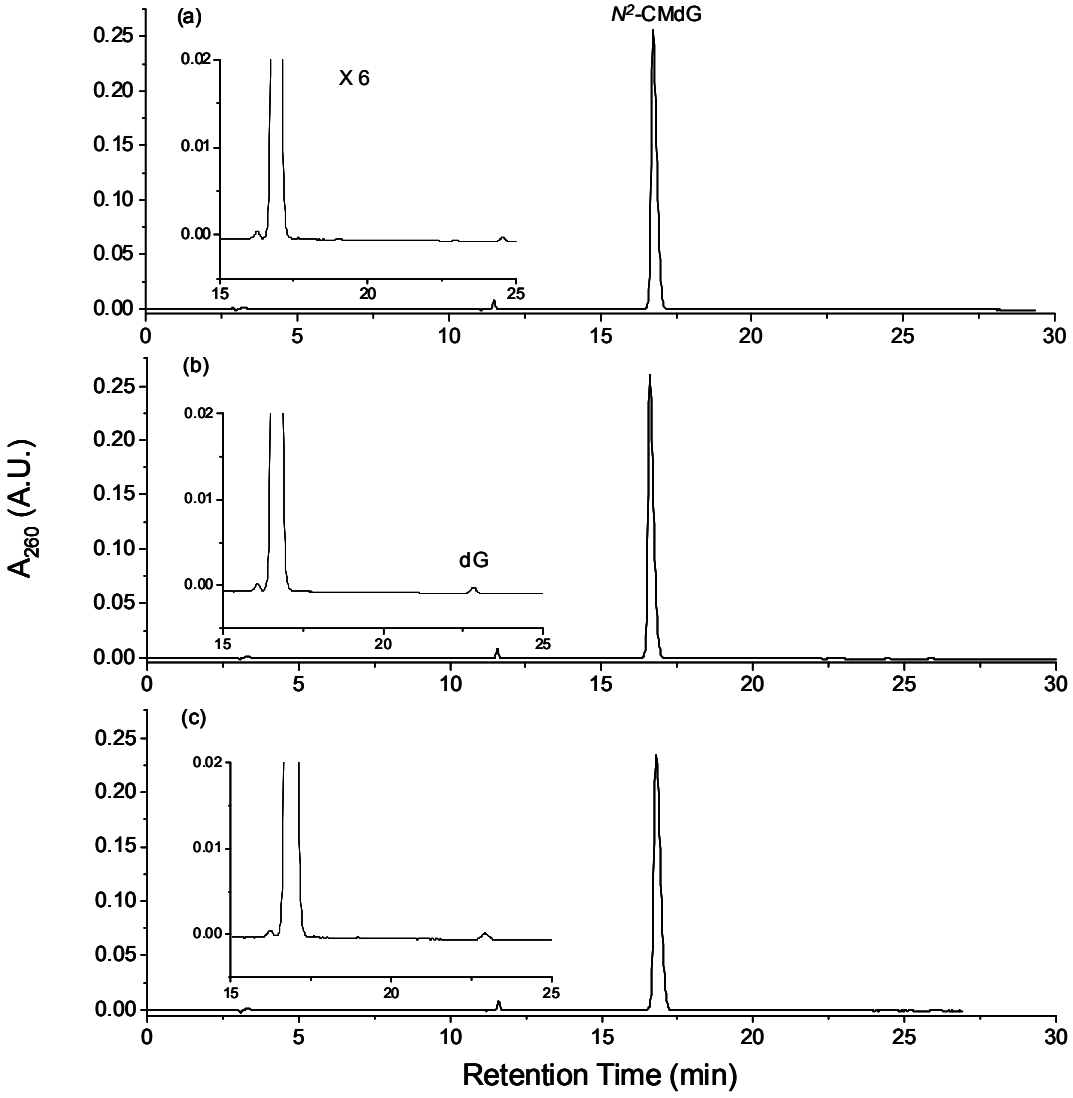

Figure 2.7 HPLC traces for the separation of aliquots removed from the N^2-CMdG solution after incubation at 37°C in PBS buffer for 0 (a), 2 (b) and 7 (c) days, respectively. Shown in the insets are the expanded chromatograms to visualize better the dG peak.

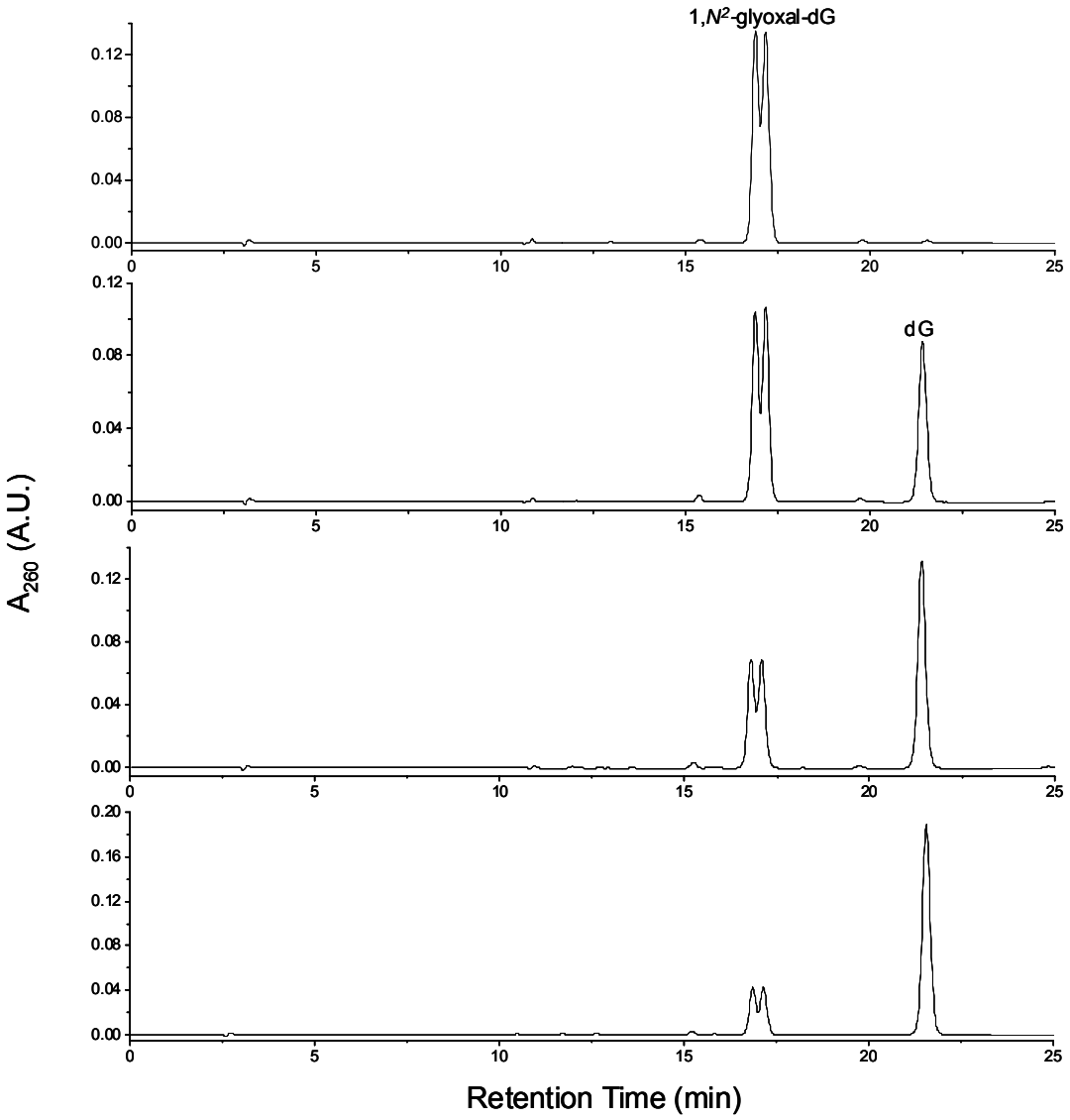

Figure 2.8 HPLC traces for the separation of aliquots removed from the 1,N^2-glyoxal-dG solution after incubation at 37 °C in PBS buffer for 0 hr (a), 4 hr (b), 8 hr (c) and 2 days (d), respectively. The doublet peaks with the retention time at 16.9 and 17.1 min correspond to the two diastereomers of 1,N^2-glyoxal-dG.

mobile phases to facilitate the protonation of the analyte. In this context, DNA was first digested with nuclease P1 to yield nucleoside 5'-monophosphates, which were dephosphorylated with alkaline phosphatase. The nucleoside mixture was subsequently separated by HPLC and detected by ESI-MS^3.

Prior to quantifying the formation of N^2-CMdG in DNA samples, we assessed the limit of detection (LOD) for our LC-MS/MS method. It turned out that, when the pure standard was analyzed by LC-MS/MS, the LOD for N^2-CMdG at an S/N of 3 was 1.8 fmol. The LOD was very similar (1.9 fmol with an S/N of 3) when the adduct was enriched from the mixture of 100 μg of DNA hydrolysate, which was doped with the [U-$^{15}N_5$]-N^2-CMdG, and analyzed by LC-MS/MS under the same conditions. The latter LOQ corresponds to the capability of detecting N^2-CMdG at a frequency of 2.8 lesions per 10^8 normal nucleosides when 100 μg of DNA is used. We monitored the *m/z* 326→210 and *m/z* 331→215 transitions for N^2-CMdG and its uniformly ^{15}N-labeled counterpart, respectively. The identity of the component eluting at 18.7 min in the SIC of Figure 2.9 was determined to be N^2-CMdG based on the same retention time and similar tandem mass spectra as those observed for [U-$^{15}N_5$]-N^2-CMdG (MS/MS shown in Figure 2.10a & 2.10b). In this context, aside from the most abundant ion at *m/z* 215, there were abundant interference ions present in Figure 2.10b. MS^3 analysis monitoring the further cleavage of the ion of *m/z* 210 was subsequently carried out. When compared to LC-MS/MS, LC-MS^3 provided better specificity for identifying and quantifying N^2-CMdG (Figure 2.10c & 2.10d). The component eluting at 15.7 min in Figure 2.9 was identified as 1,N^2-glyoxal-dG adduct based on similar retention time and tandem MS

spectra compared to the added [U-$^{15}N_5$]-1,N^2-glyoxal-dG internal standard (MS/MS and MS^3 spectra shown in Figure 2.11). However, due to the unstable nature of 1,N^2-glyoxal-dG, we did not quantify this adduct. The origin of the peak eluting at 16.9 min in Figure 2.9b remains unclear. On the grounds that LC-MS/MS of [U-$^{15}N_5$]-1,N^2-glyoxal-dG or [U-$^{15}N_5$]-N^2-CMdG under the same conditions gives a single peak in the corresponding selected-ion chromatograms (Figures 2.12 and 2.13), it is unlikely that the 16.9-min fraction arises from the conversion of either internal standard to a chemical entity with the same molecular weight. We speculate that it might be due to some isobaric interference present in the sample.

Our LC-MS/MS/MS quantification results revealed that, under physiological conditions, N^2-CMdG was formed at a frequency of approximately 2 lesions per 10^6 nucleosides in calf thymus DNA treated with 10 μM glyoxal. The level of N^2-CMdG increased from 7 to 134 adducts per 10^6 nucleosides when the concentration of glyoxal increased from 25 to 500 μM (Figure 2.14a). However, this adduct was not detectable in the control calf thymus DNA that was incubated under the same conditions but without the addition of glyoxal, suggesting that, if this adduct is present in calf thymus DNA, it should exist at a level that is lower than 2.8 lesions per 10^8 nucleosides.

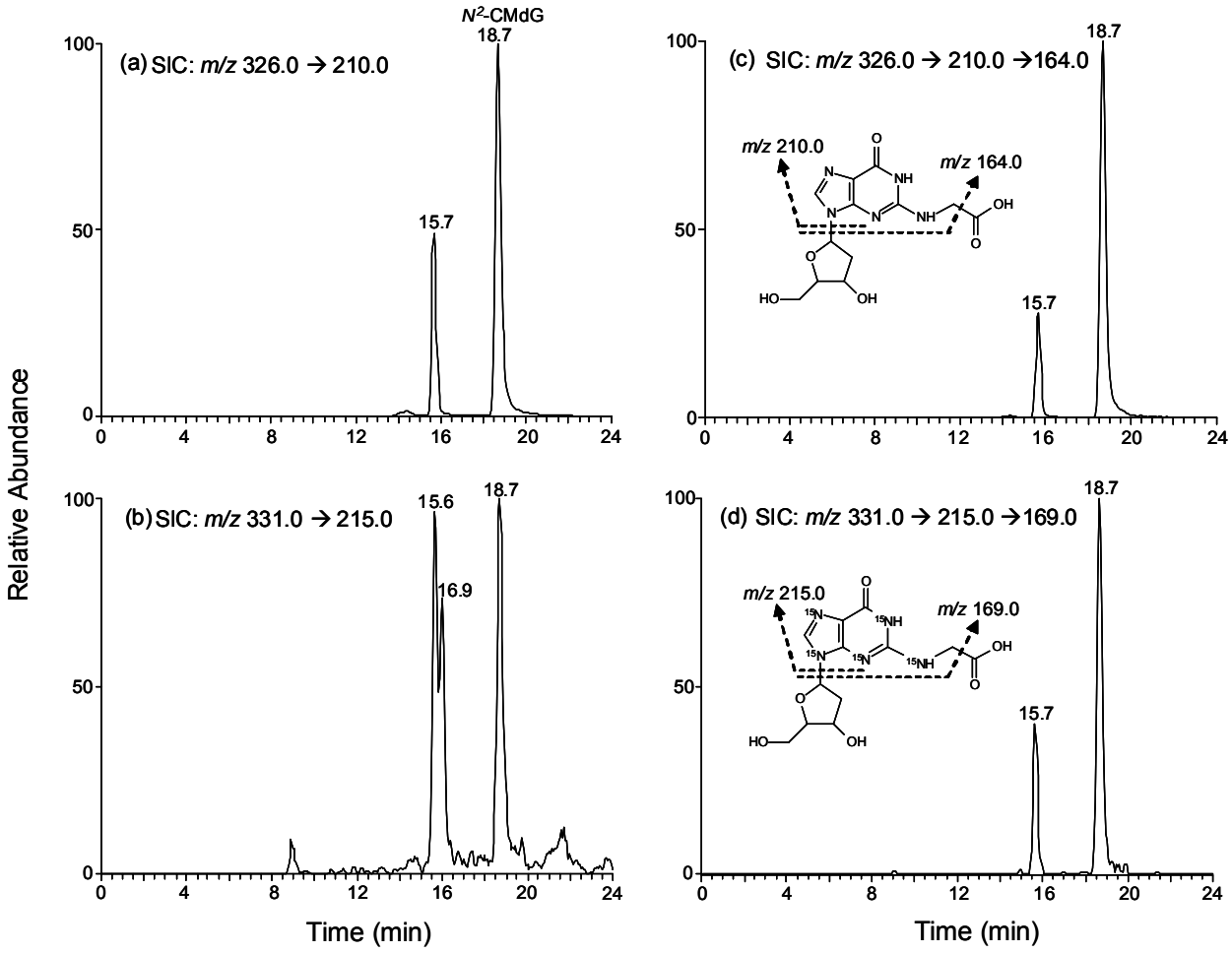

Figure 2.9 Selected-ion chromatograms (SICs) for monitoring *m/z* 326→ 210 (a) and *m/z* 326→ 210→ 164 (c) (for unlabeled N^2-CMdG) as well as the *m/z* 331→ 215 (b) and *m/z* 331→ 215→ 169 (d) (for [U-$^{15}N_5$]-N^2-CMdG) transitions of the digestion mixtures of calf thymus DNA which was treated with 250 μM of glyoxal. The peak at 15.7 min in Figure 3b was identified as1,N^2-glyoxal-dG based on its co-elution with the added [U-$^{15}N_5$]-1,N^2-glyoxal-dG, and the one at 16.9 min in Figure 2.9b might be due to the presence of isobaric interferences, as evidenced by the absence of the corresponding peak in the SIC obtained from MS/MS/MS analysis (Figure 2.9d and discussion in text).

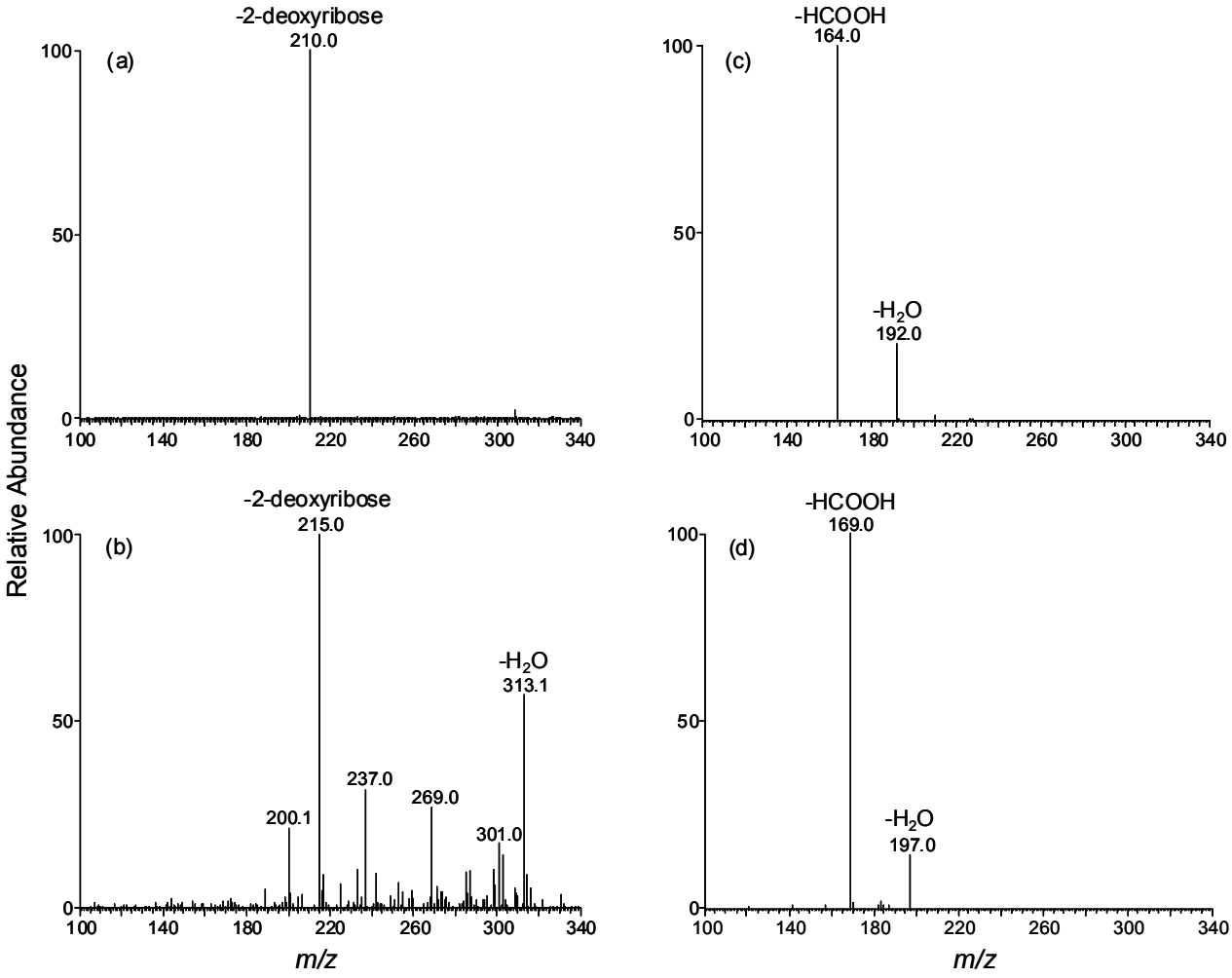

Figure 2.10 Product-ion spectra of the ions *m/z* 326 (a), *m/z* 331 (b) and MS^3 spectra of the ions of *m/z* 210 (c) and *m/z* 215 (d) (a, c for unlabeled and b, d for the [U-$^{15}N_5$]-N^2-CMdG in calf thymus DNA treated with 250 μM of glyoxal, respectively).

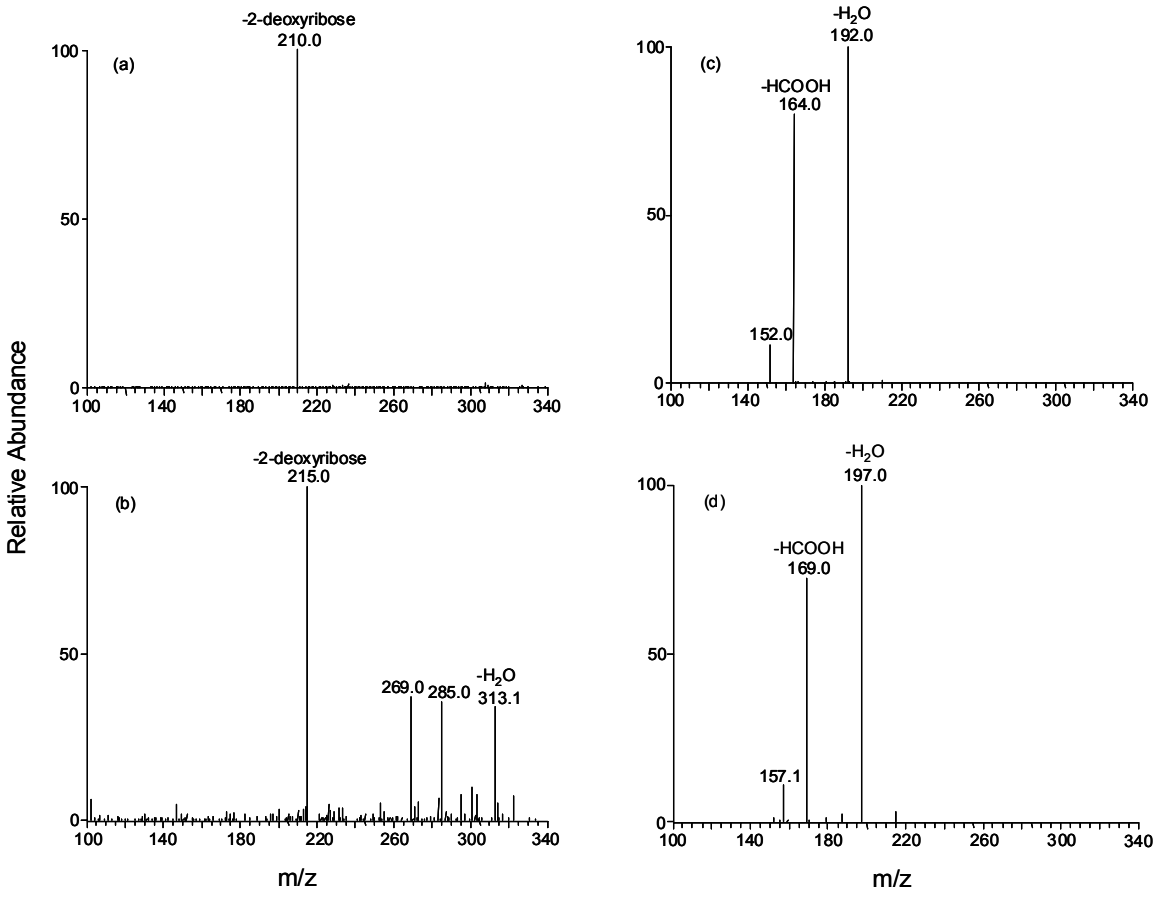

Figure 2.11 Product-ion spectra of the ion *m/z* 326 (a), *m/z* 331 (b) and MS^3 spectra of *m/z* 210 (c), *m/z* 215 (d). Panels (a) and (c) are for unlabeled, and (b) and (d) are for the [U-$^{15}N_5$]-1,N^2-glyoxal-dG in the digestion mixture of calf thymus DNA treated with 250 μM of glyoxal.

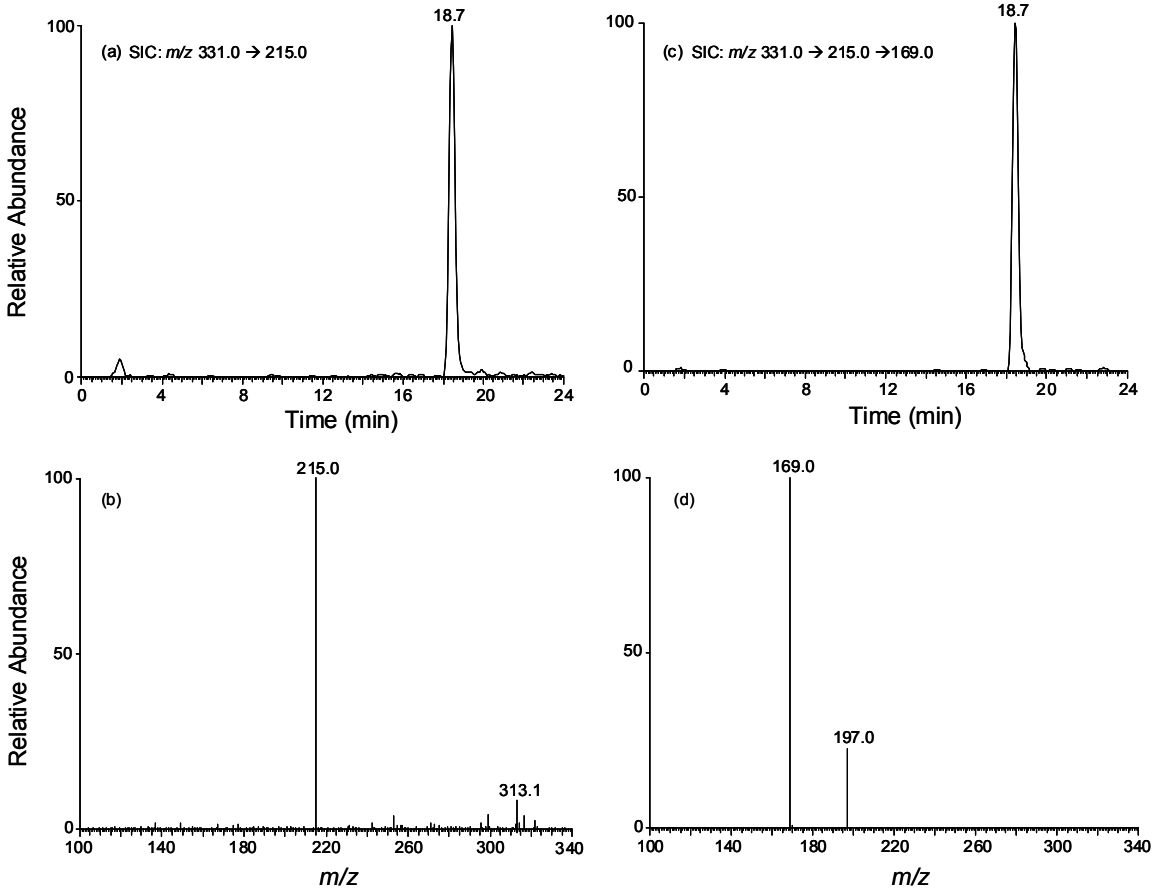

Figure 2.12 Selected-ion chromatograms (SICs) for monitoring *m/z* 331→ 215 (a) and *m/z* 331→ 215→ 169 (c) transitions for [U-$^{15}N_5$]-N^2-CMdG, and the product-ion spectra of the ion of *m/z* 331 (b) and MS^3 spectra of the ion of *m/z* 215 (d).

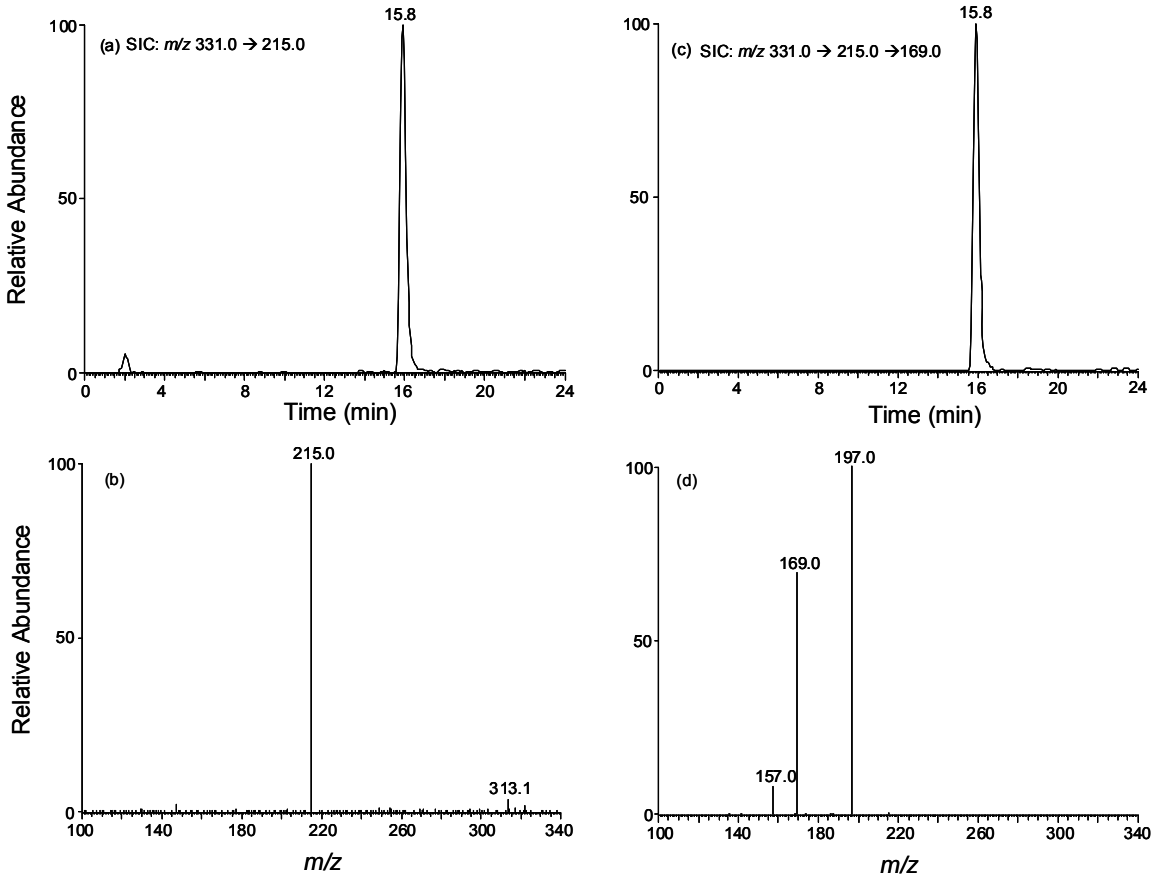

Figure 2.13 Selected-ion chromatograms (SICs) for monitoring the *m/z* 331→ 215 (a) and *m/z* 331→ 215→ 169 (c) transitions for [U-$^{15}N_5$]-1,N^2-glyoxal-dG and the product-ion spectra of the ion of *m/z* 331 (b) and MS^3 spectra of the ion of *m/z* 215 (d).

Our LC-MS/MS/MS quantification results revealed that, under physiological conditions, N^2-CMdG was formed at a frequency of approximately 2 lesions per 10^6 nucleosides in calf thymus DNA treated with 10 μM glyoxal. The level of N^2-CMdG increased from 7 to 134 adducts per 10^6 nucleosides when the concentration of glyoxal increased from 25 to 500 μM (Figure 2.14a). However, this adduct was not detectable in the control calf thymus DNA that was incubated under the same conditions but without the addition of glyoxal, suggesting that, if this adduct is present in calf thymus DNA, it should exist at a level that is lower than 2.8 lesions per 10^8 nucleosides.

We further quantified N^2-CMdG produced in calf thymus DNA upon D-glucose treatment. It turned out that N^2-CMdG could be detected in all DNA samples treated with D-glucose. Treatment of calf thymus DNA with 2, 5, 10, 25 and 50 mM of D-glucose resulted in the formation of N^2-CMdG at levels of 0.32 ± 0.06, 0.50 ± 0.03, 0.68 ± 0.07, 1.8 ± 0.2 and 2.7 ± 0.2 lesions per 10^6 nucleosides, respectively (Figure 2.14b). Thus, the incubation of calf thymus DNA with 25 mM D-glucose induced approximately 3.5-fold more N^2-CMdG, compared to the DNA treated with 5 mM D-glucose. Taken together, N^2-CMdG can be observed in isolated DNA upon exposure to D-glucose or glyoxal, and the adduct formation is dependent on the concentrations of D-glucose and glyoxal.

Quantification of N^2-CMdG in Cultured 293T Human Kidney Epithelial Cells

By using the same LC-ESI-MS^3 coupled with isotope-dilution method, we were able to quantify the formation of N^2-CMdG in genomic DNA isolated from 293T human kidney epithelial cells exposed with glyoxal. LC-MS^3 again revealed unambiguously the

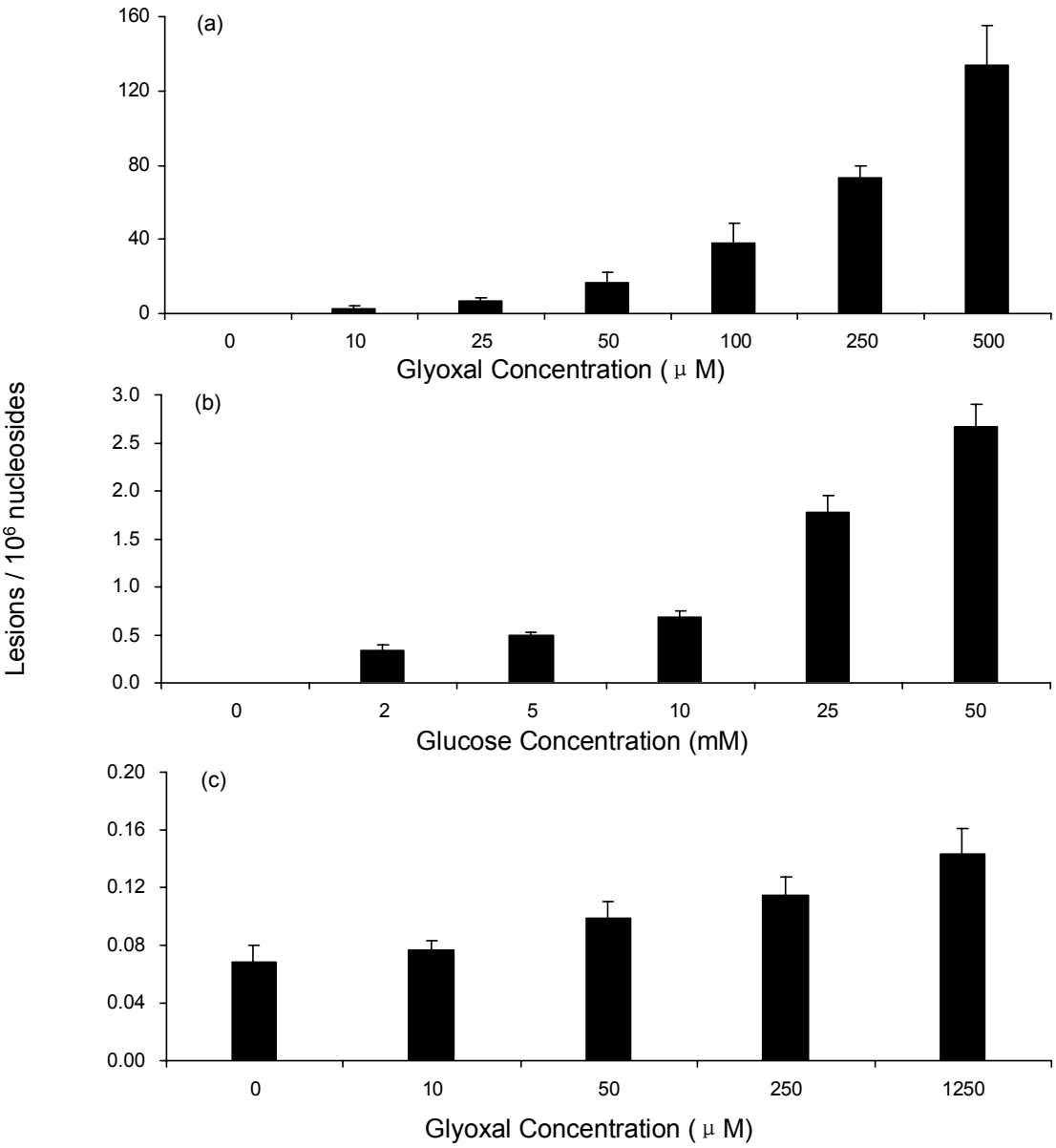

Figure 2.14 The dose-dependent formation of N^2-CMdG in calf thymus DNA, either untreated or treated with glyoxal (a), glucose (b) and in DNA isolated from glyoxal-treated 293T human kidney cells treated with glyoxal(c).

formation of N^2-CMdG in 293T cells upon treatment with glyoxal (Figures 2.15 & 2.16). The quantification results further demonstrated the dose-dependent formation of N^2-CMdG (Figure 2.14c). The yield of N^2-CMdG increased from 0.07 to 0.15 lesions per 10^6 nucleosides when the concentration of glyoxal rose from 10 to 1250 μM. It is of note that N^2-CMdG can be detected in untreated 293T cells at a frequency of approximately 0.07 lesions per 10^6 nucleosides. The much less efficient formation of N^2-CMdG in 293T cells than in calf thymus DNA might be attributed to several factors. First, not all glyoxal added to the medium is uptaken into cells, transported to the nucleus, and reacted with DNA. In addition, the package of DNA in nucleosomes in cells may also result in different frequency of adduct formation compared with isolated calf thymus DNA. Furthermore, DNA adducts in cells can be repaired, whereas those formed in isolated calf thymus DNA are not.

Quantification of N^2-CMdG and N^2-CEdG in Healthy Rat Tissues, Human Buffy Coat Samples, Human Mononuclear CD 34$^-$ Cells, Healthy and Diabetic Mouse Livers

Owing to the presence of the carboxylic moiety in N^2-CEdG and a better sensitivity afforded by positive- than the negative-ion mode, we quantified this adduct by LC-MS in the positive-ion mode where 0.1% formic acid was added to mobile phases to the protonation of the analyte. We monitored the *m/z* 340→224→178 and *m/z* 343→227→181 transitions for the two diastereomers of N^2-CEdG and their D_3-labeled counterparts, respectively. The components eluting at 20.1 and 23.6 min in the SIC of Figure 2.17 were determined to be R-N^2-CEdG and S-N^2-CEdG, respectively, based on

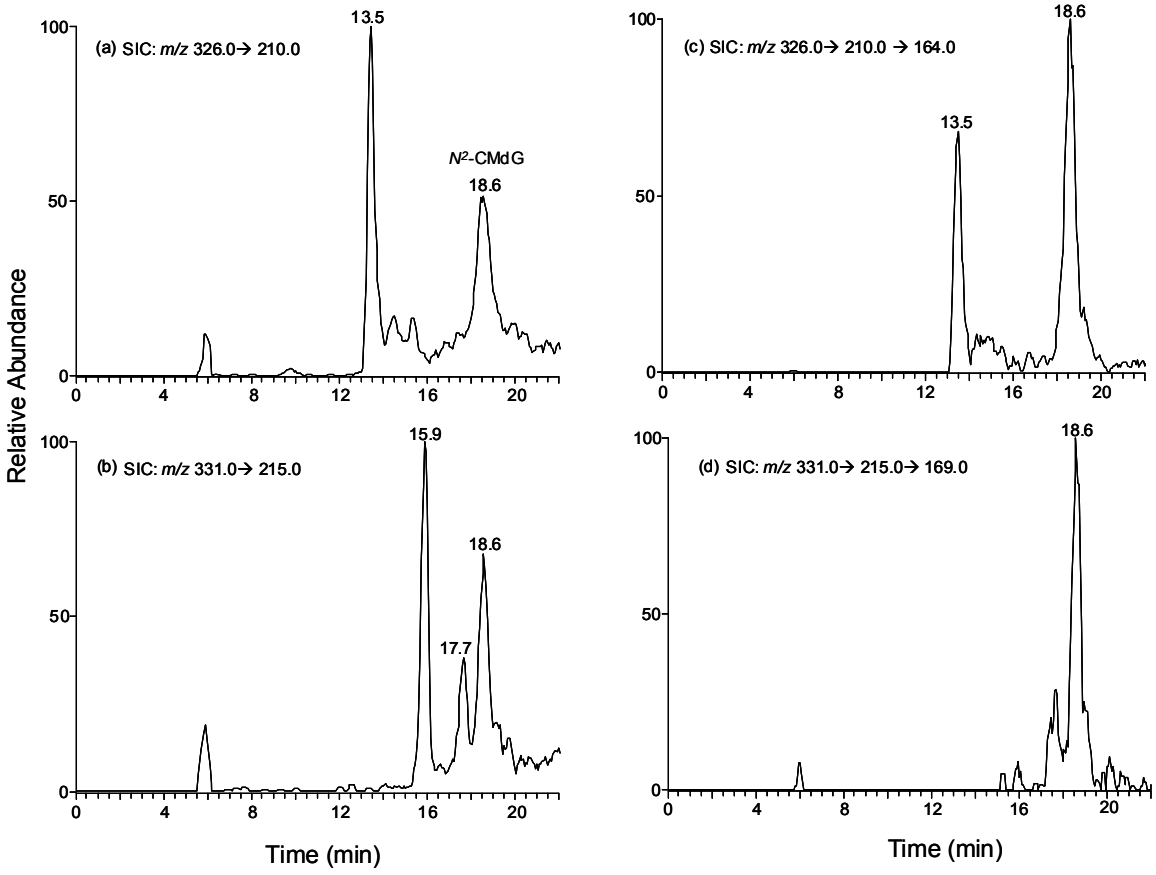

Figure 2.15 Selected-ion chromatograms for monitoring the *m/z* 326→ 210 (a) and *m/z* 326→ 210→ 164 (c) (for unlabeled N^2-CMdG), *m/z* 331→ 215 (b) and *m/z* 331→ 215→ 169 (d) (for [U-$^{15}N_5$]-N^2-CMdG) transitions of the digestion mixtures of the nuclear DNA extracted from 293T cells, which were treated with 50 μM of glyoxal.

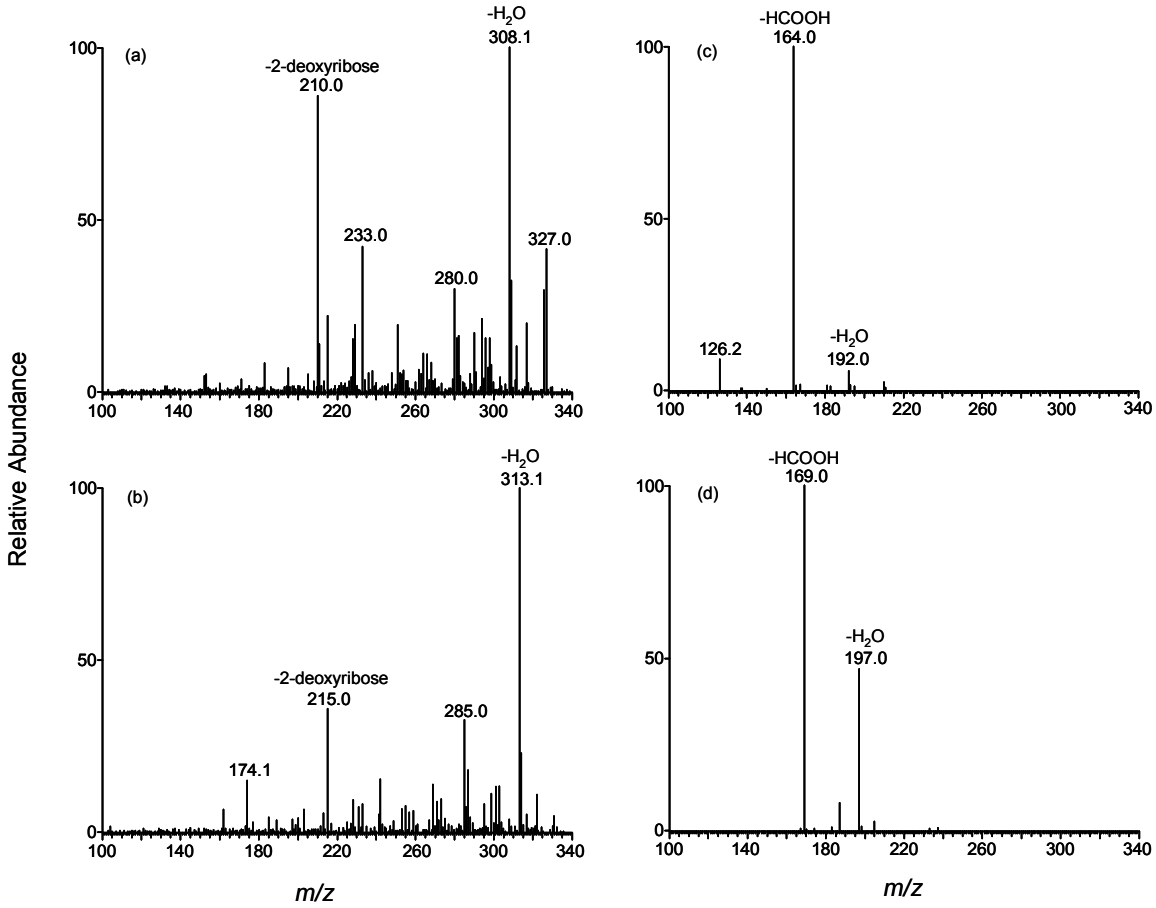

Figure 2.16 Product-ion spectra of the ion *m/z* 326 (a), *m/z* 331 (b) and MS^3 spectra of *m/z* 210 (c), *m/z* 215 (d). Panels (a) and (c) are for unlabeled, and (b) and (d) are for [U-$^{15}N_5$]-N^2-CMdG in the nuclear DNA from 293T cells, respectively.

the same retention time and similar tandem mass spectra as those observed for D_3-N^2-CEdG isomers (MS/MS/MS spectra shown in the inset). In MS^3 spectrum of unlabeled N^2-CEdG, the losses of 18 and 46 Da are attributed to the neutral losses of water and formic acid to gives the ions of *m/z* 206 and 178, respectively.

Our LC-MS/MS/MS quantification results revealed that, the level of N^2-CEdG in M13, G81 and HS35 samples ranged from 0.1-0.4 lesions per 10^6 nucleosides, while N^2-CMdG was not detectable (Figure 2.18a). Among these three samples, M13 and HS35 exhibited similar levels of R- and S-N^2-CEdG, which are higher than those found in G81. However, N^2-CMdG, R- and S-N^2-CEdG could be detected in $CD34^-$ human mononuclear cells (Figure 2.19) as well as the lung, liver, heart and kidney tissues of rats (Figure 2.18b). Different rat tissues displayed different levels of these lesions. More importantly, the formation of these three lesions is found to be significantly higher in liver tissue from mice with Akita diabetes (at frequencies of 2-6 lesions per 10^7 nucleosides), compared to the liver tissues of the control healthy animals (Figure 2.19). Akita diabetes represents a Type-1 diabetic model generated by mutant insulin-2 gene (*156*).

Discussion

Humans are exposed to glyoxal and methylglyoxal from a variety of sources. The exposure of DNA and isolated nucleosides to glyoxal and methylglyxoal facilitated the preferential formation of adducts with dG relative to other nucleosides (*157*). In light of the relatively high yield of 1,N^2-glyoxal-dG adduct, it was proposed that this adduct could be a potential biomarker for the assessment of glyoxal exposure (*30, 151*). Aside

from 1,N^2-glyoxal-dG, two other glyoxal adducts of dG were found to be present in the reaction mixture of glyoxal with calf thymus DNA, i.e., Gx_2-dG and N^2-CMdG (*35*). Among these three adducts, 1,N^2-glyoxal-dG adduct was found to undergo spontaneous decomposition to dG at pH 7.4 and 37°C (*32, 35*). Indeed, our results revealed that, when incubated in PBS buffer at 37°C, more than 70% of 1,N^2-glyoxal-dG could be decomposed to dG within one day. Likewise, the Gx_2-dG was unstable and can be partially transformed to render N^2-CMdG; the same transformation was also observed in single-stranded DNA after prolonged incubation (*35*).

N^2-CMdG, however, is very stable; we found that only 0.43 % of N^2-CMdG was decomposed after a 7-day incubation under the same conditions. Therefore, N^2-CMdG is the only stable adduct formed in calf thymus DNA upon treatment with glyoxal and we only assessed the formation of N^2-CMdG in isolated DNA and cultured human cells. Our data revealed a dose-responsive formation of N^2-CMdG in calf thymus DNA upon glyoxal exposure. The yield of N^2-CMdG increased from 2 to 134 lesions per 10^6 nucleosides when calf thymus DNA was exposed with 10-500 μM of glyoxal (Figure 2.14a).

Under physiological conditions, glucose can undergo degradation to form α-ketoaldehydes including glyoxal, methylglyoxal and 3-deoxyglucosone (*9*). Thus, hyperglycemia may also stimulate the formation of N^2-CMdG in DNA. In this respect, it was observed that the incubation of guanosine with glucose under aerobic conditions at 37 °C for 3 weeks could give rise to N^2-carboxymethyl-guanosine as the major product (*153*).

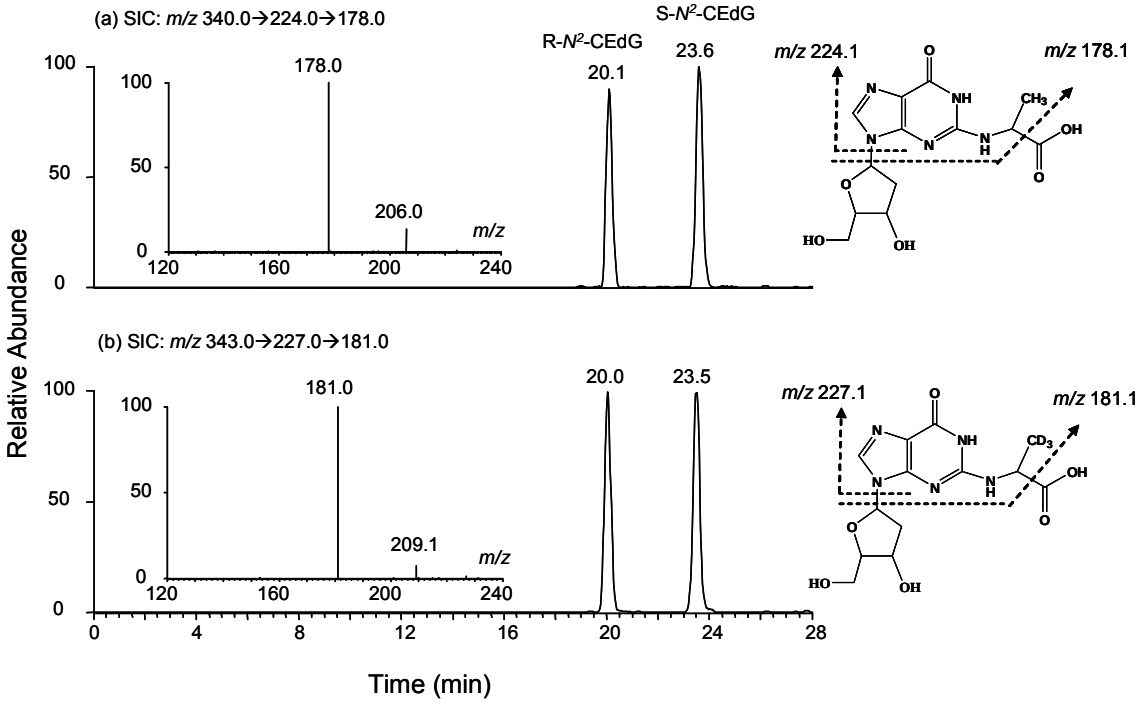

Figure 2.17 Selected-ion chromatograms for monitoring the *m/z* 340→ 224→ 178 (a) and *m/z* 343→ 227→ 181 transitions for unlabeled R-N^2-CEdG, S-N^2-CEdG and [U-$^2H_3$]-R-N^2-CEdG, [U-$^2H_3$]-S-N^2-CEdG in the digestion mixtures of the nuclear DNA from human buffy coat samples. Two insets are MS^3 spectra of the ions of *m/z* 224 (a) and *m/z* 227 (b), respectively.

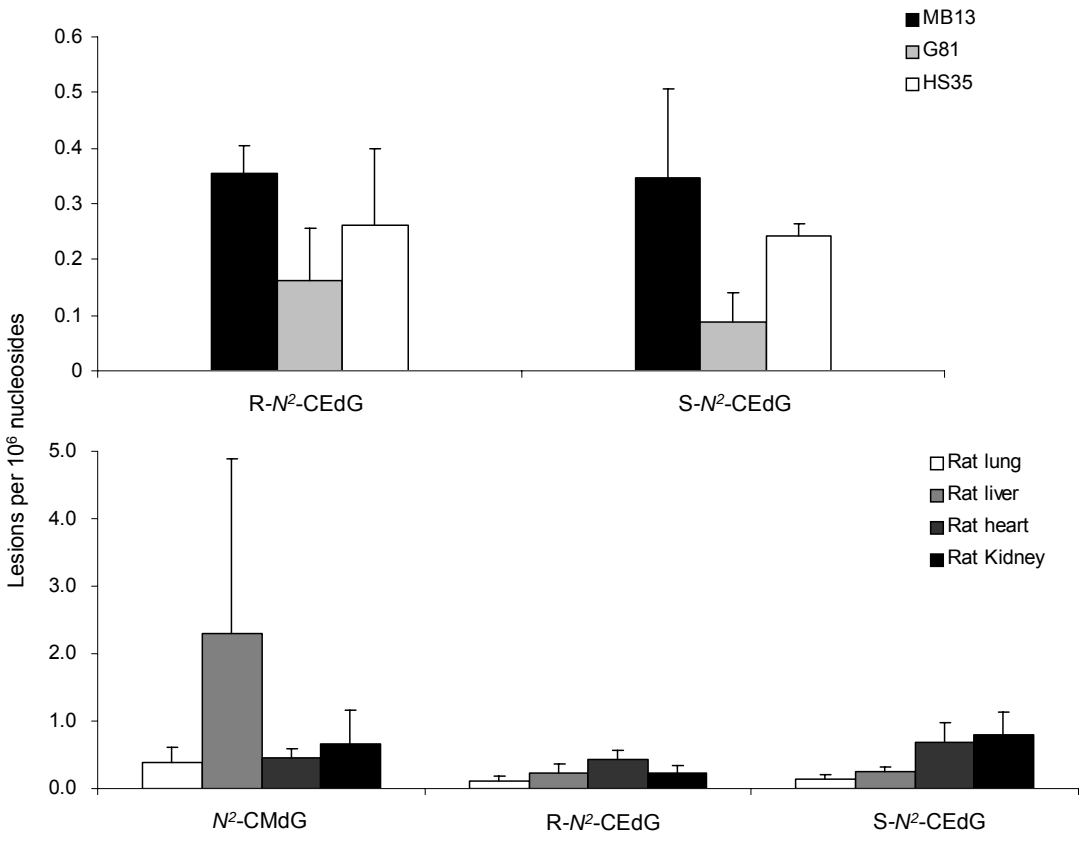

Figure 2.18 Quantification of N^2-CMdG, R-N^2-CEdG and S-N^2-CEdG in human buffy coat samples, lung/liver/heart/kidney of healthy rats. The data represent the means and standard deviations of results from three independent DNA extractions and LC-MS^3 measurements.

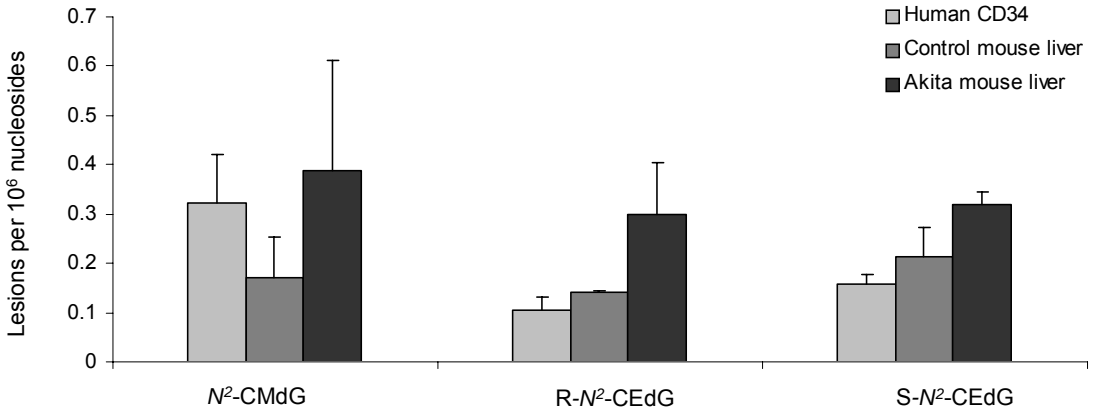

Figure 2.19 Quantification of N^2-CMdG, R-N^2-CEdG and S-N^2-CEdG in $CD34^-$ human mononuclear cells and liver tissues of healthy and Akita diabetic mice. The data represent the means and standard deviations of results from three independent DNA extractions and LC-MS^3 measurements.

We monitored the formation of N^2-CMdG in the reaction mixture where calf thymus DNA was incubated with 2, 5, 10, 25 and 50 mM of D-glucose under physiological conditions for 2 days. It turned out that N^2-CMdG could be detected in all DNA samples exposed to D-glucose. The level of N^2-CMdG in isolated calf thymus DNA treated with 25 mM of glucose was approximately 3.5 fold higher than that in DNA exposed with 5 mM glucose (Figure 2.14b). In this respect, the glucose concentration in blood samples of healthy human subjects is around 3.6-5 mM; however, it can reach up to 30 mM for diabetic patients. Our experimental result, therefore, suggests that hyperglycemia may stimulate the formation of N^2-CMdG in DNA.

To understand the biological implications of N^2-CMdG, it is important to assess its formation in human cells. Along this line, N^2-CEdG, a DNA advanced glycation endproduct induced by methylglyoxal, was found to occur frequently in kidney and aorta cells of diabetic and uremic patients as well as in human breast cancer tissues (*44*, *155*). Exposure of cultured human cells to methylglyoxal or glucose further stimulated the formation of N^2-CEdG (*158*). Here we assessed the formation of N^2-CMdG in 293T human kidney epithelial cells that were either untreated or treated with glyoxal. Our results showed that N^2-CMdG was induced endogenously in 293T cells, and the treatment of these cells with glyoxal further enhanced the formation of N^2-CMdG (Figure 2.14c). It is worth mentioning that we did not quantify the formation of N^2-CMdG in 293T cells treated with D-glucose because of the much lower rate for the formation of this product in calf thymus DNA treated with D-glucose (1.8 adduct per 10^6 normal nucleosides when exposed with 25 mM of D-glucose) than with glyoxal (72 adducts per 10^6 normal

nucleosides when treated with 250 μM of glyoxal) and due to its relatively low rate of formation in 293T cells upon exposure to glyoxal (Figure 2.14).

In light of the above quantification results, we hypothesize that N^2-CMdG and N^2-CEdG may serve as molecular biomarkers for monitoring the progression of diabetes. The level of N^2-CMdG and N^2-CEdG were quantified by the established LC-MS method in different biological samples. Our data indicate that those lesions could be detected in $CD34^-$ human mononuclear cells (Figure 2.19) and the lung, liver, heart and kidney tissues of rats (Figure 2.18b). It is worth noting that the levels of these lesions are significantly higher in diabetic mouse livers compared to the healthy controls (Figure 2.19). To further test our hypothesis, we assessed the levels of N^2-CMdG and N^2-CEdG in human patient buffy coat samples. Owing to the low frequency of formation, N^2-CMdG could not be detected in any of the buffy coat samples; however, both diastereomers of N^2-CEdG could be detected (Figure 2.18a).

Glyoxal exhibits tumor promoting activity on rat glandular stomach carcinogenesis pretreated with *N*-methyl-*N'*-nitro-*N*-nitrosoguanidine (*159*). In addition, glyoxal has been shown to be a potent mutagen in mammalian cells (*160*). The majority of glyoxal-induced mutations was G:C→ T:A followed by G:C→ C:G transversions as well as deletions and frameshift mutations, with 83% of the single-base substitutions occurring at G:C base pairs (*160*). Previous studies demonstrated that methylglyoxal-DNA adducts could induce single strand breaks and high mutation frequencies in *E. coli* cells (*48*) and G:C→ C:G and G:C→ T:A transversions in supF gene in mammalian cells (*161*). The facile formation of N^2-CMdG and N^2-CEdG may

account, in part, for the mutations occurring at G:C site. Future studies on the cytotoxic and mutagenic properties of N^2-CMdG and N^2-CEdG will further illuminate the relationship between glyoxal, methylglyoxal exposure and the risk of cancer development.

References

(1) Muratakamiya, N., Kamiya, H., Iwamoto, N. and Kasai, H. (1995) Formation of a mutagen, glyoxal, from DNA treated with oxygen-free radicals. *Carcinogenesis 16*, 2251-2253.

(2) Moree-Testa, P. and Saint-Jalm, Y. (1981) Determination of [alpha]-dicarbonyl compounds in cigarette smoke. *J. Chromatogr. A 217*, 197.

(3) Nagao, M., Fujita, Y., Wakabayashi, K., Nukaya, H., Kosuge, T. and Sugimura, T. (1986) Mutagens in coffee and other beverages. *Environ. Health Perspect. 67*, 89-91.

(4) Kalapos, M. P. (1999) Methylglyoxal in living organisms - Chemistry, biochemistry, toxicology and biological implications. *Toxicol. Lett. 110*, 145-175.

(5) Phillips, S. A., Mirrlees, D. and Thornalley, P. J. (1993) Modification of the glyoxalase system in streptozotocin-induced diabetic rats - effect of the aldose reductase inhibitor statil. *Biochem. Pharmacol. 46*, 805-811.

(6) Frankel, E. N. (1983) Volatile lipid oxidation-products. *Prog. Lipid Res. 22*, 1-33.

(7) Loidlstahlhofen, A. and Spiteller, G. (1994) Alpha-hydroxyaldehydes, products of lipid-peroxidation. *Biochim. Biophys. Acta. Lipids Lipid Metabol. 1211*, 156-160.

(8) Thornalley, P. J., Langborg, A. and Minhas, H. S. (1999) Formation of glyoxal, methylglyoxal and 3-deoxyglucosone in the glycation of proteins by glucose. *Biochem. J. 344*, 109-116.

(9) Han, Y., Randell, E., Vasdev, S., Gill, V., Gadag, V., Newhook, L. A., Grant, M. and Hagerty, D. (2007) Plasma methylglyoxal and glyoxal are elevated and

related to early membrane alteration in young, complication-free patients with Type 1 diabetes. *Mol. Cell. Biochem. 305*, 123-131.

(10) Lapolla, A., Flamini, R., Vedova, A. D., Senesi, A., Reitano, R., Fedele, D., Basso, E., Seraglia, R. and Traldi, P. (2003) Glyoxal and methylglyoxal levels in diabetic patients: quantitative determination by a new GC/MS method. *Clin. Chem. Lab. Med. 41*, 1166-1173.

(11) Ueda, Y., Miyata, T., Goffin, E., Yoshino, A., Inagi, R., Ishibashi, Y., Izuhara, Y., Saito, A., Kurokawa, K. and de Strihou, C. V. (2000) Effect of dwell time on carbonyl stress using icodextrin and amino acid peritoneal dialysis fluids. *Kidney Int. 58*, 2518-2524.

(12) Raj, D. S. C., Choudhury, D., Welbourne, T. C. and Levi, M. (2000) Advanced glycation end products: A nephrologist's perspective. *Am. J. Kidney Dis. 35*, 365-380.

(13) McLellan, A. C., Thornalley, P. J., Benn, J. and Sonksen, P. H. (1994) Glyoxalase system in clinical diabetes-mellitus and correlation with diabetic complications. *Clin. Sci. 87*, 21-29.

(14) Gao, Y. and Wang, Y. S. (2006) Site-selective modifications of arginine residues in human hemoglobin induced by methylglyoxal. *Biochemistry 45*, 15654-15660.

(15) Oya, T., Hattori, N., Mizuno, Y., Miyata, S., Maeda, S., Osawa, T. and Uchida, K. (1999) Methylglyoxal modification of protein - Chemical and immunochemical characterization of methylglyoxal-arginine adducts. *J. Biol. Chem. 274*, 18492-18502.

(16) Mostafa, A. A., Randell, E. W., Vasdev, S. C., Gill, V. D., Han, Y., Gadag, V., Raouf, A. A. and El Said, H. (2007) Plasma protein advanced glycation end products, carboxymethyl cysteine, and carboxyethyl cysteine, are elevated and related to nephropathy in patients with diabetes. *Mol. Cell. Biochem. 302*, 35-42.

(17) Wang, H. X., Cao, H. C. and Wang, Y. S. (2010) Quantification of N-2-carboxymethyl-2 '-deoxyguanosine in calf thymus DNA and cultured human kidney epithelial cells by capillary high-performance liquid chromatography-tandem mass spectrometry coupled with stable isotope dilution method. *Chem. Res. Toxicol. 23*, 74-81.

(18) Frischmann, M., Bidmon, C., Angerer, J. and Pischetsrieder, M. (2005) Identification of DNA adducts of methylglyoxal. *Chem. Res. Toxicol. 18*, 1586-1592.

(19) Shapiro, R. and Hachmann, H. (1966) Reaction of guanine derivatives with 1,2-dicarbonyl compounds. *Biochemistry 5*, 2799-2807.

(20) Staehelin, M. (1959) Inactivation of virus nucleic acid with glyoxal derivatives. *Biochim. Biophys. Acta 31*, 448-454.

(21) Olsen, R., Molander, P., Ovrebo, S., Ellingsen, D. G., Thorud, S., Thomassen, Y., Lundanes, E., Greibrokk, T., Backman, J., Sjoholm, R. and Kronberg, L. (2005) Reaction of glyoxal with 2 '-deoxyguanosine, 2 '-deoxyadenosine, 2 '-deoxycytidine, cytidine, thymidine, and calf thymus DNA: Identification of DNA adducts. *Chem. Res. Toxicol. 18*, 730-739.

(22) Li, Y. Y., Cohenford, M. A., Dutta, U. and Dain, J. A. (2008) The structural

modification of DNA nucleosides by nonenzymatic glycation: an in vitro study based on the reactions of glyoxal and methylglyoxal with 2 '-deoxyguanosine. *Anal. Bioanal. Chem. 390*, 679-688.

(23) Olsen, R., Ovrebo, S., Thorud, S., Lundanes, E., Thomassen, Y., Greibrokk, T. and Molander, P. (2008) Sensitive determination of a glyoxal-DNA adduct biomarker candidate by column switching capillary liquid chromatography electrospray ionization mass spectrometry. *Analyst 133*, 802-809.

(24) Pluskota-Karwatka, D., Pawlowicz, A. J., Tomas, M. and Kronberg, L. (2008) Formation of adducts in the reaction of glyoxal with 2 '-deoxyguanosine and with calf thymus DNA. *Bioorg. Chem. 36*, 57-64.

(25) Schneider, M., Thoss, G., Hubner-Parajsz, C., Kientsch-Engel, R., Stahl, P. and Pischetsrieder, M. (2004) Determination of glycated nucleobases in human urine by a new monoclonal antibody specific for N-2-carboxyethyl-2 '-deoxyguanosine. *Chem. Res. Toxicol. 17*, 1385-1390.

(26) Cao, H. C., Jiang, Y. and Wang, Y. S. (2007) Stereospecific synthesis and characterization of oligodeoxyribonucleotides containing an N-2-(1-carboxyethyl)-2 '-deoxyguanosine. *J. Am. Chem. Soc. 129*, 12123-12130.

(27) Li, H., Nakamura, S., Miyazaki, S., Morita, T., Suzuki, M., Pischetsrieder, M. and Niwa, T. (2006) N-2-carboxyethyl-2 '-deoxyguanosine, a DNA glycation marker, in kidneys and aortas of diabetic and uremic patients. *Kidney Int. 69*, 388-392.

(28) Seidel, W. and Pischetsrieder, M. (1998) Reaction of guanosine with glucose under oxidative conditions. *Bioorg. Med. Chem. Lett. 8*, 2017-2022.

(29) Hong, H. Z. and Wang, Y. S. (2005) Formation of intrastrand cross-link products between cytosine and adenine from UV irradiation of d((Br)CA) and duplex DNA containing a 5-bromocytosine. *J. Am. Chem. Soc. 127*, 13969-13977.

(30) Synold, T., Xi, B. X., Wuenschell, G. E., Tamae, D., Figarola, J. L., Rahbar, S. and Termini, J. (2008) Advanced glycation end products of DNA: quantification of N-2-(1-carboxyethyl)-2 '-deoxyguanosine in biological samples by liquid chromatography electrospray ionization tandem mass spectrometry. *Chem. Res. Toxicol. 21*, 2148-2155.

(31) Bugger, H., Boudina, S., Hu, X. X., Tuinei, J., Zaha, V. G., Theobald, H. A., Yun, U. J., McQueen, A. P., Wayment, B., Litwin, S. E. and Abel, E. D. (2008) Type 1 diabetic Akita mouse hearts are insulin sensitive but manifest structurally abnormal mitochondria that remain coupled despite increased uncoupling protein 3. *Diabetes 57*, 2924-2932.

(32) Dutta, U., Cohenford, M. A. and Dain, J. A. (2005) Nonenzymatic glycation of DNA nucleosides with reducing sugars. *Anal. Biochem. 345*, 171-180.

(33) Kasai, H., Iwamoto-Tanaka, N. and Fukada, S. (1998) DNA modifications by the mutagen glyoxal: adduction to G and C, deamination of C and GC and GA cross-linking. *Carcinogenesis 19*, 1459-1465.

(34) Yuan, B., Cao, H., Jiang, Y., Hong, H. and Wang, Y. (2008) Efficient and accurate bypass of N^2-(1-carboxyethyl)-2'-deoxyguanosine by DinB DNA polymerase *in vitro* and *in vivo*. *Proc. Natl. Acad. Sci. USA 105*, 8679-8684.

(35) Takahashi, M., Okamiya, H., Furukawa, F., Toyoda, K., Sato, H., Imaida, K. and

Hayashi, Y. (1989) Effects of glyoxal and methylglyoxal administration on gastric carcinogenesis in wistar rats after initiation with N-methyl-N'-nitro-N-nitrosoguanidine. *Carcinogenesis 10*, 1925-1927.

(36) MurataKamiya, N., Kamiya, H., Kaji, H. and Kasai, H. (1997) Glyoxal, a major product of DNA oxidation, induces mutations at G:C sites on a shuttle vector plasmid replicated in mammalian cells. *Nucleic Acids Res. 25*, 1897-1902.

(37) Pischetsrieder, M., Seidel, W., Munch, G. and Schinzel, R. (1999) N-2-(1-carboxyethyl)deoxyguanosine, a nonenzymatic glycation adduct of DNA, induces single-strand breaks and increases mutation frequencies. *Biochem. Biophys. Res. Commun. 264*, 544-549.

(38) Murata-Kamiya, N., Kamiya, H., Kaji, H. and Kasai, H. (2000) Methylglyoxal induces G: C to C: G and G: C to T: A transversions in the supF gene on a shuttle vector plasmid replicated in mammalian cells. *Mutat. Res. 468*, 173-182.

CHAPTER 3

Investigating the Effect of 6-Thioguanine on the Cytosine Methylation *In-Vitro* and *In-Vivo*

Introduction

Thiopurine drugs, which include 6-thioguanine (^{S}G) and 6-mercaptopurine (Scheme 1), are commonly used for the treatment of acute lymphoblastic leukemia, inflammatory bowl disease, autoimmune hepatitis and other pathological conditions (*52, 53*). Azathioprine (Scheme 3.1), which is converted to 6-mercaptopurine *in vivo*, is a standard immunosuppressant prescribed to prevent graft rejection in organ transplant patients (*52*). Although the exact mechanisms underlying the cytotoxic effects of these thiopurines remain elusive, it is known that the activation of the thiopurine drugs requires the formation of thioguanine nucleotides and their incorporation into nucleic acids (*52*).

Compared to guanine, the increased chemical reactivity of 6-thioguanine may contribute to the cytotoxic effects of the thiopurine drugs. After being incorporated into DNA, 6-thioguanine can be methylated by *S*-adenosyl-L-methionine (*S*-AdoMet) to form S^6-methylthioguanine (S^6mG) (*73*) or oxidized to guanine-S^6-sulfonic acid (^{SO3H}G) upon exposure to UVA light (*74*). Both S^6mG and ^{SO3H}G exhibit considerable miscoding properties (*73-76*), and a recent replication study with single-stranded M13 shuttle vector demonstrated that, in *E. coli* cells, these two modified nucleosides could lead to G→A transition at frequencies of 94% and 77%, respectively (*77*). The S^6mG:T base pairs arising from DNA replication can trigger the post-replicative mismatch repair system (*73,*

162), which may account for the cytotoxicity of the thiopurine drugs. Moreover, our recent replication experiments showed that 6-thioguanine is mutagenic in *E. coli* cells, and it can give rise to G→A transition mutation at a frequency of ~11%, raising the possibility that the replication-produced ^{S}G:T base pair may trigger directly the post-replicative mismatch repair pathway (*77*) .

DNA methylation occurs in the genomes of diverse organisms and, in higher eukaryotes, methylation of cytosine occurs predominantly at CpG dinucleotide sites in the promoter and initial exons of genes (*84*). In this respect, each protein revealed by biochemical experiments to be involved in the establishment, maintenance, or interpretation of genomic methylation pattern in mammals is encoded by an essential gene, underscoring the biological importance of CpG methylation (*87*). In human cells, the CpG methylation pattern is established and maintained by DNA (cytosine-5)-methyltransferases (*87*). In addition, a family of human proteins exhibit high binding affinity to DNA sequences bearing the methylated CpG dinucleotide (*80*); upon binding to methylated DNA, these methyl-CpG binding proteins may further recruit histone-modifying enzymes to promote chromatin condensation and gene silencing (*88*).

Previous studies revealed that the covalent modifications of nucleobases at CpG dinucleotide site could perturb cytosine methylation by DNA methyltransferases. In this context, earlier studies showed that the replacement of the guanine residue at CpG site with an 8-oxo-7,8-dihydroguanine (8-oxoG) resulted in diminished methylation of its 5' neighboring cytosine catalyzed by DNA methyltransferases; the substitution of guanine at methylated CpG site with an 8-oxoG or O^6-methylguanine (O^6mG), however, enhanced

the methylation of the opposing cytosine in the complementary strand (*92, 93, 163, 164*). Furthermore, Subach *et al.* (*94*) showed that benzo[*a*]pyrene (B[*a*]P) guanine adduct (+)-*trans*-B[*a*]P-N^2-dG inhibited the binding and the methylation by both SssI and HhaI methyltransferases. However, the isomeric (+)-*cis*-B[*a*]P-N^2-dG adduct allowed for normal binding of methyltransferases and did not result in apparent change in methylation efficiencies. On the other hand, Sowers and coworkers (*95*) demonstrated recently that 5-chlorocytosine or 5-bromocytosine present at the CpG dinucleotide site behaves like a 5-methylcytosine and directs the methylation of the opposing cytosine residue in the complementary strand.

Previous studies also revealed that the presence of a 6-thioguanine in DNA can perturb a number of enzymatic reactions including T4 DNA ligase-mediated DNA ligation (*165*), RNase H-induced cleavage of DNA/RNA heteroduplexes (*57*), and topoisomerase II-catalyzed DNA cleavage (*166*). In light of these previous findings, we reason that the replacement of the guanine residue at CpG site with a 6-thioguanine may interfere with CpG methylation by DNA methyltransferases, thereby perturbing the epigenetic pathways of gene regulation. As a first step toward testing this hypothesis, we developed an LC-MS/MS method and examined how 6-thioguanine in DNA affects the methylation of cytosine residues at CpG site by two DNA methyltransferases, i.e., the bacterial *Hpa*II methylase and human DNMT1. *Hpa*II methylates the internal cytosine residue at unmethylated or hemimethylated CCGG site (*167*), and DNMT1 methylates preferentially the cytosine residue at hemi-methylated CpG site (*168*). Our results revealed that the presence of a 6-thioguanine at CpG site could indeed perturb the

cytosine methylation mediated by the two methyltransferases, and the perturbation is dependent on both the nature of the methyltransferase and the location of ^{S}G with respect to the cytosine to be methylated. Moreover, we showed that the treatment of Jurkat T, HL-60, CCRF-CEM, K-562 cells with 6-thioguanine could lead to an appreciable drop in the level of global cytosine methylation. Together, our results support that the thiopurine drugs may exert their cytotoxic effects by perturbing the epigenetic pathway of gene regulation.

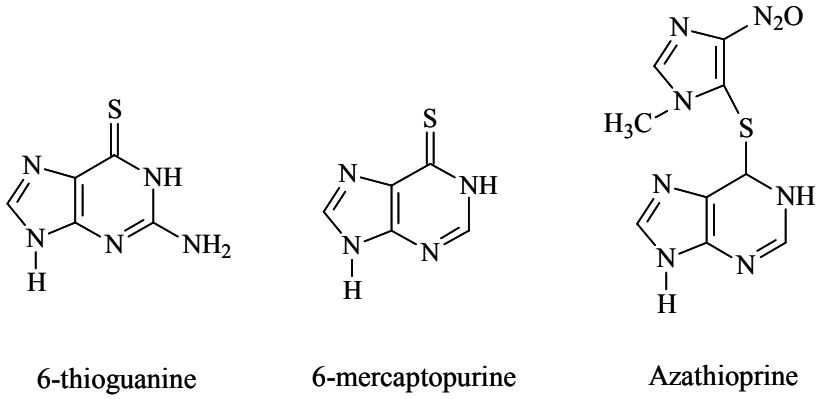

Scheme 3.1 Chemical structures of 6-thioguanine, 6-mercaptopurine and azathioprine.

Experimental Procedures

Chemicals and Enzymes

All chemicals and enzymes, unless otherwise noted, were obtained from Sigma-Aldrich (St. Louis, MO). Reagents for solid-phase DNA synthesis were obtained from Glen Research (Sterling, VA, USA). Unmodified oligodeoxynucleotides (ODNs) used in this study were purchased from Integrated DNA Technologies (Coralville, IA). Human maintenance DNA methyltransferase DNMT1, *Hpa*II methylase, BciVI and uracil-DNA glycosylase (UDG) were from New England Biolabs (Ipswich, WA). Jurkat T (Clone E6-1) acute lymphoblastic leukemia cells, penicillin, streptomycin, and RPMI-1640 media were purchased from ATCC (Manassas, VA, USA).

Preparation of ODN Substrates Containing 6-Thioguanine and 5-Methylcytosine

ODNs containing ^{S}G and 5-methylcytosine (^{m}C) were synthesized on a Beckman Oligo 1000S DNA synthesizer (Fullerton, CA) at 1-μmol scale. After solid-phase synthesis, the controlled pore glass support was treated with 1.0 M DBU (1,8-diazabicyclo[5.4.0]undec-7-ene) in anhydrous acetonitrile at room temperature for 5 hrs to remove the cyanoethyl protecting group on the thionucleoside. The solid support was subsequently treated with 50 mM NaSH in concentrated NH_4OH solution at room temperature for 24 hrs to complete the deprotection. The synthesized 15mer ODNs, i.e., d(ACC^{m}C^{S}GGTGACACACC) and d(ACC^{m}CG^{S}GTGACACACC), were purified by HPLC and their identities were confirmed by electrospray ionization-mass spectrometry (ESI-MS) and tandem MS (MS/MS) measurements. Likewise, we synthesized and

characterized the 24-mer ^{S}G-bearing ODNs (the top strands for Substrates **2** and **3**, Table 3.1).

The above 15-mer ^{S}G-bearing ODNs were ligated with d(TGGCAGGTATCCAGT) in the presence of template DNA to afford d(TGGCAGGTATCCAGTACC^{m}CXYTGACACACC) ("XY" represents ^{S}GG and G^{S}G in the top strand for Substrates **5** and **6**, respectively. Table 3.1). The ligation reaction was performed at 16 °C overnight with 5 nmol each of the above two ODNs along with the template DNA and 1200 units of T4 DNA ligase in a buffer containing 50 mM Tris-HCl (pH 7.5), 10 mM $MgCl_2$, 10 mM DTT, 1 mM ATP and 25 μg/mL BSA. The ligation products were purified by employing 15%, 1:19 cross-linked polyacrylamide gels containing 8 M urea. The substrates were then isolated from the gel and desalted by ethanol precipitation. The purity of the resulting ODNs was confirmed by polyacrylamide gel electrophoresis (PAGE) analysis and their identities were verified by ESI-MS and MS/MS.

HPLC

The ODNs were purified on a Beckman HPLC system with pump module 125 and a UV detector (module 126). A 4.6 × 250 mm Apollo C18 column (5 μm in particle size and 300 Å in pore size, Alltech Associate Inc., Deerfield, IL) was used. Triethylammonium acetate (TEAA, 50 mM, pH 6.6, Solution A) and a mixture of 50 mM TEAA and acetonitrile (70/30, v/v, Solution B) were employed as mobile phases. The flow rate was 0.8 mL/min. A gradient of 0-20% B in 5 min, 20-45% B in 40 min, and

45-100% B in 5 min was employed for the separation. The purified ODNs were desalted on the same HPLC system with H_2O as mobile phase A and acetonitrile as mobile phase B, and a gradient of 0% B in 20 min, 0-50% B in 5 min, and 50% B in 25 min was used.

Methylation of Cytosine Residues in Duplex DNA by DNMT1 and HpaII

Each of the six double-stranded DNA substrates listed in Table 1 was annealed in the DNMT1 reaction buffer, which contained 50 mM Tris-HCl, 1 mM EDTA, 1 mM dithiothreitol (DTT), and 5% glycerol. The resulting hemimethylated duplex DNA (10 pmol) was incubated with DNMT1 (3 units) in the presence of *S*-AdoMet (20 nmol) at 37°C for 1, 2 and 4 hrs. The enzyme was subsequently inactivated by heating at 65°C for 20 min and removed by chloroform extraction. The aqueous layer was dried by using a Savant Speed-Vac (Thermo Savant Inc., Holbrook, NY, USA).

For the *Hpa*II-mediated methylation, ODNs were hybridized in the reaction buffer supplied by the vendor, which contained 50 mM Tris-HCl (pH 7.5), 10 mM EDTA, and 5 mM β-mercaptoethanol. To the annealed duplex solution (10 pmol) were added *Hpa*II (4 units) and *S*-AdoMet (4.8 nmol), and the reaction mixture was incubated at 37 °C for 10, 20, 40 and 60 min. *Hpa*II was subsequently inactivated by heating the solution to 70°C for 15 min and removed by chloroform extraction, and the aqueous layer was dried.

BciVI Digestion

The dried residues obtained from the above methylation reactions were redissolved in doubly distilled water and incubated with 1 unit of BciVI in a buffer

containing 50 mM potassium acetate, 20 mM Tris-acetate, 10 mM magnesium acetate and 1 mM DTT at 37°C for 1 hr. The BciVI was inactivated by heating at 65°C for 20 min and removed by chloroform extraction. The reaction mixture was dried by using Savant Speed-Vac and reconstituted in doubly distilled water for LC-MS/MS analysis. After the above restriction cleavage, the DNA fragments of interest were liberated as 6- (for Substrates **1**-**3**) or 7-mer ODNs (for Substrates **4**-**6**), which were subjected to LC-MS/MS analysis for the identification and quantification of cytosine methylation.

UDG Digestion

Some methylation reaction mixtures were also treated with UDG to produce short ODNs for the LC-MS measurements. In this respect, the products arising from the 10-pmol methylation reaction was treated with UDG (~0.4 unit) in a buffer containing 20 mM Tris-HCl (pH 8.0), 1 mM DTT and 1 mM EDTA at 37°C for 4 hrs. The UDG cleavage reaction mixture was quenched by adding piperidine until its final concentration reached 0.25 M. The resulting solution was incubated at 60°C for 1 hr to induce DNA strand cleavage at the UDG-produced abasic site. The mixture was extracted with chloroform to remove the UDG and the aqueous layer was dried. The dried residues were redissolved in water for LC-MS/MS analysis.

During the course of the study, we noted that the 6-thioguanine-bearing ODN was partially degraded during the UDG digestion and the subsequent hot piperidine treatment, which affected the measurement of the methylation level of cytosine residue that is situated in the same strand as ^{S}G. However, the UDG digestion does not affect the

Table 3.1 Substrates employed for the *in-vitro* methylation assay.

5′-TGG CAG GTA TCC AGU ACC C XY TGA-3′ 3′-ACC GTC CAT AGG TCA TGG G^{m}CC ACT-5′	**1.** XY=GG **2.** XY=^{S}GG **3.** XY=G^{S}G
5′-TGG CAG GTA TCC AGT ACC ^{m}CXY TGA CAC ACC-3′ 3′-ACC GTC CAT AGG TCA UGG GCC ACT-5′	**4.** XY=GG **5.** XY=^{S}GG **6.** XY=G^{S}G

measurement of the methylation of cytosine that is in the opposite strand with respect to ^{S}G. Most data were obtained from the cleavage with BciVI.

During the course of the study, we noted that the 6-thioguanine-bearing ODN was partially degraded during the UDG digestion and the subsequent hot piperidine treatment, which affected the measurement of the methylation level of cytosine residue that is situated in the same strand as ^{S}G. However, the UDG digestion does not affect the measurement of the methylation of cytosine that is in the opposite strand with respect to ^{S}G. Most data were obtained from the cleavage with BciVI.

LC-MS/MS Analysis and Data Processing

The extent of cytosine methylation in synthetic duplex DNA was quantified by on-line LC-MS/MS experiments, which were carried out using an Agilent 1100 capillary HPLC pump (Agilent Technologies, Palo Alto, CA) and an LTQ linear ion-trap mass spectrometer (Thermo Electro Inc., San Jose, CA). A 0.5 × 150 mm Zorbax SB-C18 column (particle size 5 μm, Agilent Technologies) was used for the separation of ODNs after the restriction enzyme digestion, and the flow rate was 6.0 μL/min. A gradient of 5 min of 0-20% methanol followed by a 35 min of 20-50% methanol in 400 mM 1,1,1,3,3,3-hexafluoroisopropanol (HFIP, pH was adjusted to 7.0 by addition of triethylamine) was employed (*169*). The voltage for electrospray was 4.0 kV, and the ion transport tube of the mass spectrometer was maintained at 300°C to minimize the formation of HFIP adducts of ODNs.

The specific precursor ions for the methylated and unmethylated sequences were chosen for fragmentation to acquire the tandem mass spectra. The integrated peak areas (IAs), which were found in the selected-ion chromatogram (SIC) plotted for the formation of three abundant fragment ions of the ODNs containing a methylated and unmethylated cytosine at CpG site, were used to calculate the percentage of methylation:

$$\textit{Methylation percentage (\%)} = \frac{IA(methylated)}{IA(methylated) + IA(unmethylated)} \times 100\%$$

Cell Culture, Drug Treatment, and DNA Isolation

Jurkat T, HL-60, CCRF-CEM, K-562 and HCT-116 cells were cultured separately in ATCC recommended media with 10% (v/v) fetal bovine serum (FBS) at 37°C in a 5% CO_2 atmosphere. When the confluence level of the cells reached about 60%, the old media were removed and the cells were cultured, for 24 hrs, in fresh media alone (served as control) or in the same media containing 6-thioguanine (1 or 3 μM) or 5-aza-2'-deoxycytidine (5-aza-dC, 5 μM).

DNA Isolation

The above drug- or mock-treated cells (~2×10^7 cells) were harvested by centrifugation, and the cell pellets were washed with phosphate buffered saline (PBS) and resuspended in a lysis buffer containing 10 mM Tris-HCl (pH 8.0), 0.1 M EDTA, and 0.5% SDS. The cell lysates were then treated with 20 μg/mL of RNase A at 37°C for 1 hr and subsequently with 100 μg/mL of proteinase K at 50°C for 3 hrs. Genomic DNA was

isolated by extraction with phenol/chloroform/isoamyl alcohol (25:24:1, v/v) and desalted by ethanol precipitation. The DNA pellet was redissolved in water and its concentration was measured by UV absorbance at 260 nm.

DNA Digestion and HPLC Quantification of Global Cytosine Methylation

The above cellular DNA (50 μg) was denatured by heating to 95°C and chilled immediately on ice. The denatured DNA was subsequently digested with 2 units of nuclease P1 and 0.008 unit of calf spleen phosphodiesterase in a buffer containing 30 mM sodium acetate (pH 5.5) and 1 mM zinc acetate at 37°C for 4 hrs. To the digestion mixture were then added 12.5 units of alkaline phosphatase and 0.05 unit of snake venom phosphodiesterase in a 50-mM Tris-HCl buffer (pH 8.6). The digestion was continued at 37°C for 3 hrs, and the enzymes were removed by chloroform extraction. The aqueous DNA layer was dried by using a Speed-vac and the dried DNA was redissolved in water. The amount of nucleosides in the mixture was quantified by UV absorbance measurements.

The above digested nucleoside mixtures were separated by HPLC on an Agilent 1100 capillary pump (Agilent Technologies, Palo Alto, CA) with a UV detector monitoring at 260 nm and a Peak Simple Chromatography Data System (SRI Instruments Inc., Las Vegas, NV, USA). A 4.6×250 mm Polaris C18 column (5 μm in particle size, Varian Inc., Palo Alto, CA) was used for the separation of the enzymatic digestion mixture. A solution of 10 mM ammonium formate (pH 6.3, solution A) and a mixture of 10 mM ammonium formate and acetonitrile (70:30, v/v, solution B) were employed as

mobile phases. A gradient of 5 min 0-4%B, 40 min 4-30% B and 5 min 30-100% B was employed, and the flow rate was 0.80 mL/min. Under these conditions, we were able to resolve 5-methyl-2'-deoxycytidine (5-mdC) from other nucleosides. The global methylation in cells was quantified based on the peak areas of 5-mdC and 2'-deoxycytidine (dC) with the consideration of the extinction coefficients of the two nucleosides at 260 nm (5020 and 7250 L mol^{-1} cm^{-1} for 5-mdC and dC, respectively).

The identities and purities of the nucleosides were assessed by LC-MS/MS under the same conditions as described above for the analysis of the methylation reaction mixtures except that different mobile phases and gradient were used (Figure 3.1). In this respect, 0.1% formic acid in water and 0.1% formic acid in methanol were employed as mobile phases A and B, respectively, and a gradient of 0-20% B in 5 min followed by 20-45% B in 35 min was employed.

Results

Although it is known that the DNA 6-thioguanine is the ultimate metabolite for the thiopurine drugs to exert their cytotoxic effects (*52*), the molecular mechanisms through which the DNA 6-thioguanine results in cell death remain not very clear. In light of the previous findings that the chemical modifications of cytosine and guanine residues at CpG dinucleotide site can perturb the enzymatic methylation of cytosine at this site (*92-95, 163, 164*), we postulate that the incorporation of ^{S}G into DNA may perturb the epigenetic pathway of gene regulation by altering the DNA methyltransferase-mediated cytosine methylation. To test this hypothesis, we set out to assess how the presence of

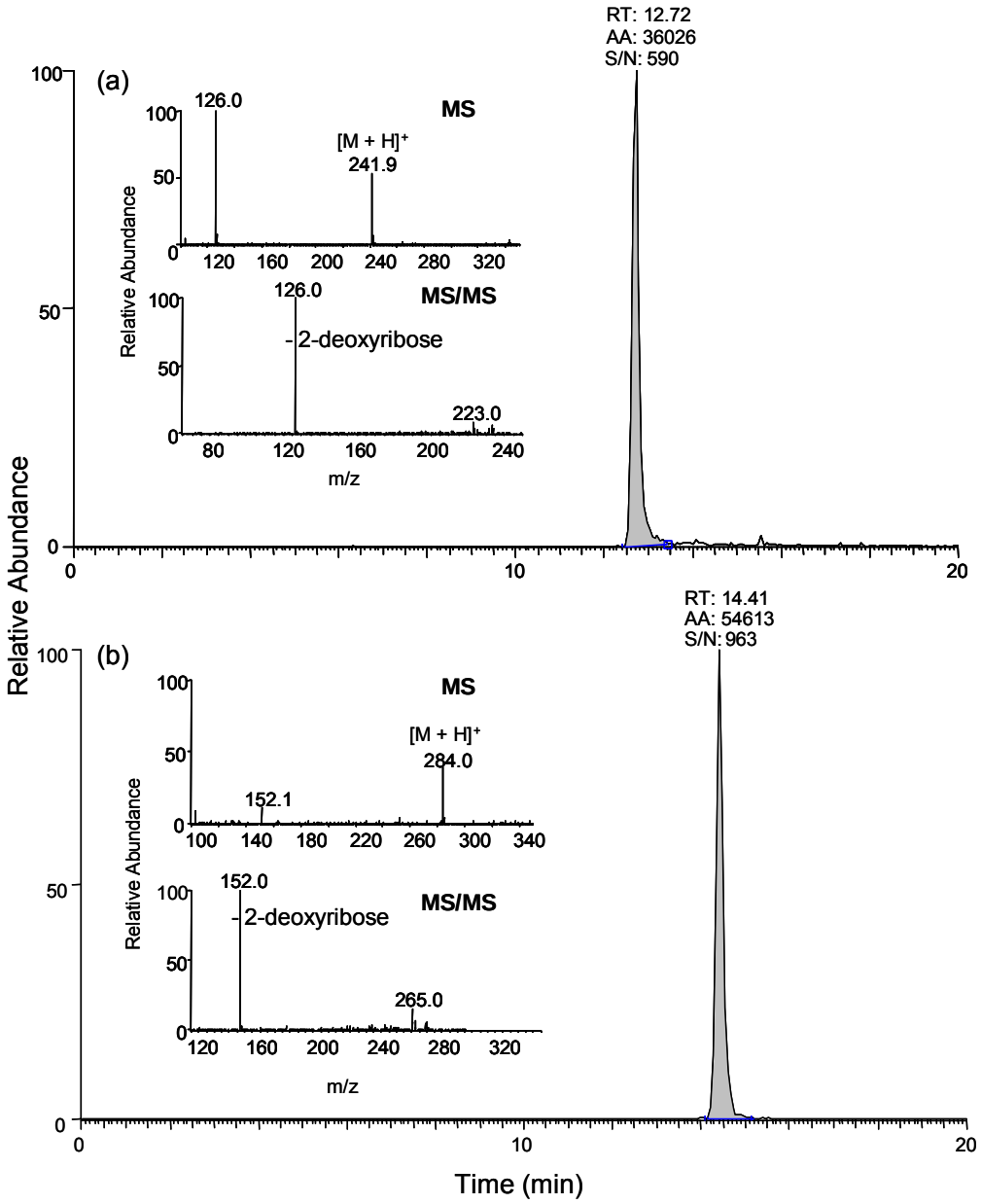

Figure 3.1 LC-MS/MS analyses of the 5-mdC (a) and guanosine (G, b) fractions. Shown are the extracted-ion chromatograms for the $[M + H]^+$ ions of 5-mdC (a) and G (b). Shown in the insets are the MS and MS/MS (for the $[M + H]^+$ ions of the two nucleosides). We also monitored the formation of other canonical ribonucleosides and 2'-deoxyribonucleosides; except for the presence of trace amounts of 5-mdC in the G fraction (<2%) and trace amount of G in the 5-mdC fraction (<2%), other nucleosides were not detectable.

6-thioguanine in synthetic duplex DNA affects the methylation of cytosine residues by purified DNA methyltransferases including human DNMT1 and bacterial *Hpa*II methylase.

Preparation of ODNs Containing 6-Thioguanine and 5-Methylcytosine

To assess how the presence of 6-thioguanine perturbs the methylation of cytosine residues at CpG sites by DNA methyltransferases, we designed two sets of DNA substrates. The first set has three substrates where the bottom strand contains a $C^{m}CGG$ sequence motif and the top strand carries CCGG, $CC^{S}GG$ or $CCG^{S}G$ (Substrates **1-3** in Table 3.1). These three substrates allow us to investigate how the presence of ^{S}G at CCGG site affects the methylation of the internal cytosine at this site in the same strand. The second set has another three substrates where the bottom strand bears CCGG sequence motif and the top strand contains $C^{m}CGG$, $C^{m}C^{S}GG$, or $C^{m}CG^{S}G$ (Substrates **4-6** in Table 3.1). These three substrates facilitate us to ask how the existence of ^{S}G in the methylated strand perturbs the methylation of the internal cytosine at CCGG site in the opposite strand.

It is worth noting that the top strands of Substrates **4, 5** and **6** were designed originally for protein binding assays, and it turned out to be somewhat difficult to assess, by using LC-MS/MS, the level of methylation in the bottom strand if the 30-mer duplex DNA was used. Thus, we chose to employ a 24mer bottom strand for the methylation experiments. We compared the DNMT1-mediated methylation of Substrate **4** with the corresponding substrate where the top strand does not carry the 6-nucleotide overhang.

Our results showed that these two substrates exhibited no significant difference toward the DNMT1-mediated methylation (Data not shown).

LC-MS/MS Analysis of Cytosine Methylation at CpG Site in ODNs

Figure 3.2 illustrates the method that we employed for examining the effect of 6-thioguanine on the methylation of cytosine at CpG site. In this context, the substrates carry a unique BciVI recognition site, thereby enabling the cleavage of the bottom initially methylated strand to two ODNs, e.g., d(TCAC^{m}CGG) and d(pGTACTGGATACCTGCCA) for Substrate **1**. The corresponding cleavage of the top strand in Substrate **1** renders d(TGGCAGGTATCCAGUACC) and d(pCGGTGA), where the underlined "C" can be methylated or unmethylated.

Indeed LC-MS/MS analysis of the BciVI cleavage products of the methylation reaction mixture of Substrate **1** showed the elution of the short 6- and 7-mer ODNs at ~23 min, and the long 17- and 18-mer ODNs at ~29 min (Figure 3.3). In this respect, the 6-mer methylated product d(p^{m}CGGTGA) and its unmethylated counterpart, i.e., d(pCGGTGA), eluted at 23.2 min and 22.9 min, respectively (Figure 3.4a&b). The identities of the BciVI-produced ODNs were confirmed by MS/MS analysis. For instance, the product-ion spectra of the $[M - 2H]^{2-}$ ions of the 6-mer ODNs (Figure 3.4c&d) showed the formation of w_n ions, that is, the w_1, w_2, w_3, w_4, and w_5, and [a_n-Base] ions, namely, the [a_2-G], [a_3-G] and [a_5-G] ions [Nomenclature for fragment ions follows that described by McLuckey *et al.* (*118*). "A", "G", and "C" represent adenine, guanine and cytosine, respectively]. The [a_2-G], [a_3-G] and [a_5-G] ions of d(p^{m}CGGTGA) exhibited

14 Da higher in mass than the corresponding fragments formed from the unmethylated d(pCGGTGA). The MS/MS results clearly support the methylation of cytosine residue at CpG site (Figure 3.4c&d).

The LC-MS/MS analysis combined with BciVI digestion also allowed for the monitoring of the methylation of other DNA substrates listed in Table 3.1, and example LC-MS/MS results are shown in Figures 3.5&3.6. In this context, it is worth emphasizing that our LC-MS/MS results revealed only the expected BciVI cleavage products; no other products could be detected, which underscores the specificity of BciVI cleavage.

6-Thioguanine Perturbs Cytosine Methylation at CpG Site by Both Human DNMT1 and Bacterial HpaII

Based on the peak areas found in the SICs (Figure 3.4a&b), we were able to quantify the extent of cytosine methylation by using the equation described in Materials and Methods. It is worth noting that, in the above quantification studies, the ionization and fragmentation efficiencies for the methylated 6- or 7-mer ODNs were assumed to be the same as their unmethylated counterparts. To assess whether this might introduce substantial error to the quantification, we digested an equi-molar mixture of hemimethylated Substrate **1** and the corresponding fully methylated duplex ODN, in which the internal cytosine at CCGG site in the top strand is also methylated, with BciVI and subjected the digestion mixture to LC-MS/MS analysis under the same experimental conditions as described above. It turned out that the efficiency for forming the three abundant fragment ions from the methylated substrate is approximately 10% greater than

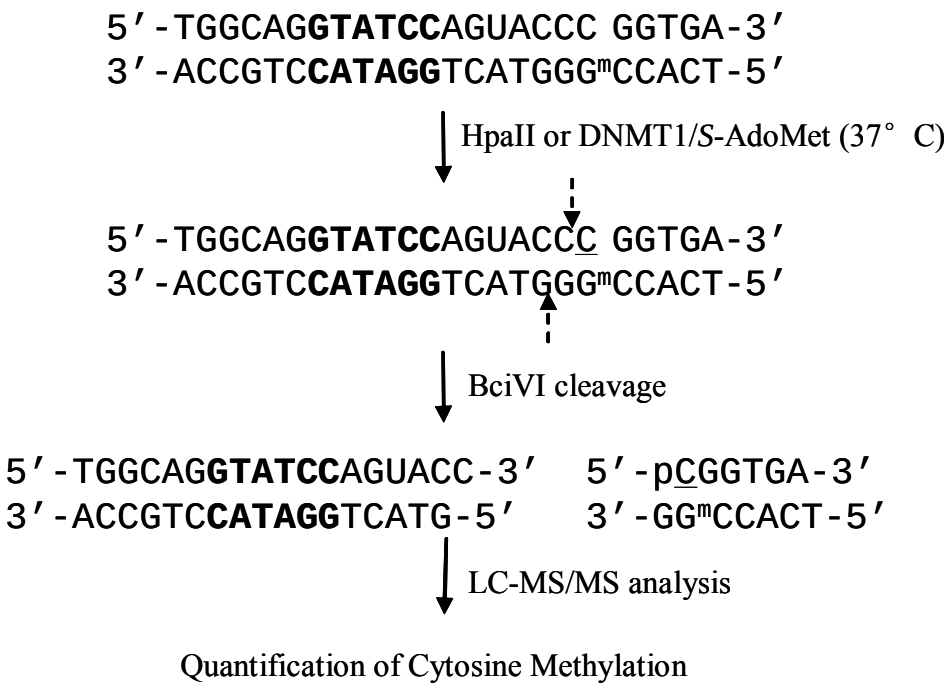

Figure 3.2 The experimental procedures for assessing the DNA methyltransferase-mediated cytosine methylation in synthetic duplex DNA. The underlined "C" represents unmethylated or methylated cytosine. The recognition site of BciVI is highlighted in bold and the cleavage sites of BciVI are indicated by broken arrows.

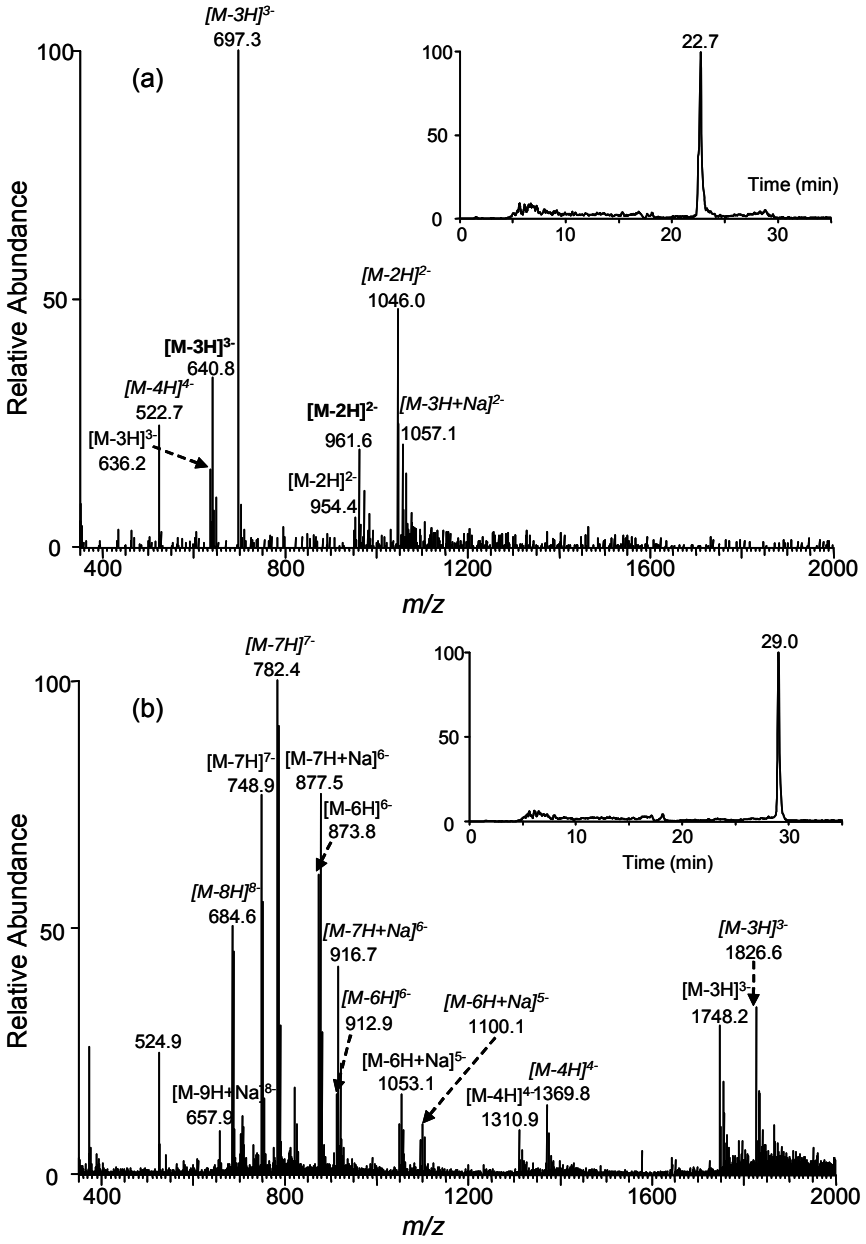

Figure 3.3 Negative-ion ESI-MS of BciVI fragments from the DNMT1-mediated methylation reaction mixture of Substrate 1. (a) ESI-MS of the short BciVI fragments averaged from the 22.7-min peak found in the SIC (shown in the inset) for monitoring the formation of d(pCGGTGA). Multiply charged ions for d(pCGGTGA), d(p^{m}CGGTGA), and d(TCAC^{m}CGG) are designated in normal, bold, and italic fonts, respectively. (b) ESI-MS of the longer BciVI fragments averaged from the 29.0-min peak found in the SIC for monitoring the formation of d(pGTACTGGATACCTGCCA). Multiply charged ions for d(pGTACTGGATACCTGCCA) and d(TGGCAGGTATCCAGUACC) are labeled in normal and italic fonts, respectively.

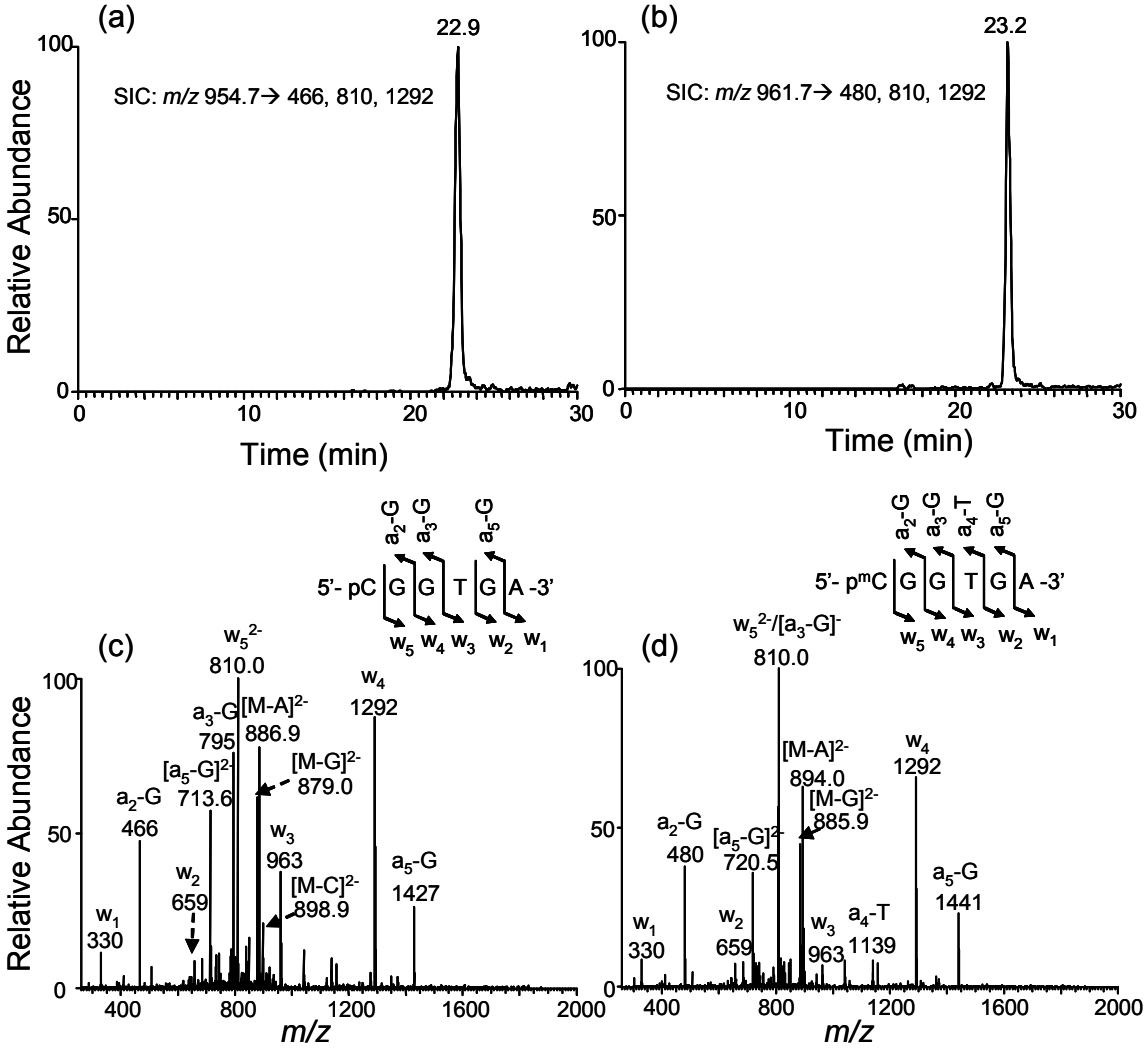

Figure 3.4 LC-MS/MS for monitoring the restriction fragments of interest with or without methylation at CpG site [i.e., d(pCCGTGA) and d(p^{m}CGGTGA), which were from the BciVI cleavage of Substrate **1** after in-vitro methylation]. Shown in (a) and (b) are the SICs for monitoring the formation of indicated fragment ions of these two ODNs, and illustrated in (c) and (d) are the MS/MS of the $[M - 2H]^{2-}$ ions of the two ODNs (*m/z* 954.7 and 961.7). Nomenclature for fragment ions follows that described by McLuckey *et al.* (*118*)

that for the unmethylated substrate. Thus, the above assumption does not result in significant error in measuring the level of methylation.

Our quantification data, summarized in Figure 3.7, revealed that the incorporation of ^{S}G into CpG site affected the methylation of nearby cytosine in duplex DNA by both human maintenance DNA methyltransferase DNMT1 and bacterial *Hpa*II methylase. The presence of ^{S}G at CpG site suppressed strongly the methylation of its 5' adjacent cytosine by both DNMT1 and *Hpa*II (i.e., Substrate **2** vs. Substrate **1**, Figure 3.7a and 3.7c). On the other hand, when ^{S}G was located immediately 3' to the CpG site on the unmethylated strand of a hemimethylated target (Substrate **3** vs. Substrate **1**), it did not bear any significant effect on cytosine methylation mediated by DNMT1 (Figure 3.7a). Substrate **3**, however, displayed greatly diminished tendency toward *Hpa*II-mediated cytosine methylation when compared to Substrate **1** (Figure 3.7c). Interestingly, relative to the control substrate, a higher level of *Hpa*II-mediated methylation was found for substrates where either guanine at CCGG site in the opposing strand was replaced with a ^{S}G (compare Substrate **4** with Substrates **5** and **6**, Figure 3.7d). However, the replacement of guanine at CpG site, but not the substitution of the flanking guanine 3' to the CpG site, stimulated the DNMT1-mediated CpG methylation in the opposing strand (Figure 3.7b).

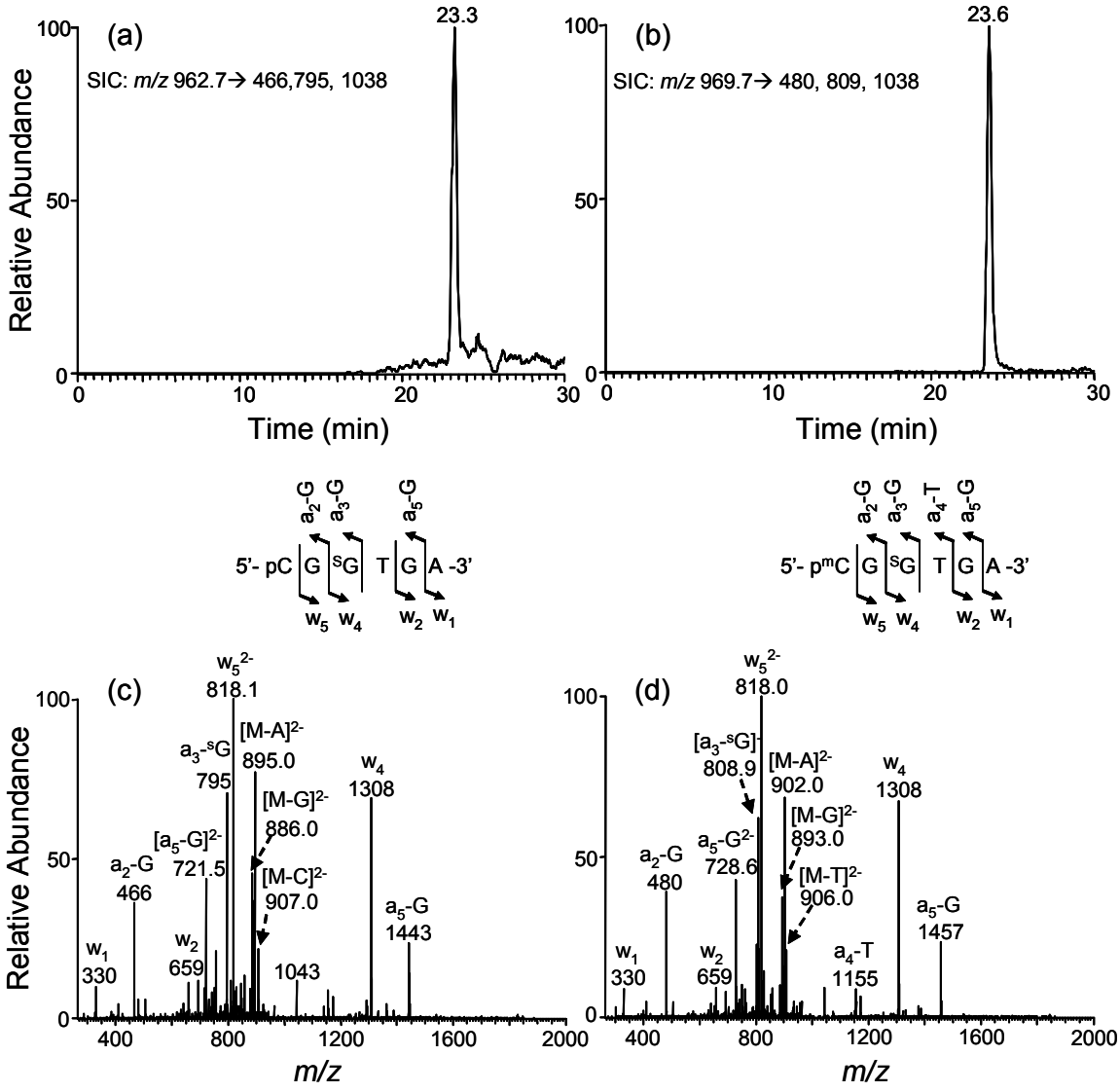

Figure 3.5 LC-MS/MS for monitoring the restriction fragments of interest with or without methylation at CpG site [i.e. d(pCG^{S}GTGA) and d(p^{m}CG^{S}GTGA), from the BciVI digestion of methylation reaction mixture of Substrate **3**]. Shown in (a) and (b) are the SICs for the formation of indicated fragment ions of the two ODNs, and illustrated in (c) and (d) are the MS/MS of the $[M-2H]^{2-}$ ions of the two ODNs (*m/z* 962.7 and 969.7).

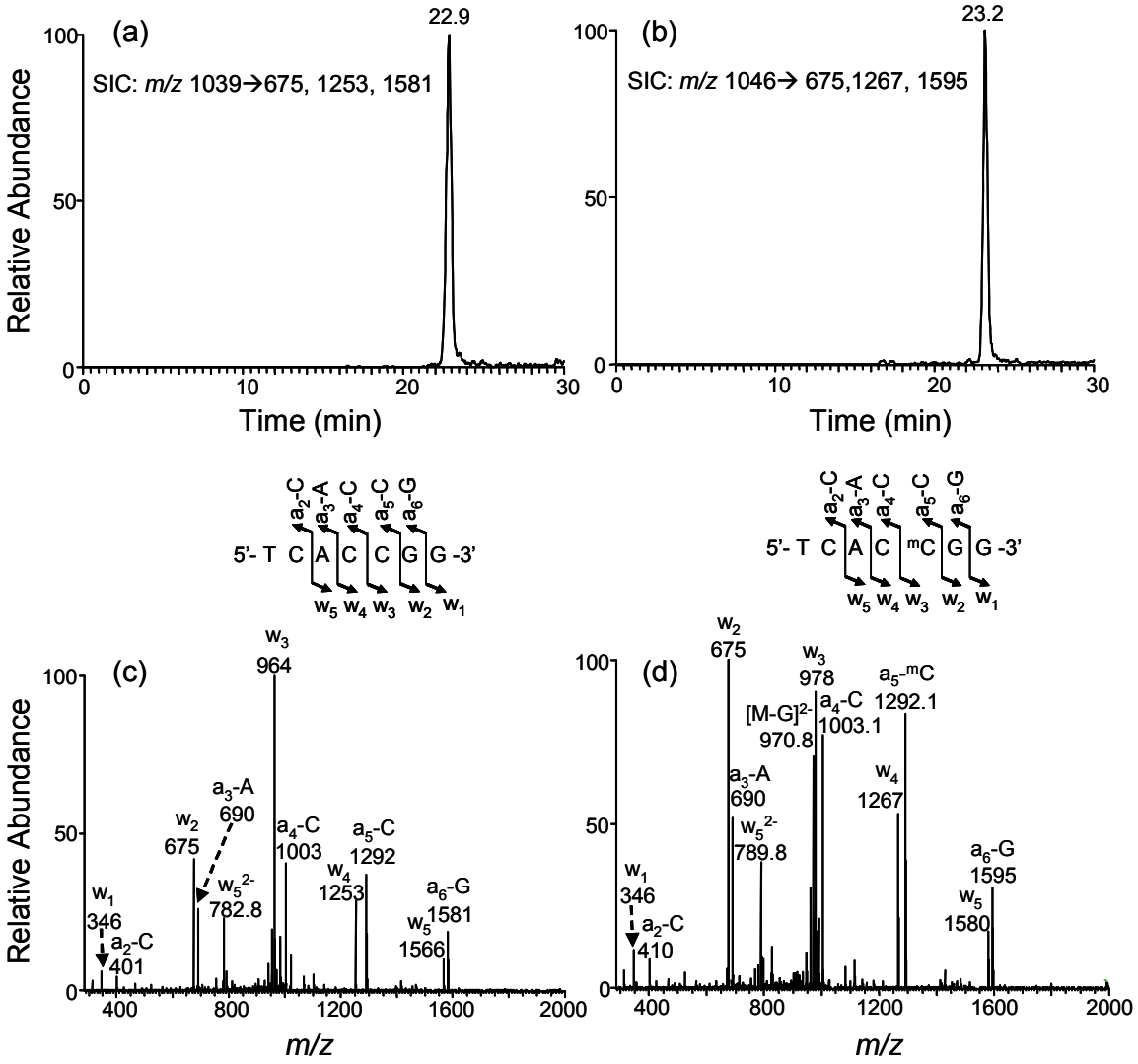

Figure 3.6 LC-MS/MS for monitoring the restriction fragments of interest with or without methylation at CpG site [i.e. d(TCACCGG) and d(TCAC^{m}CGG), from the BciVI digestion of the methylation reaction mixture of Substrate **4**]. Depicted in (a) and (b) are the SICs for the formation of indicated fragment ions of these two ODNs, and illustrated in (c) and (d) are the MS/MS of the $[M-2H]^{2-}$ ions of the two ODNs (*m/z* 1039.2 and 1046.2).

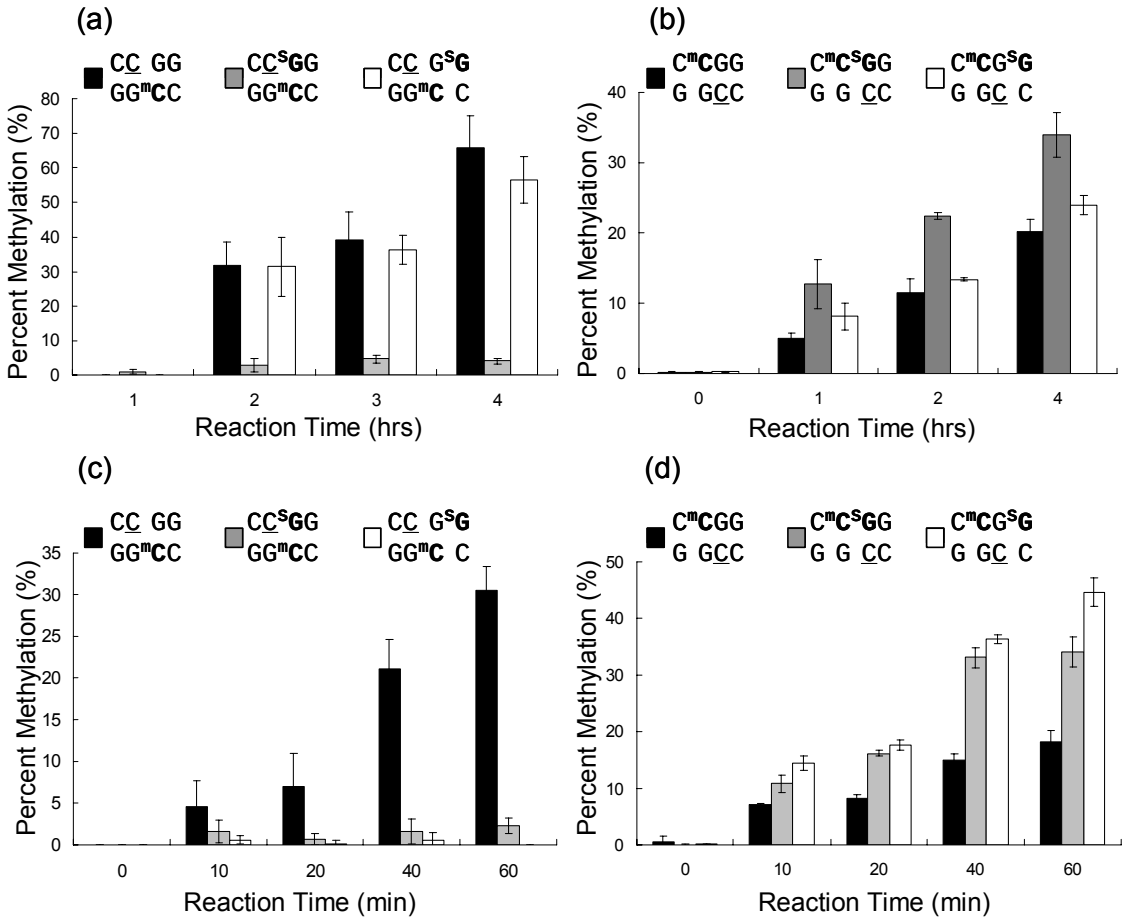

Figure 3.7 Levels of cytosine methylation in different substrates induced by DNMT1 and *Hpa*II methyltransferases. (a) DNMT1-induced methylation of cytosine at CpG site in Substrates **1**, **2** and **3** (Table 1). (b) DNMT1-catalyzed methylation of cytosine at CpG site in Substrates **4**, **5** and **6** (Table 1). (c) *Hpa*II-mediated methylation of cytosine at CpG site in Substrates **1**, **2** and **3**. (d) *Hpa*II-catalyzed methylation of cytosine at CpG site in Substrates **4**, **5** and **6**. The target cytosine residues to be methylated are underlined. The data represent the means and standard deviation of three independent methylation reactions and LC-MS/MS measurements. All results shown in panel (b) were obtained from UDG digestion, and the rest results were from BciVI cleavage (See Materials and Methods).

6-ThioguanineTreatment Leads to Decrease in Global Cytosine Methylation in Jurkat T, HL-60, CCRF-CEM and K-562 Leukemia Cells

After having demonstrated the inhibitory effect of 6-thioguanine on the methylation of its neighboring 5' cytosine by DNA methyltransferases, we next assessed whether 6-thioguanine can act as an inhibitor for cytosine methylation in human cells. On the grounds that thiopurine drugs have been successfully employed for treating acute lymphoblastic leukemia (ALL) (*52*) and aberrant cytosine methylation has been detected for a number of genes in bone marrow samples from ALL patients and two ALL cell lines (Jurkat-T and NALM-6 cells) (*170*), we chose to employ Jurkat T cells for this experiment. To this end, we treated Jurkat T cells with 6-thioguanine (at a concentration of 1 or 3 μM) or 5-aza-2'-deoxycytidine (5 μM) for 24 hrs. We then isolated the genomic DNA from the cells, digested the DNA with nuclease P1 and alkaline phosphatase, and assessed the level of cytosine methylation by HPLC analysis of the resulting nucleoside mixtures. Under optimized HPLC conditions (See Materials and Methods), we were able to resolve dC and 5-mdC from each other and from other nucleosides (Figure 3.8 and Figures 3.9&3.1). From the integrated peak areas for dC and 5-mdC observed in the HPLC traces (Figure 3.8) and the extinction coefficients for the two nucleosides at 260 nm, we were able to quantify the percentage of cytosine methylation in cells that are untreated or treated with 6-thioguanine or 5-aza-2'-deoxycytidine.

It turned out that the culturing of Jurkat T cells in a medium containing 1 or 3-μM of 6-thioguanine for 24 hrs led to appreciable decreases in global cytosine methylation, i.e., the percentage of cytosine methylation decreased from 3.92 ± 0.04% in untreated

cells to 3.42 ± 0.04% and 3.39 ± 0.18% in cells treated with 1 and 3-μM of 6-thioguanine, respectively (Figure 3.10a). Similar treatment with 5-μM of 5-aza-2'-deoxycytidine, a well-known inhibitor for cytosine methylation (*171*), resulted in the decrease of the percentage of cytosine methylation to 1.96 ± 0.15% (Figure 3.10a).

It is worth noting that the extents of decrease in cytosine methylation are modest, by 13-16% relative to the control untreated cells; however, the difference in the level of global cytosine methylation between ^{S}G-treated and untreated cells is statistically significant ($P < 0.0001$, Figure 3.10a). Likewise, we found decreased global cytosine methylation in three other leukemia lines including HL-60, CCRF-CEM, K-562 upon the same ^{S}G treatment (Figure 3.10b & Table 3.2). The level of global cytosine methylation in HL-60 cells dropped, relative to the control untreated cells, by 3.3 and 9.4% upon a 24-h treatment with 1 μM and 3 μM ^{S}G, respectively, whereas somewhat less pronounced, but statistically significant decreases were found for CCRF-CEM cells (4.5 and 7.3%) and K-562 cells (2.7 and 4.8%). However, global cytosine methylation was not affected in human colon cancer HCT-116 cells upon the same ^{S}G treatment (Figure 3.10b & Table 3.2). In addition, the above drop in methylation level reflects the decrease in cytosine methylation in newly synthesized DNA in the background of previously methylated DNA that is not expected to change during the drug treatment.

Discussion

Thiopurine drugs have been available to medical practitioners as effective anticancer and immunosuppressive agents for more than half a century (*52*, *53*). Although

the biochemical mechanisms through which the thiopurines exert their cytotoxic effects remain elusive, the formation of thioguanine nucleotides and their subsequent incorporation into nucleic acids are known to be essential for the drugs to be effective (*52*). In this context, ^{S}G in DNA is chemically more reactive than guanine; it can be methylated by *S*-AdoMet to give S^6mG and the resulting S^6mG:T base pair may trigger the post-replicative mismatch repair pathway, which may account for the therapeutic effects of the thiopurine drugs (*73*). In addition, a recent study suggested that 6-thioguanine, because of its miscoding potential, may trigger the post-replicative mismatch repair pathway without being converted to S^6mG (*77*). In higher eukaryotes, cytosine methylation at CpG dinucleotide site is known to be important in gene regulation and essential for embryonic viability (*87*), and aberrant cytosine methylation is associated with cancer development (*172, 173*). We hypothesize that the thiopurine drugs may exert their anti-neoplastic effect via perturbing the methylation of cytosine at CpG site by DNA methyltransferases, thereby interfering with the epigenetic pathways of gene regulation.

To gain experimental evidence for supporting this hypothesis, we first developed an LC-MS/MS coupled with restriction enzyme digestion method and assessed the human DNMT1- and *Hpa*II-mediated methylation of cytosine in synthetic duplex DNA where a guanine residue at CCGG site was replaced with a ^{S}G. Our quantification results illustrated that the substitution of the guanine residue at CpG site with a ^{S}G inhibited greatly the methylation of the adjoining 5' cytosine by DNMT1; however, little effect on the methylation of CpG dinucleotide was observed when the guanine 3' neighboring to

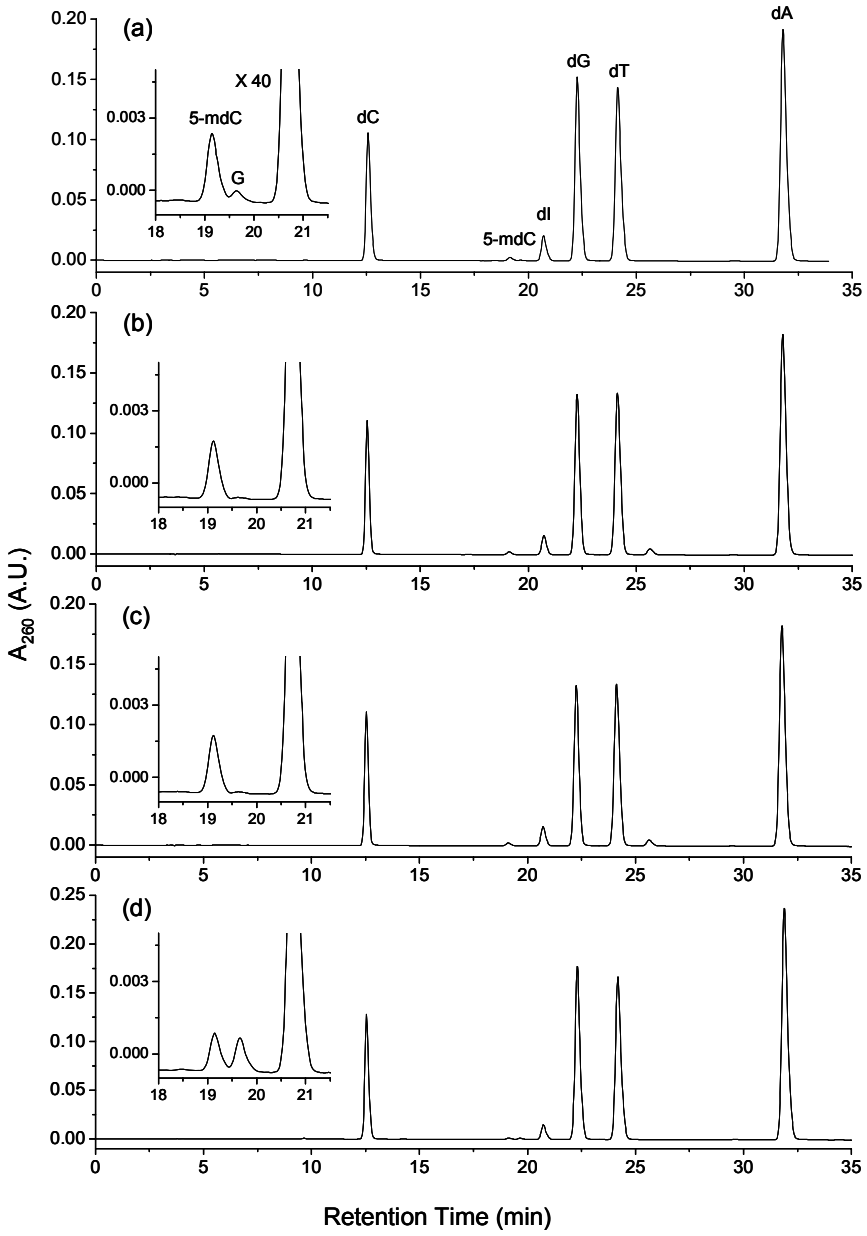

Figure 3.8 The HPLC traces for the separation of nucleoside mixtures produced from the digestion of genomic DNA isolated from Jurkat T cells that were: (a) untreated; (b) treated with 1 μM ^{S}G; (c) treated with 3 μM ^{S}G; (d) treated with 5 μM 5-aza-dC. Shown in the insets are the expanded chromatograms to visualize better the 5-mdC peak. "dI" and "G" represent 2'-deoxyinosine and guanosine, respectively. The former arises from the deamination of 2'-deoxyadenosine during enzymatic digestion. It is worth noting that the amount of RNA present in the isolated DNA varied from sample to sample, which resulted in different amounts of G in the nucleoside mixtures.

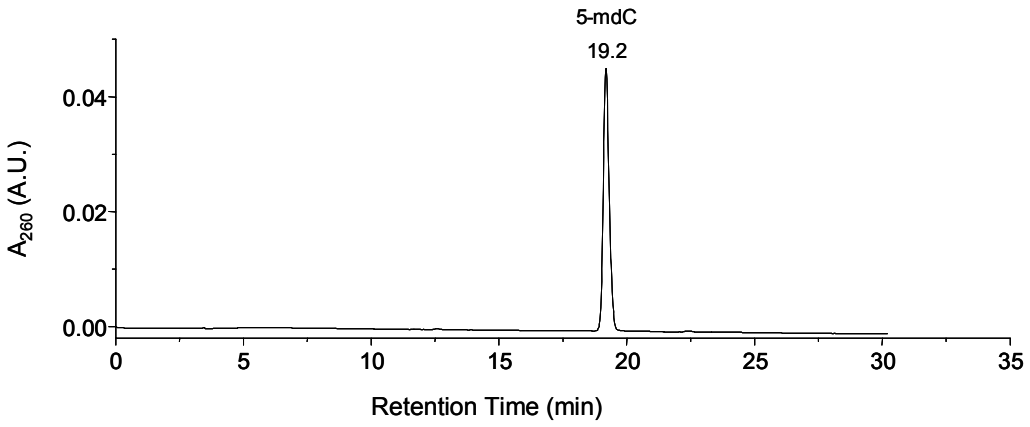

Figure 3.9 HPLC trace for the separation of standard 5-mdC. The HPLC conditions were the same as those described for the separation of nucleoside mixtures from the digestion of genomic DNA isolated from Jurkat cells.

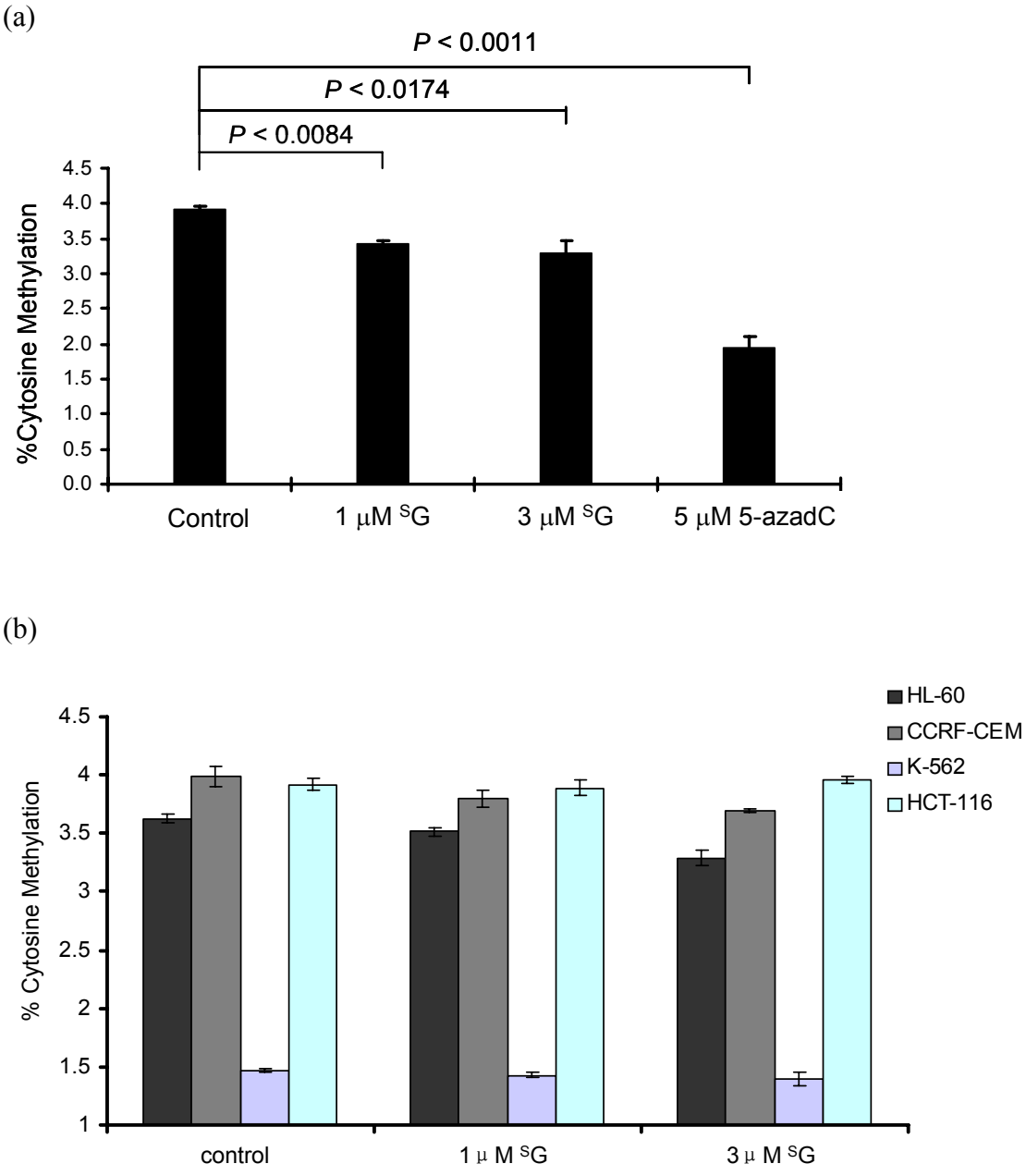

Figure 3.10 6-Thioguanine treatment results in decreased global cytosine methylation in Jurkat T (a), and HL-60, CCRF-CEM, K-562 and HCT-116 cells (b). Plotted are the percentages of global cytosine methylation in genomic DNA isolated from human cancer cells that were untreated or treated with ^{S}G. The data represent the means and standard deviations of results from three independent drug treatments and HPLC measurements.

Table 3.2 .Percentage of global cytosine methylation in human cancer cells

	Jurkat T (%)	HL-60 (%)	CCRF-CEM (%)	K-562 (%)	HCT-116 (%)
Control	3.92±0.06	3.63±0.04	3.98±0.09	1.47±0.01	3.92±0.05
1 μM ^{S}G	3.42±0.07	3.51±0.04	3.80±0.07	1.43±0.02	3.89±0.07
3 μM ^{S}G	3.29±0.17	3.29±0.07	3.70±0.02	1.40±0.06	3.96±0.03

CpG site was replaced with a ^{S}G. In addition, the substitution of either guanine at CCGG site with a ^{S}G inhibited the *Hpa*II-catalyzed methylation of the internal cytosine residue in the same strand. By contrast, the replacement of either guanine residue at C^{m}CGG site leads to enhanced CpG methylation in the opposing strand by *Hpa*II methylase, and only the change of the guanine residue at methylated CpG site with a ^{S}G stimulated the DNMT1-mediated methylation at CpG site in the opposing strand. The above results with the two different methyltransferases are consistent with the previous findings that the CpG dinucleotide is sufficient for DNMT1 binding and methylation (*168*), whereas *Hpa*II binding and methylation requires the CCGG sequence motif (*167*).

The mechanism for the different effects of ^{S}G on cytosine methylation remains unclear. Nevertheless, previous X-ray structural studies with M. HhaI methyltransferase demonstrated that the methylation necessitated the flipping of cytosine residue out of DNA double helix and the fitting of this nucleobase into the catalytic pocket of the methyltransferase (*174*). On the basis of the increased atomic radius, bond length and the altered hydrogen bonding property of sulfur (*175*), we speculate that, when 6-thioguanine lies on the 3' side of the target cytosine to be methylated, it may result in compromised binding between DNA and the methyltransferase, thereby resulting in abolished cytosine methylation. When the guanine residing on the opposite strand of the target CpG site was replaced with an ^{S}G, the weakened hydrogen bonding interaction between ^{S}G and cytosine(*75*) may render the facile flipping of the target cytosine from the double helix structure thereby enhancing the methylation of cytosine residue.

Our results are consistent with the previous studies about the effect of other guanine modifications on the methyltransferase-mediated cytosine methylation. In this regard, it was found that the substitution of guanine at CpG site with an 8-oxoG inhibited the methylation of its vicinal 5' cytosine (*92, 163*) . It was also observed that replacing the guanine at methylated CpG site with an 8-oxoG or O^6mG stimulated the methylation of the opposing cytosine in the complementary strand (*92, 93, 163, 164*).

The results from the above *in-vitro* biochemical experiments suggest that the incorporation of ^{S}G into the nascent DNA strand during DNA replication may result in diminished maintenance cytosine methylation, thereby perturbing the epigenetic pathway of gene regulation. By quantifying the level of global cytosine methylation with a direct HPLC method, we further showed that the treatment of Jurkat T, HL-60, CCRF-CEM and K-562 cells with 1 or 3 μM 6-thioguanine for 24 hrs could lead to a significant decrease in global cytosine methylation. Along this line, by measuring the ^{3}H/^{14}C ratio in DNA isolated from cells pulse-labeled with L-[methyl-^{3}H]methionine and [2-^{14}C]thymidine, Hogarth, De Abreu and their coworkers (*176, 177*) showed that the treatment of MOLT-F4 human malignant lymphoblastic cells with ^{S}G or 6-mercaptopurine could give rise to a lower level of cytosine methylation in newly synthesized DNA. In addition, Hogarth et al. (*177*) observed that the treatment of MOLT-F4 cells with ^{S}G or MP could lead to a decrease in the enzymatic activity of DNMT1 in the whole cell lysate and a drop in the level of the DNMT1 protein. The decreased level of DNMT1 protein was also observed in cells treated with 5-aza-dC and this decrease was attributed to the degradation of DNMT1 by the proteasomal pathway (*178*). Although it remains

unexplored whether the ^{S}G-induced decrease in DNMT1 protein level also arises from the proteasomal pathway, it is highly plausible that this pathway may also play an important role. 5-azacytidine and 5-aza-dC are in clinical trials for the treatment of various hematopoietic and solid malignancies but they are considered too toxic and mutagenic for long-term preventive therapy (*179*), whereas mercaptopurine along with methotrexate has been routinely used in the maintenance therapy for childhood ALL (*53*).The more potent inhibition of cytosine methylation exerted by 5-aza-dC than by thiopurines may account for the different pharmacological performances for the two types of drugs.

Taken together, the results from the present study support that the thiopurine drugs may exert their cytotoxic effects, at least in part, by perturbing the epigenetic pathway *in vivo*. In this context, it is worth noting that, in DNA samples isolated from peripheral blood mononuclear cells of patients receiving 6-mercaptopurine or azathioprine, approximately 0.01-0.1% of guanine are replaced with 6-thioguanine (*180, 181*). This level is orders of magnitude greater than the levels of typical guanine modification products induced by reactive oxygen species or alkylating agents.

References

(1) Elion, G. B. (1989) The purine path to chemotherapy. *Science 244*, 41-47.

(2) Pui, C. H. and Evans, W. E. (1998) Acute lymphoblastic leukemia. *N. Engl. J. Med. 339*, 605-615.

(3) Swann, P. F., Waters, T. R., Moulton, D. C., Xu, Y. Z., Zheng, Q. G., Edwards, M. and Mace, R. (1996) Role of postreplicative DNA mismatch repair in the cytotoxic action of thioguanine. *Science 273*, 1109-1111.

(4) O'Donovan, P., Perrett, C. M., Zhang, X. H., Montaner, B., Xu, Y. Z., Harwood, C. A., McGregor, J. M., Walker, S. L., Hanaoka, F. and Karran, P. (2005) Azathioprine and UVA light generate mutagenic oxidative DNA damage. *Science 309*, 1871-1874.

(5) Gu, C. N. and Wang, Y. S. (2007) In vitro replication and thermodynamic studies of methylation and oxidation modifications of 6-thioguanine. *Nucleic Acids Res. 35*, 3693-3704.

(6) Zhang, X. H., Jeffs, G., Ren, X. L., O'Donovan, P., Montaner, B., Perrett, C. M., Karran, P. and Xu, Y. Z. (2007) Novel DNA lesions generated by the interaction between therapeutic thiopurines and UVA light. *DNA Repair 6*, 344-354.

(7) Yuan, B. F. and Wang, Y. S. (2008) Mutagenic and cytotoxic properties of 6-thioguanine, S-6-methylthioguanine, and guanine-S-6-sulfonic acid. *J. Biol. Chem. 283*, 23665-23670.

(8) Waters, T. R. and Swann, P. F. (1997) Cytotoxic mechanism of 6-thioguanine: hMutS alpha, the human mismatch binding heterodimer, binds to DNA containing

S-6-methylthioguanine. *Biochemistry 36*, 2501-2506.

(9) Robertson, K. D. (2005) DNA methylation and human disease. *Nat. Rev. Genet. 6*, 597-610.

(10) Bestor, T. H. (2000) The DNA methyltransferases of mammals. *Hum. Mol. Genet. 9*, 2395-2402.

(11) Hendrich, B. D. and Willard, H. F. (1995) Epigenetic regulation of gene-expression - The effect of altered chromatin structure from yeast to mammals. *Hum. Mol. Genet. 4*, 1765-1777.

(12) Klose, R. J. and Bird, A. P. (2006) Genomic DNA methylation: the mark and its mediators. *Trends Biochem. Sci. 31*, 89-97.

(13) Turk, P. W., Laayoun, A., Steven, S. S. and Weitzman, S. A. (1995) DNA adduct 8-hydroxyl-2'-deoxyguanosine (8-hydroxyguanine) affects function of human DNA methyltransferase. *Carcinogenesis 16*, 1253-1255.

(14) Weitzman, S. A., Turk, P. W., Milkowski, D. H. and Kozlowski, K. (1994) Free-radical adducts induce alterations in DNA cytosine methylation. *Proc. Natl. Acad. Sci. USA 91*, 1261-1264.

(15) Tan, N. W. and Li, B. F. L. (1990) Interaction of oligonucleotides containing 6-O-methylguanine with human DNA (cytosine-5-)-methyltransferase. *Biochemistry 29*, 9234-9240.

(16) Smith, S. S., Kan, J. L. C., Baker, D. J., Kaplan, B. E. and Dembek, P. (1991) Recognition of unusual DNA structures by human DNA (cytosine-5) methyltransferase. *J. Mol. Biol. 217*, 39-51.

(17) Subach, O. M., Maltseva, D. V., Shastry, A., Kolbanovskiy, A., Klimasauskas, S., Geacintov, N. E. and Gromova, E. S. (2007) The stereochemistry of benzo[a]pyrene-2 '-deoxyguanosine adducts affects DNA methylation by SssI and HhaI DNA methyltransferases. *FEBS J. 274*, 2121-2134.

(18) Valinluck, V. and Sowers, L. C. (2007) Endogenous cytosine damage products alter the site selectivity of human DNA maintenance methyltransferase DNMT1. *Cancer Res. 67*, 946-950.

(19) Ling, Y. H., Chan, J. Y., Beattie, K. L. and Nelson, J. A. (1992) Consequences of 6-thioguanine incorporation into DNA on polymerase, ligase, and endonuclease reactions. *Mol. Pharmacol. 42*, 802-807.

(20) Krynetskaia, N. F., Krynetski, E. Y. and Evans, W. E. (1999) Human RNase H-mediated RNA cleavage from DNA-RNA duplexes is inhibited by 6-deoxythioguanosine incorporation into DNA. *Mol. Pharmacol. 56*, 841-848.

(21) Krynetskaia, N. F., Cai, X. J., Nitiss, J. L., Krynetski, E. Y. and Relling, M. V. (2000) Thioguanine substitution alters DNA cleavage mediated by topoisomerase II. *FASEB J. 14*, 2339-2344.

(22) Quint, A. and Cedar, H. (1981) Invitro methylation of DNA with Hpa-II methylase. *Nucleic Acids Res. 9*, 633-646.

(23) Yoder, J. A., Soman, N. S., Verdine, G. L. and Bestor, T. H. (1997) DNA (cytosine-5)-methyltransferases in mouse cells and tissues. Studies with a mechanism-based probe. *J. Mol. Biol. 270*, 385-395.

(24) Apffel, A., Chakel, J. A., Fischer, S., Lichtenwalter, K. and Hancock, W. S. (1997)

Analysis of oligonucleotides by HPLC-electrospray ionization mass spectrometry. *Anal. Chem. 69*, 1320-1325.

(25) McLuckey, S. A., Vanberkel, G. J. and Glish, G. L. (1992) Tandem mass-spectrometry of small, multiply charged oligonucleotides. *J. Am. Soc. Mass Spectrom. 3*, 60-70.

(26) Taylor, K. H., Pena-Hernandez, K. E., Davis, J. W., Arthur, G. L., Duff, D. J., Shi, H., Rahmatpanah, F. B., Sjahputera, O. and Caldwell, C. W. (2007) Large-scale CpG methylation analysis identifies novel candidate genes and reveals methylation hotspots in acute lymphoblastic leukemia. *Cancer Res. 67*, 2617-2625.

(27) Jones, P. A. and Taylor, S. M. (1980) Cellular differentiation, cytidine analogs and DNA methylation. *Cell 20*, 85-93.

(28) Jones, P. A. and Baylin, S. B. (2002) The fundamental role of epigenetic events in cancer. *Nat. Rev. Genet. 3*, 415-428.

(29) Esteller, M. (2002) CpG island hypermethylation and tumor suppressor genes: a booming present, a brighter future. *Oncogene 21*, 5427-5440.

(30) O'Gara, M., Horton, J. R., Roberts, R. J. and Cheng, X. (1998) Structures of HhaI methyltransferase complexed with substrates containing mismatches at the target base. *Nat. Struct. Biol. 5*, 872-877.

(31) Platts, J. A., Howard, S. T. and Bracke, B. R. F. (1996) Directionality of hydrogen bonds to sulfur and oxygen. *J. Am. Chem. Soc. 118*, 2726-2733.

(32) Lambooy, L. H., Leegwater, P. A., van den Heuvel, L. P., Bokkerink, J. P. and De

Abreu, R. A. (1998) Inhibition of DNA methylation in malignant MOLT F4 lymphoblasts by 6-mercaptopurine. *Clin. Chem. 44*, 556-559.

(33) Hogarth, L. A., Redfern, C. P., Teodoridis, J. M., Hall, A. G., Anderson, H., Case, M. C. and Coulthard, S. A. (2008) The effect of thiopurine drugs on DNA methylation in relation to TPMT expression. *Biochem. Pharmacol. 76*, 1024-1035.

(34) Ghoshal, K., Datta, J., Majumder, S., Bai, S., Kutay, H., Motiwala, T. and Jacob, S. T. (2005) 5-Aza-deoxycytidine induces selective degradation of DNA methyltransferase 1 by a proteasomal pathway that requires the KEN box, bromo-adjacent homology domain, and nuclear localization signal. *Mol. Cell. Biol. 25*, 4727-4741.

(35) Jackson-Grusby, L., Laird, P. W., Magge, S. N., Moeller, B. J. and Jaenisch, R. (1997) Mutagenicity of 5-aza-2'-deoxycytidine is mediated by the mammalian DNA methyltransferase. *Proc. Natl. Acad. Sci. USA 94*, 4681-4685.

(36) Warren, D. J., Andersen, A. and Slordal, L. (1995) Quantitation of 6-thioguanine residues in peripheral-blood leukocyte DNA obtained from patients receiving 6-mercaptopurine-based maintenance therapy. *Cancer Res. 55*, 1670-1674.

(37) Cuffari, C., Li, D. Y., Mahoney, J., Barnes, Y. and Bayless, T. M. (2004) Peripheral blood mononuclear cell DNA 6-thioguanine metabolite levels correlate with decreased interferon-gamma production in patients with Crohn's disease on AZA therapy. *Dig. Dis. Sci. 49*, 133-137.

CHAPTER 4

Identification and Quantification of 6-Thioguanine and Its Metabolites in Human Cancer Cells upon 6-Thioguanine Treatment

Introduction

Thiopurines, including 6-mercaptopurine (6-MP) and 6-thioguanine (^{S}G), have been widely used in the treatment of childhood acute lymphoblastic leukemia (ALL) (*53*). Another thiopurine, azathioprine, which is converted to 6-MP *in vivo*, is a commonly prescribed immunosuppressant for the treatment of inflammatory bowel diseases, autoimmune conditions and following transplantation (*52*). 6-MP and azathioprine were separately approved by FDA for the treatment of ALL in children in 1953 (*54*)and for the prolongation of renal allograft survival in 1963 (*55*).

Thiopurines are inactive prodrugs and, to exert their cytotoxic effect, these prodrugs need to be metabolically activated (i.e., to thioguanine nucleotides) and incorporated into DNA (Scheme 4.1) (*52*). During metabolism, ^{S}G is converted to its corresponding nucleoside monophosphate (^{S}GMP) in a single-step reaction catalyzed by hypoxanthine phosphoribosyltransferase (HPRT), whereas three enzymatic steps are required to convert 6-MP and azathioprine to ^{S}GMP. ^{S}GMP is then phosphorylated by kinases to give ^{S}GDP and ^{S}GTP, and ^{S}GDP can be converted to ^{S}dGTP through the sequential actions of ribonucleotide reductase and kinase (*56*). Thiopurine methyltransferase (TPMT), which exhibits genetic polymorphism, catalyzes the *S*-methylation of thiopurines. Clinical studies revealed that TPMT-deficient patients

accumulate excessive ^{S}G nucleotides in erythrocytes and are susceptible to develop severe hematopoietic toxicity or even death from neutropenic sepsis (*60-62*). In addition, S^6-methylthioinosine-5'-monophosphate is a potent inhibitor for *de novo* purine synthesis, which may constitute an alternative mechanism for the cytotoxicity of 6-MP (*63*).

The incorporation of 6-thioguanine into the nucleotide pool or DNA was found to perturb various cellular pathways. In this vein, ^{S}GTP, a nucleotide metabolite of azathioprine, was shown to block the activation of Rac1, a GTP-binding protein, in human CD4+ T lymphocytes upon CD28 costimulation (*182*). Additionally, ^{S}G in DNA can lead to global cytosine demethylation (*91*) and it can induce single-strand breaks, interstrand cross-links, DNA-protein cross-links, and chromatid damage (*58, 72, 183, 184*).

The increased chemical reactivity of ^{S}G relative to guanine may also contribute to the cytotoxic effects of thiopurine drugs. In this context, Swann et al. (*73*) found that DNA ^{S}G can be methylated spontaneously to S^6-methylthioguanine (S^6mG) in the presence of *S*-adenosyl-L-methionine (*S*-AdoMet). The coding property of S^6mG directs the misincorporation of thymine to give S^6mG:T base pair during DNA replication, which is recognized by post-replicative mismatch repair (MMR) machinery; futile cycles of repair synthesis may give rise to cell death. Our recent replication study demonstrated that both 6-thio-2'-deoxyguanosine (^{S}dG) and S^6-methylthio-2'-deoxyguanosine (S^6mdG) are mutagenic in *Escherichia coli* (*E. coli*) cells and could lead to G→A mutations at frequencies of 10% and 94%, respectively (*77*). ^{S}G:T mispair is known to be recognized more readily by MMR machinery than the S^6mG:T mispair (*162, 185*).

Scheme 4.1 Thiopurines and their metabolism to form 6-thioguanine nucleotides. HPRT, hypoxanthine phosphoribosyltransferase; IMPD, inosine monophosphate dehydrogenase; GMPS, guanosine monophosphate synthase; ^{S}GMP, 6-thioguanosine monophosphate; d^{S}GTP, 6-thio-2'-deoxyguanosine triphosphate.

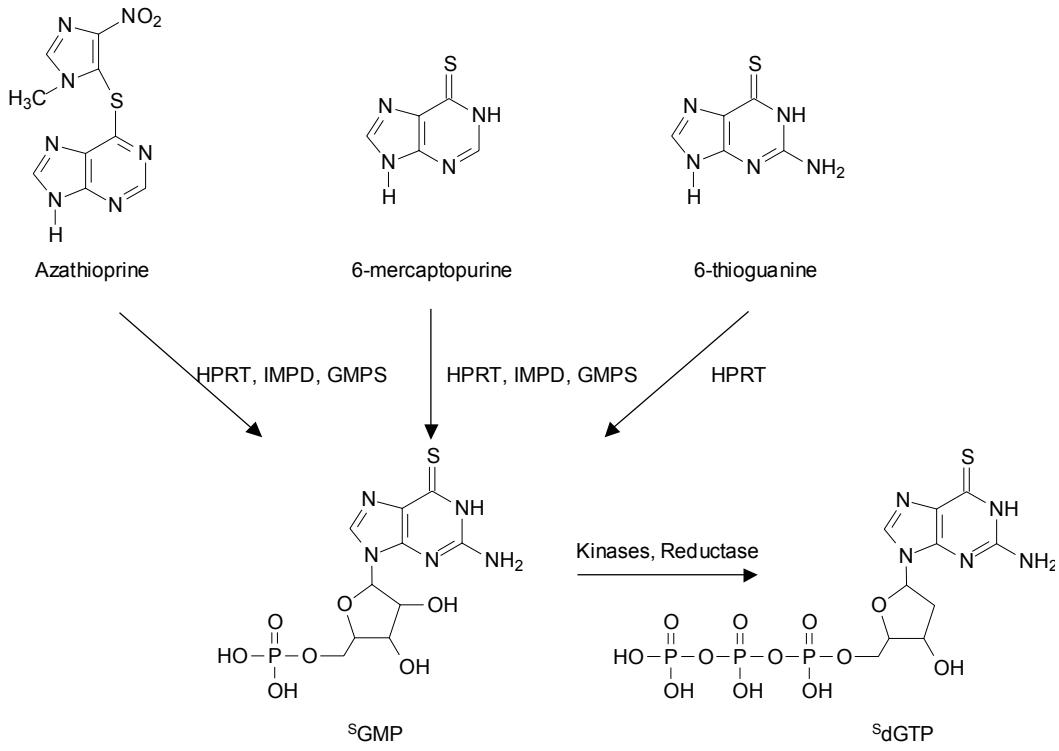

Thus, we hypothesized that the ^{S}G:T mispair arising from *in vivo* DNA replication may invoke directly the post-replicative MMR pathway without having the ^{S}G being converted to *S*^{6}mG (*77*). In order to evaluate the relative contributions of ^{S}G:T and *S*^{6}mG:T mispairs in provoking the post-replicative mismatch repair pathways, it is necessary to quantify accurately the amounts of ^{S}dG and its methylated metabolite, *S*^{6}mdG, in genomic DNA of ^{S}G-treated leukemic cells.

Reverse-phase HPLC with UV or fluorescence detection was used to monitor thiopurine nucleosides and nucleotides (*186-189*). In addition, anion-exchange HPLC was employed to determine the mono-, di- and triphosphate forms of thiopurine nucleotides (*187*). Moreover, erythrocyte 6-thioguanine and 6-methylmercaptopurine nucleotides were hydrolyzed by acid to its component nucleobases and subsequently analyzed by LC-MS/MS, though stable isotope-labeled standards were not used (*190*). However, none of the above-described methods have been used to measure the levels of ^{S}dG and *S*^{6}mdG in cellular DNA. In the latter respect, *S*^{6}mdG was detected in DNA of cultured Chinese hamster ovary cells by using radiolabeling with L-[^{3}H-methyl]methionine and it was estimated that approximately 1.6 out of 10^{4} ^{S}G could be methylated to *S*^{6}mG (*73*). Nevertheless, the method requires the use of radioisotopes, and it has not been applied for measuring the levels of ^{S}dG and *S*^{6}mdG in DNA of ^{S}G-treated leukemic cells.

Herein, we developed an LC-MS/MS with the stable isotope dilution method for the sensitive, accurate and simultaneous quantification of ^{S}dG and *S*^{6}mdG in genomic

DNA of cultured human cancer cells exposed with ^{S}G. We also quantified, by using LC-MS/MS, the ^{S}GTP in the nucleotide pool of cells treated with 6-thioguanine.

Experimental Procedures

Chemicals and Enzymes

All chemicals and enzymes, unless otherwise specified, were from Sigma-Aldrich (St. Louis, MO). [U-$^{15}N_5$]-2'-deoxyguanosine ([U-$^{15}N_5$]-dG) and CD_3I were purchased from Cambridge Isotope Laboratories (Andover, MA). Proteinase K was obtained from New England Biolabs (Ipswich, WA). Cancer cell lines, which included Jurkat T, CCRF-CEM, HL-60, K-562 and HCT-116 cells, and cell culture reagents were purchased from ATCC (Manassas, VA, USA).

Synthesis and Characterization of [U-$^{15}N_5$]-6-Thio-2'-deoxyguanosine

The title compound was prepared at microscale following previously published method for the synthesis of the corresponding unlabeled compound (*191*). Briefly, [U-$^{15}N_5$]-dG (1.5 mg, 5.5 μmol) was dried three times by evaporation in anhydrous pyridine and suspended in 0.5 mL of anhydrous pyridine, which was cooled in an ice bath under argon atmosphere. To the solution was added trifluroacetic anhydride (12 μL, 83 μmol). After a 40-min incubation, 14 mg of NaSH in 250 μL of anhydrous DMF was added. After another 24 hrs, the reaction mixture was poured into a 1-mL vigorously stirred solution of 0.16 M ammonium bicarbonate. The solution was then concentrated to dryness. The residue was triturated with methanol and filtered. The filtrate was

concentrated to dryness again and the residue was triturated with 0.1 M TEAA and filtered. The desired [U-$^{15}N_5$]-6-thio-2'-deoxyguanosine ([U-$^{15}N_5$]-^{S}dG) was purified by HPLC on a Beckman system with pump module 125 and a UV detector (module 126). A 4.6×250 mm Apollo C18 column (5 μm in particle size and 300 Å in pore size, Grace Inc., Deerfield, IL) was used and the wavelength of the UV detector was set at 340 nm. A solution of 10 mM ammonium formate (pH 6.3, solution A) and a mixture of 10 mM ammonium formate and acetonitrile (70:30, v/v, solution B) were employed as mobile phases. The flow rate was 0.80 mL/min, and a gradient of 5 min 0-10% B, 40 min 10-35% B and 1 min 35-100% B was used. After purification, the identity of [U-$^{15}N_5$]-^{S}dG was confirmed by both high-resolution ESI-QTOF MS and ion trap LC-MS/MS analyses (see Results).

Synthesis and Characterization of D_3-S^6mdG

This compound was synthesized at microscale following previously reported procedures for the synthesis of the corresponding unlabeled compound (*192*). Briefly, ^{S}dG (1.8 mg, 6.3 μmol) was dissolved in 250 mM phosphate buffer (1 mL, pH 8.5), to which solution was added 2 μL CD_3I (30 μmol). The solution was stirred overnight, and the reaction mixture was concentrated to dryness. The desired D_3-S^6mdG was purified by using the above-described HPLC method with the wavelength of the UV detector being set at 312 nm. The structure of D_3-S^6mdG was confirmed by both high-resolution ESI-QTOF MS and ion trap LC-MS/MS analyses (see Results).

Cell Culture, 6-Thioguanine Treatment, and DNA Isolation

Cells were cultured in ATCC-recommended medium at 37°C under 5% CO_2 atmosphere. All media were supplemented with 10% fetal bovine serum, 100 I.U./mL penicillin, and 100 μg/mL streptomycin. After growing to 70% confluence (at a density of 10^6 cells/mL), cells were cultured in fresh medium containing 0, 1 and 3 μM of 6-thioguanine and incubated for 24 hrs.

After treatment, the adherent HCT-116 cells (~ 2×10^7 cells) were first detached by trypsin-EDTA treatment. The leukemic cells (~ 2×10^7 cells) and the detached HCT-116 cells were harvested by centrifugation to remove the medium. The cell pellets were subsequently washed twice with 1×PBS and resuspended in a lysis buffer containing 10 mM Tris-HCl (pH 8.0), 0.1 M EDTA, and 0.5% SDS. The cell lysates were then treated with RNase A (20 μg/mL) at 37°C for 1 hr and subsequently with proteinase K (100 μg/mL) at 50°C for 3 hrs. Genomic DNA was isolated by extraction with phenol/chloroform/isoamyl alcohol (25:24:1, v/v) and desalted by ethanol precipitation. The DNA pellet was redissolved in water and its concentration was measured by UV absorbance at 260 nm.

Nucleotide Extraction

After 6-thioguanine treatment, cell pellets were harvested from the drug- or mock-treated cells (~ 2×10^7 cells), washed with PBS buffer and resuspended in 10 mM sodium citrate (pH 4.5) at a final volume of 400 μL. The mixture was sonicated for 1 min, to which solution was added 4 μL of 50 mM DTT. The resulting solution was incubated

at 37°C for 30 min. After centrifugation at 13,000 rpm for 5 min, the supernatant was transferred out and filtrated using 3000-molecular weight cut-off Microcon ultracentrifugation units. The ultrafiltrates were then subjected to LC-MS/MS analysis.

Enzymatic Digestion

For the enzymatic digestion of DNA, nuclease P1 (4 units) was added to a mixture containing 100 μg cellular DNA, 100 fmol D_3-S^6mdG, 2 pmol [U-$^{15}N_5$]-^{S}dG, 30 mM sodium acetate (pH 5.5) and 1 mM zinc acetate, and the mixture was incubated at 37°C for 4 hrs. To the digestion mixture was then added 30 units of alkaline phosphatase in a 50 mM Tris-HCl buffer (pH 8.6), the digestion was continued at 37°C for 2.5 hrs, and the enzymes were subsequently removed by chloroform extraction. The aqueous DNA layer was dried and the dried residues were reconstituted in distilled water. The amount of nucleosides in the mixture was quantified by UV absorbance measurements.

HPLC Enrichment

HPLC removal of unmodified nucleosides in the digestion mixture of cellular DNA was carried out by using a 4.6×250 mm Apollo C18 column (5 μm in particle size and 300 Å in pore size, Grace Inc., Deerfield, IL). An Agilent 1100 HPLC system with a capillary pump (Agilent Technologies) and a UV detector was used, and a Peak Simple Chromatography Data System was employed for data collection (SRI Instruments Inc., Las Vegas, NV, USA). A solution of 10 mM ammonium formate (pH 4.0, solution A) and a mixture of 10 mM ammonium formate and acetonitrile (70:30, v/v, pH 4.0, solution B)

were used as mobile phases. A gradient of 5 min 0-12% B, 45 min 10-35% B, 1 min 35-100% B and 15 min 100% B was employed and the flow rate was 0.80 mL/min. The fractions containing S^6mdG and ^{S}dG were collected separately, dried in a Speedvac, reconstituted in distilled water and subjected to LC-MS/MS analysis. Due to high level of ^{S}dG incorporation in Jurkat T, CCRF-CEM, HL-60 and K-562 cell lines, ^{S}dG levels in DNA of these cells were directly measured by LC-MS/MS with 3 nmol of digested nucleoside mixture doped with 5 pmol [U-$^{15}N_5$]-^{S}dG.

Mass Spectrometry

Electrospray ionization-mass spectrometry (ESI-MS) and tandem MS (MS/MS) experiments were carried out on an LCQ Deca XP ion-trap mass spectrometer (Thermo Fisher Scientific, San Jose, CA). A mixture of acetonitrile and water (50:50, v/v) was used as solvent for electrospray. The spray voltage was 3.0 kV, and the temperature for the ion transport tube was maintained at 275°C. High-resolution mass spectra (HRMS) were acquired on an Agilent 6510 Q-TOF LC/MS instrument equipped with an ESI source and an Agilent HPLC-Chip Cube MS interface.

LC-MS/MS

Quantitative analysis of S^6mdG and ^{S}dG in the above DNA hydrolysates was performed by online capillary HPLC-ESI-MS/MS using an Agilent 1200 capillary HPLC pump interfaced with an LTQ linear ion trap mass spectrometer (Thermo Fisher Scientific, San Jose, CA). A 0.5×150 mm Zorbax SB-C18 column (5 μm in particle size,

Agilent Technologies) was used for the separation of the DNA hydrolysis mixture and the flow rate was 6.0 μL/min. A gradient of 0-20% methanol (in 5-min) followed by 20-80% methanol (in 40-min) in water with 0.1% formic acid was employed for the detection of ^{S}dG and S^{6}mdG. The effluent from the LC column was directed to the LTQ mass spectrometer, which was set up for MS/MS analysis, where the fragmentation of the protonated ions of unlabeled and labeled ^{S}dG and S^{6}mdG was monitored.

The level of ^{S}GTP in different cancer cells upon 6-thioguanine treatment was quantified by on-line LC-MS/MS experiments. 6-Thioguanine metabolites were separated by using a 0.5×150 mm Zorbax SB-C18 column (5 μm in particle size, Agilent Technologies) at the flow rate of 6.0 μL/min. A gradient of 40 min of 0-25% methanol followed by a 15 min of 20-60% methanol in 400 mM 1,1,1,3,3,3-hexafluoroisopropanol (HFIP, pH was adjusted to 7.0 by addition of triethylamine) was employed. The voltage for electrospray was 4.0 kV, and the ion transport tube of the mass spectrometer was maintained at 300°C to minimize the formation of HFIP adducts. The LC effluent was analyzed by MS/MS by monitoring the fragmentation of the deprotonated guanosine triphosphate (GTP) and ^{S}GTP.

Cell Viability Assay

Jurkat T, CCRF-CEM, HL-60, K-562 and HCT-116 cells were separately seeded in 6-well plates at a density of ~ 3×10^{5} cells/mL. To the cultured cells was added 6-thioguanine until its final concentration was 1.0 or 3.0 μM. After 24 or 48 hrs of

treatment, cells were stained with trypan blue and counted on a hemocytometer to measure cell viability.

Results and Discussion

6-MP and ^{S}G are widely used for treating acute lymphoblastic leukemia. It is generally believed that DNA ^{S}G is the ultimate metabolite for thiopurines to exert their cytotoxic effects (*52*). However, the cytotoxic mechanism through which DNA ^{S}G results in cell death remains elusive. Based on the observations that DNA ^{S}G can be spontaneously methylated by *S*-AdoMet to give *S*^{6}mG and the resulting *S*^{6}mG:T mispair formed from DNA replication may trigger the mismatch repair pathway, it was hypothesized that ^{S}G may confer its cytotoxic effect via futile cycles of repair synthesis triggered by DNA *S*^{6}mG (*73*).

Our recent study showed that ^{S}dG is mutagenic in *E. coli* cells, it can give rise to ~10% G→A mutation, whereas *S*^{6}mdG is highly mutagenic, with G→A mutation occurring at a frequency of 94% (*77*). This result led us to suggest that ^{S}G might trigger mismatch repair pathway without being methylated to *S*^{6}mG. As an important step toward understanding the relative contributions of these two pathways, we developed a sensitive LC-MS/MS coupled with stable isotope dilution method and quantified the levels of ^{S}dG and *S*^{6}mdG in genomic DNA of leukemic cells treated with ^{S}G.

Synthesis and Characterization of Isotope-labeled S^{6}mdG and ^{S}dG

Uniformly ^{15}N-labeled dG was reacted with trifluoroacetic anhydride in the presence of pyridine to form the putative 6-pyridyl intermediate, which was converted to

[U-$^{15}N_5$]-^{S}dG upon treatment of NaSH in DMF (Scheme 4.2a). The desired product was purified from the mixture by HPLC. High-resolution ESI MS gives *m/z* 289.0653 for the $[M+H]^+$ ion of [U-$^{15}N_5$]-^{S}dG, which is consistent with the calculated *m/z* of 289.0664 with a deviation of 3.8 ppm. Collision-induced dissociation of the ion of *m/z* 289.0 led to the formation of the fragment ion of *m/z* 173.1, which is attributed to the elimination of a 2-deoxyribose moiety (Figure 4.1b). Further fragmentation of the *m/z* 173.1 ion gave product ions of *m/z* 155.1, 139.1 and 129.0, which were originated from the losses of a $^{15}NH_3$, an H_2S, and a $C(^{15}NH)_2$, respectively, from the uniformly ^{15}N-labeled nucleobase portion (Figure 4.1c).

D_3-S^6mdG was prepared from the reaction of ^{S}dG with CD_3I in a phosphate buffer (Scheme 4.2b) and purified from the reaction mixture by HPLC. High-resolution ESI MS gives *m/z* 301.1145 for the $[M+H]^+$ ion of D_3-S^6mdG, which is consistent with the calculated *m/z* of 301.1157 with a deviation of 3.9 ppm. MS/MS of the ion of *m/z* 300.9 (Figure 4.2a) shows the predominant fragment ion of *m/z* 185.2, which again arises from the elimination of a 2-deoxyribose moiety (Figure 4.2b).

Analytical Strategy for the Quantification of ^{S}dG and S^6mdG by LC-MS/MS

^{S}G has been shown to be more efficacious than 6-MP in human ALL cell lines and in lymphoblasts from childhood ALL both in preclinical (*193*) and clinical studies (*194*). In addition, ^{S}G has more direct intracellular activation pathway to form ^{S}G nucleotide than 6-MP (Scheme 4.1); therefore, we decided to use ^{S}G to treat human ALL cells. Viewing that the peak concentration of ^{S}G in plasma was in the range of 0.2-1.2 μM after

Scheme 4.2 Synthesis of stable isotope-labeled 6-thio-2'-deoxyguanosine (a) and S^6-methylthio-2'-deoxyguanosine (b).

(a)

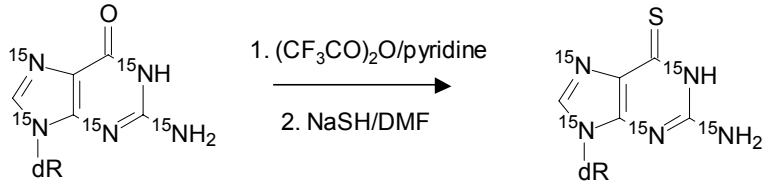

(b)

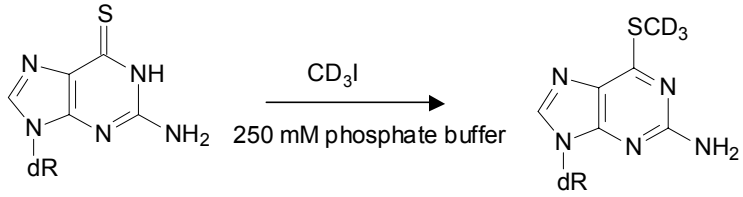

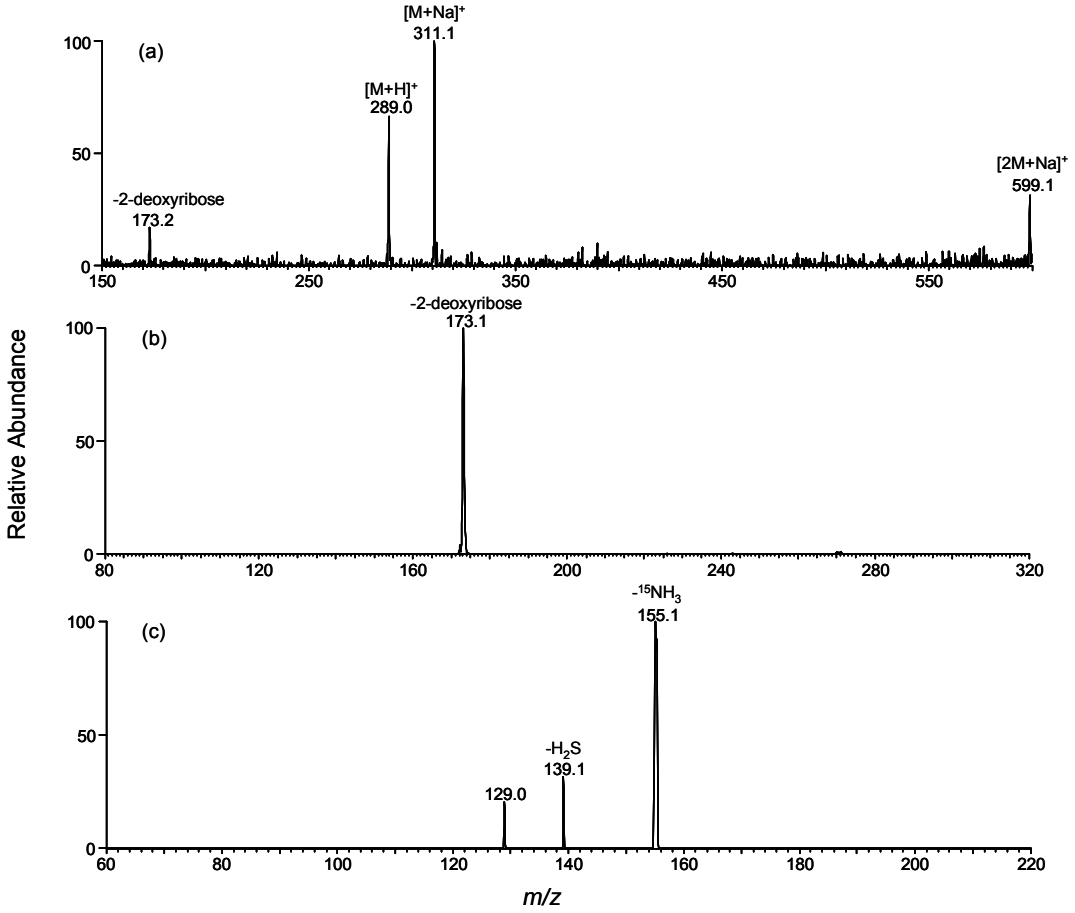

Figure 4.1 Positive ESI-MS of [U-$^{15}N_5$]-^{S}dG (a), and the MS/MS of the $[M+H]^+$ ion of *m/z* 289.0 (b), and shown in (c) is the MS/MS/MS of the ion of *m/z* 173.1 found in (b).

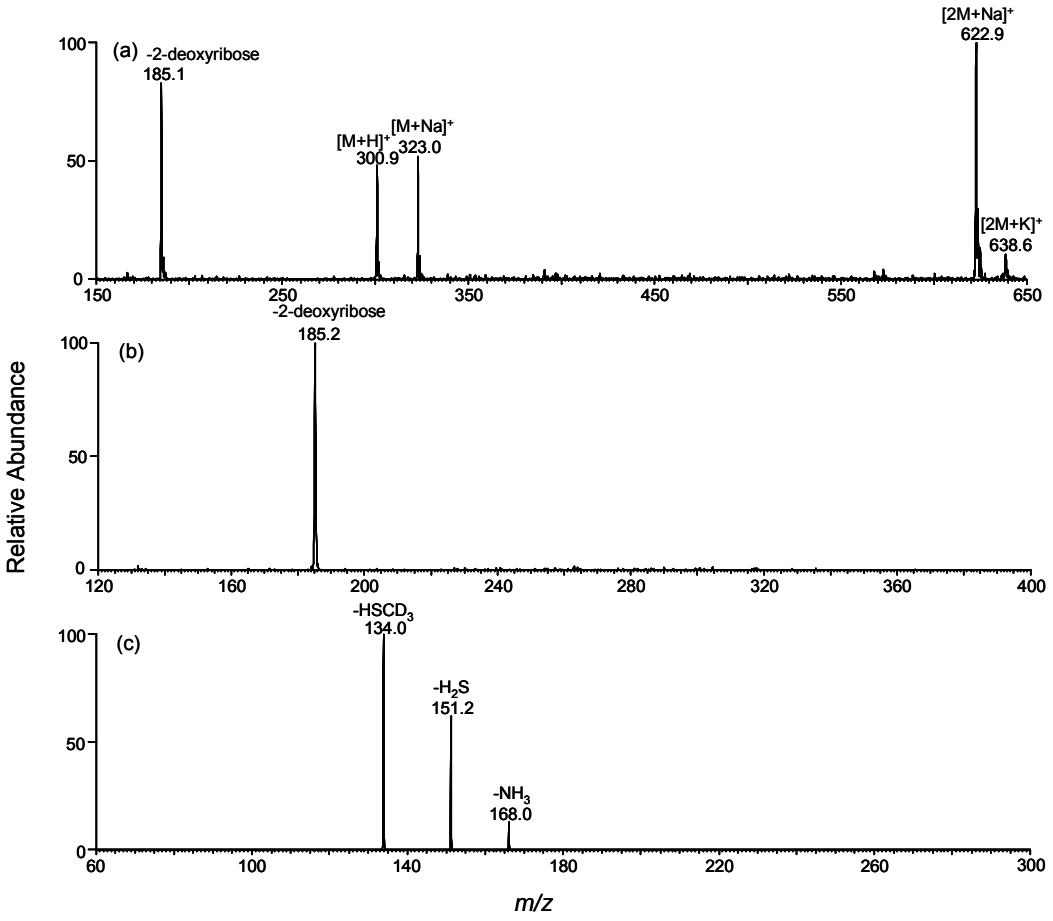

Figure 4.2 Positive ESI-MS of D_3-S^6mdG (a), and the MS/MS of the $[M+H]^+$ ion of *m/z* 301.0 (b).

oral ^{S}G administration (60 mg/m^2) and 1.3-4.1 μM after continuous intravenous infusion (20 mg/m^2/h) (*194*), we treated human ALL cells with 1 and 3 μM of ^{S}G for 24 hrs and isolated the genomic DNA from the treated and control untreated cells. To quantify ^{S}dG and *S*^{6}mdG in genomic DNA isolated from ^{S}G-treated human cancer cell lines, we first digested the DNA with nuclease P1 to yield nucleoside 5'-monophosphates, which were subsequently dephosphorylated with alkaline phosphatase. Due to the trace amount of *S*^{6}mdG present in DNA, the nucleoside mixture was subsequently separated by offline HPLC, and the fractions containing these two lesions were collected and dried. After being reconstituted in H_2O, ^{S}dG and *S*^{6}mdG were analyzed by LC-ESI-MS/MS. Owing to the better sensitivity afforded by the positive- than the negative-ion mode, we quantified ^{S}dG and *S*^{6}mdG by LC-MS/MS in the positive-ion mode, where we added 0.1% formic acid to the mobile phases to facilitate the protonation of the analytes. The quantitation of these two lesions was based on the peak area ratio between the analyte and its isotope-labeled counterpart found in the selected-ion chromatograms (SICs) and the constructed calibration curves (Figure 4.3).

We monitored the *m/z* 284→168 and *m/z* 289→173 transitions for ^{S}dG and its uniformly ^{15}N-labeled counterpart, respectively. The identity of the component eluting at 20.4 min in the SIC of Figure 1a was determined to be ^{S}dG based on the same retention time (Figure 4.4b) and similar tandem mass spectrum as those observed for [U-$^{15}N_5$]-^{S}dG (Figure 4.5a&b). The component eluting at 16.2 min in Figure 1a was identified as 8-oxodG. In this context, 8-oxodG and ^{S}dG bear the same nominal molecular weight and these two nucleosides undergo the same fragmentation in MS/MS, i.e., with the loss of

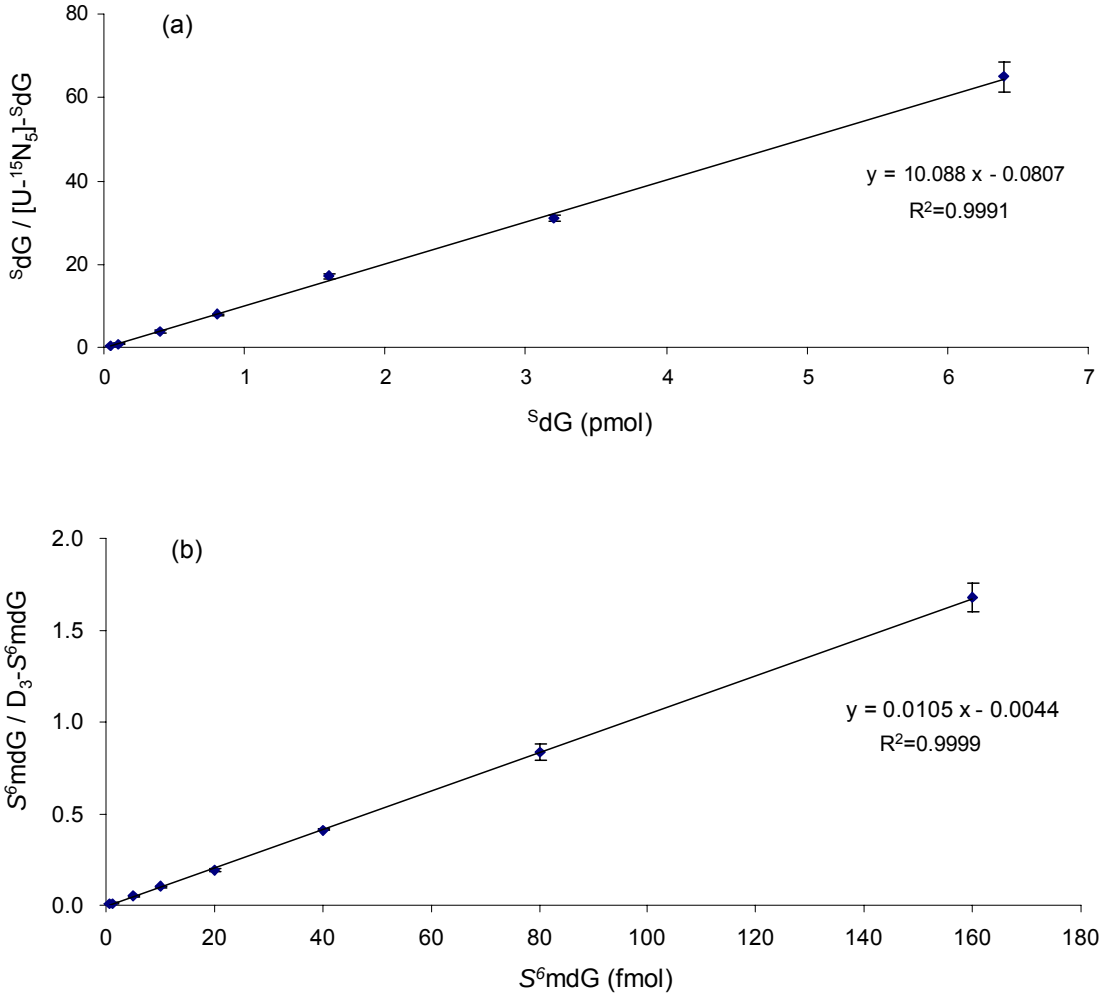

Figure 4.3 Calibration curves for the quantification of ^{S}dG (a) and S^6mdG (b). The amounts of [U-^{15}N$_5$]-^{S}dG (a) and D$_3$-S^6mdG (b) added were 100 fmol. Error bars represent standard deviations resulting from three independent measurements.

2-deoxyribose being the dominant fragmentation pathway. However, 8-oxodG and ^{S}dG can be well resolved by capillary HPLC under the conditions we employed. Furthermore, fragmentations of the nucleobase moieties of 8-oxodG and ^{S}dG gave distinctive MS/MS/MS; the spectrum of ^{S}dG displays the loss of an NH_3, $C(NH)_2$ and H_2S (Figure 4.1c depicts the MS/MS/MS for the uniformly ^{15}N-labeled ^{S}dG), whereas that of 8-oxodG shows the predominant losses of H_2O (*m/z* 150.1) and NH_3 (*m/z* 151.0) molecules (Figure 4.6b).

S^{6}mdG and D_3-*S*^{6}mdG were monitored by the *m/z* 298→182 and *m/z* 301→185 transitions, respectively. The fraction eluting at 23.4 min in the SIC shown in Figure 1c was identified as *S*^{6}mdG based on the same retention time (Figure 4.4d) and similar MS/MS as those of D_3-*S*^{6}mdG (MS/MS are shown in Figure 4.5c&d). In this context, aside from the most abundant ion at *m/z* 182, there was another ion of *m/z* 253.1 present in Figure 2c. Viewing that the corresponding fragment could not be found in the MS/MS of the internal standard (Figure 4.5d), we speculate that the latter fragment ion might arise from some isobaric species present in the sample.

Quantification of ^{S}dG and S^{6}mdG in Leukemia Cells upon ^{S}G Treatment

LC-MS/MS with the isotope dilution method constitutes a reliable quantification method. In this study, we added isotope-labeled [U-$^{15}N_5$]-^{S}dG and D_3-*S*^{6}mdG to the samples prior to the enzymatic hydrolysis of genomic DNA, which corrected for the potential analyte loss during various stages of sample preparation process. Limits of quantification (LOQ) for our LC-MS/MS method were assessed prior to the analysis of

cellular DNA samples. It turned out that, when the pure standards were analyzed, the LOQs at an S/N of 10 were found to be 6.8 and 0.25 fmol for ^{S}dG and *S*^{6}mdG, respectively. Due to the ion suppression induced by the co-eluting unmodified nucleosides and/or other species, the corresponding LOQs for ^{S}dG and *S*^{6}mdG in nucleoside mixtures of genomic DNA were determined to be 62 and 0.6 fmol, respectively.

We quantified the levels of ^{S}dG and *S*^{6}mdG in cellular DNA of five different cancer cell lines that were cultured for 24 hrs in a medium containing 1 or 3 μM ^{S}G. The quantification results revealed a dose-dependent incorporation of ^{S}dG in all cell lines and Jurkat T cells have the highest level of ^{S}dG incorporation in DNA; upon treatment with 1 and 3 μM of ^{S}G, genomic DNA isolated from these cells has approximately 2% and 10% of dG being replaced with ^{S}dG, respectively (Figure 4.7a). HL-60 and CCRF-CEM cells exhibit similar levels of ^{S}dG incorporation; a 24-h ^{S}G treatment induced 2-4% and 6-7% of dG replacement upon treatment with 1 and 3 μM of the drug, respectively. Among all studied leukemia cells, K-562 cells exhibit the lowest level of ^{S}dG incorporation, whereas less than 1% and 4% replacements were observed when the cells were treated with 1 and 3 μM of ^{S}G, respectively. HCT-116, a human colorectal carcinoma cell line, has also been investigated in this study because a previous study showed that ^{S}G replaced approximately 0.2% of DNA guanine in HCT-116 cells grown for 24 hrs in a medium containing 1 μM ^{S}G (*74*). We, however, observed that ^{S}G substituted approximately 0.004% and 0.2% of DNA guanine in HCT-116 cells grown for 24 hrs in a medium containing 1 and 3 μM ^{S}G (Figure 4.7b).

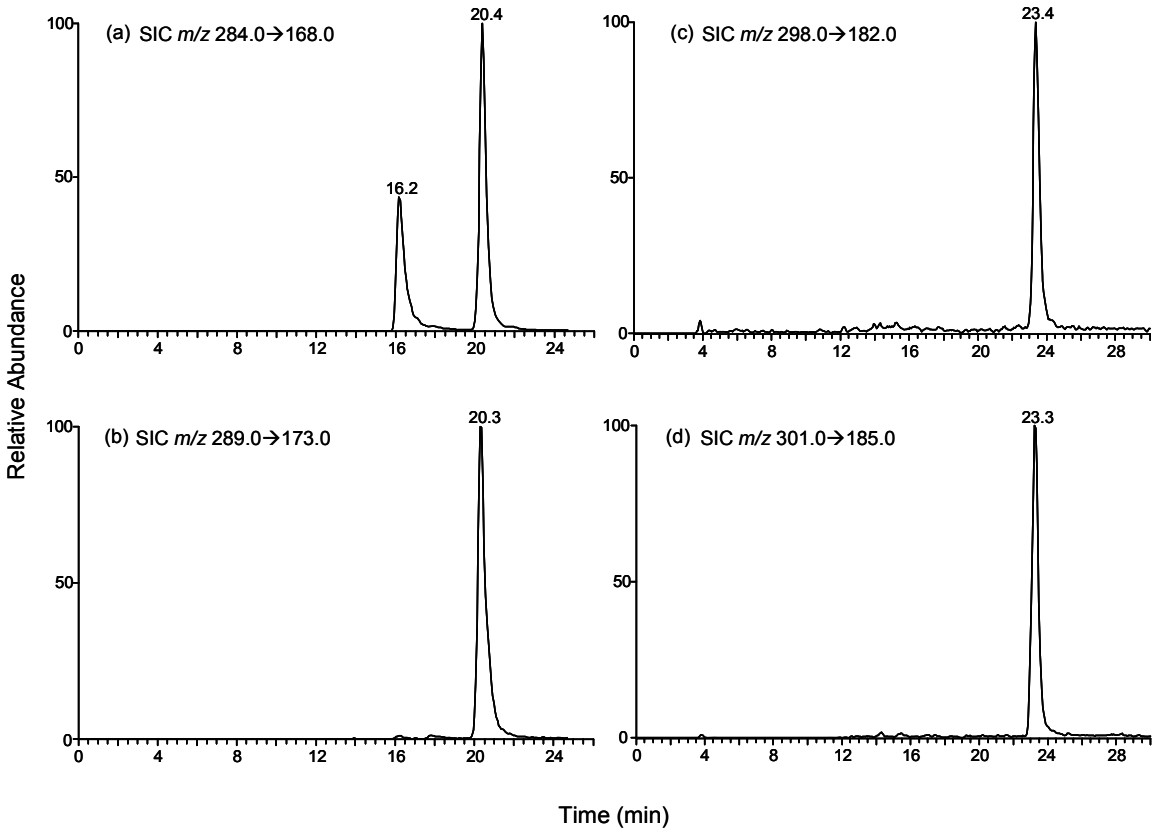

Figure 4.4 Selected-ion chromatograms (SICs) for monitoring the *m/z* 284→168 (a) and *m/z* 289→173 (b) transitions for ^{S}dG and [U-$^{15}N_5$]-^{S}dG; *m/z* 298→182 (c) and *m/z* 301→185 (d) transitions for S^6-mdG and D_3-S^6mdG, respectively, in CCRF-CEM cells treated with 3 μM 6-thioguanine for 24 hrs.

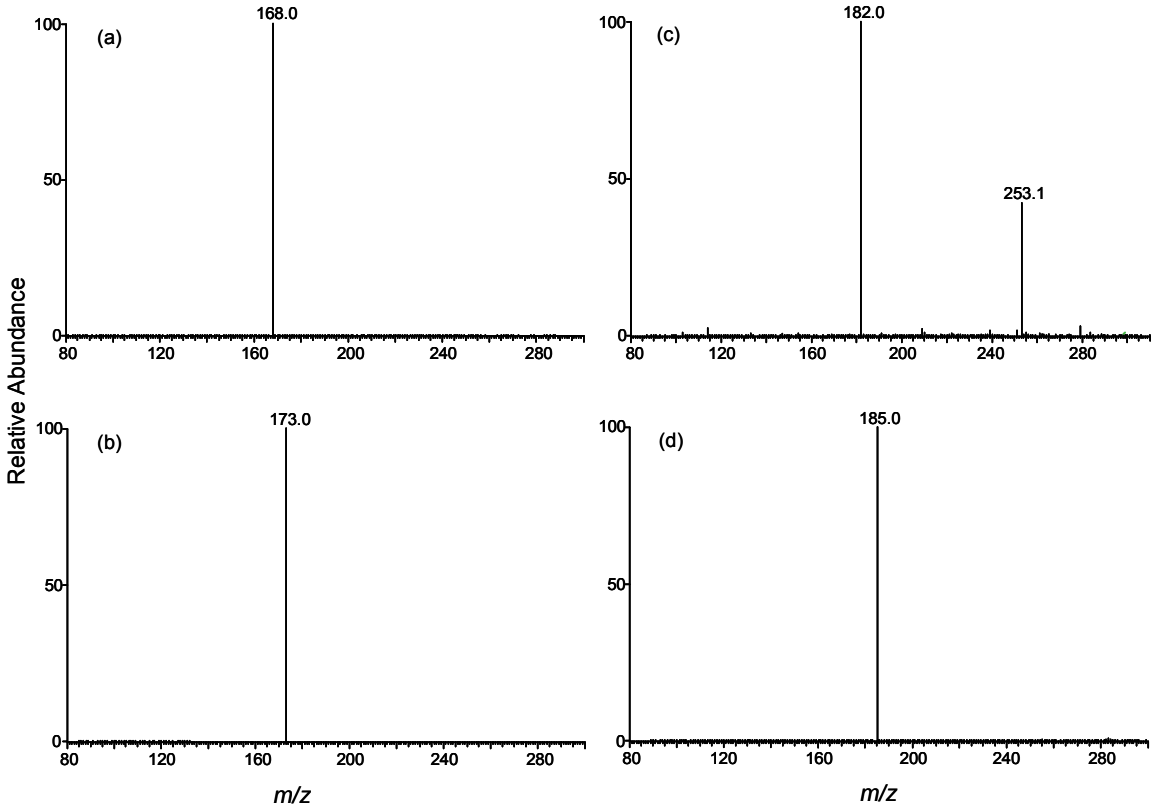

Figure 4.5 Product-ion spectra of the ions of *m/z* 284 (a), *m/z* 289 (b), *m/z* 298 (c), and *m/z* 301 (d). Panels (a) and (c) are for unlabeled, and (b) and (d) are for the [U-$^{15}N_5$]-^{S}dG and D_3-S^6mdG, respectively. The sample was the nucleoside mixture of DNA extracted from CCRF-CEM cells treated with 3 μM 6-thioguanine for 24 hrs.

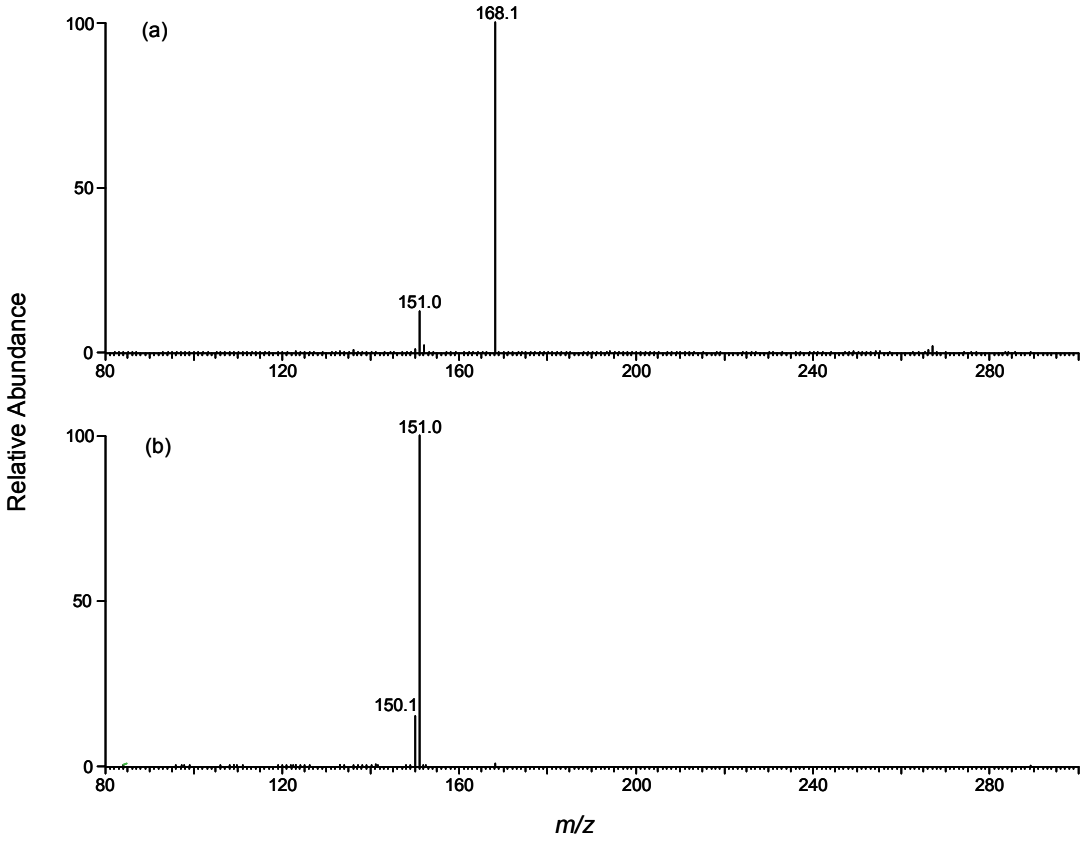

Figure 4.6 Positive-ion ESI-MS/MS (a) and MS/MS/MS (b) spectra of 8-oxo-2'-deoxyguanosine.

We also examined the cell viability in the above five cell lines upon ^{S}G treatment (shown in Figure 4.8a&b). Consistent with the incorporation rate of ^{S}G, the most pronounced cell death was found for Jurkat T cells, i.e., the cell viability dropped by 10% and 30% after a 24-hr treatment with 1 and 3 μM ^{S}G, respectively, whereas a 48-hr ^{S}G treatment resulted in 25% and 60% cell death. HL-60 and CCRF-CEM cells showed 5% and 9% cell death with the same treatment, but 9% and 30% after 48-hr incubation; in these two cell lines, the level of ^{S}dG in genomic DNA was lower than that in Jurkat T cells. Among all studied leukemia cell lines, K-562 cells displayed the maximum resistance toward ^{S}G treatment, which is in line with the lowest level of ^{S}dG incorporation being observed for this cell line (Figure 4.7a).

The accurate quantification of ^{S}dG and *S*^{6}mdG in the above cell lines also allowed for the determination of the extent of methylation of ^{S}dG in genomic DNA from the ^{S}G-treated leukemic cells. Our results revealed that the extent of *S*^{6}mdG converted from ^{S}dG was very low (Figure 4.9). Less than 2 out of 10^{5} ^{S}dG in DNA was converted to *S*^{6}mdG in Jurkat T cells treated with 3 μM of ^{S}G, followed by 4 and 7 per 10^{5} ^{S}dG being replaced in HL-60 and CCRF-CEM cells, and then 16 per 10^{5} ^{S}dG in K-562 cells. Despite the low level of ^{S}dG incorporation in HCT-116 cells, DNA isolated from this cell line was found to bear the highest level of conversion from ^{S}dG to *S*^{6}mdG, i.e., 64 and 36 out of 10^{5} ^{S}dG were substituted when the cells were treated with 1 and 3 μM ^{S}G, respectively. Considering that, in *E. coli* cells, ^{S}dG and *S*^{6}mdG can induce G→A mutation at frequencies of 10% and 94%, respectively, and several out of 10^{5} ^{S}dG in DNA are

converted to S^6mdG, we reason that the ^{S}G:T mispairs may assume the major role in triggering the MMR pathway, while the S^6mG:T mispairs may be partially involved.

To investigate whether the difference in ^{S}dG incorporation into genomic DNA in the above five cancer cell lines is due to drug uptake or drug metabolism, we assessed quantitatively the level of ^{S}GTP in the nucleotide pool of these cancer cells by using LC-MS/MS. GTP was employed as internal standard. We monitored the *m/z* 522→424 and *m/z* 538→440 transitions for GTP and ^{S}GTP, respectively. The components eluting at 37.5 min and 37.8 min in the SICs displayed in Figure 4.10a&b were attributed to GTP and ^{S}GTP based on their fragmentation patterns. In MS/MS shown in Figure 4.10c&d, the loss of 18 and 98 Da was due to the neutral loss of water and phosphoric acid from both analytes, respectively. The ion of 371.1 was attributed to the loss of guanine or 6-thioguanine, and this ion can further eliminate one and two H_3PO_4 to render the ion of *m/z* 273.3 and 176.9, respectively (Insets of Figure 4.10c&d). Our result in Figure 4.11 revealed a dose-dependent formation of ^{S}GTP in the ^{S}G-exposed leukemia cell lines (Jurkat T, CCRF-CEM, HL-60 and K-562), while ^{S}GTP was not detected in the control untreated cells. The level of ^{S}GTP in the nucleotide pool of the above four cell lines is consistent with the percentage of ^{S}G incorporation into genomic DNA. However, the amount of ^{S}GTP was found to be significantly higher in CCRF-CEM cells. In addition, we were not able to detect ^{S}GTP in the nucleotide pool of HCT-116 cells, which is in line with the extremely low level of ^{S}G incorporation into genomic DNA of this cell line treated with ^{S}G (Figure 4.7). In the future, other relevant 6-thioguanine nucleotide

metabolites need to be measured to reveal the mechanism leading to the variation in ^{S}dG incorporation into genomic DNA of different cell lines.

Our developed LC-MS/MS coupled with stable isotope dilution method facilitates the accurate detection of ^{S}dG in human ALL cells induced by ^{S}G treatment from 3 nmol of digested nucleoside mixture, which is generated from ~1 μg of DNA. Furthermore, we achieved a detection limit of 0.7 fmol of S^{6}mdG in 50 μg of digested DNA, which corresponds to 4 lesions per 10^{9} unmodified nucleobases. This method obviates the need of ^{3}H-labeling while maintaining good sensitivity and it also facilitates the monitoring of both ^{S}G and its methylated metabolite in DNA. Moreover, LC-MS/MS can provide structure information for the analytes, which allows for the unambiguous identification and accurate quantification of these two modified nucleosides in DNA.

Taken together, we developed a sensitive LC-MS/MS coupled with stable isotope dilution method for the simultaneous quantification of the levels of ^{S}dG and S^{6}mdG in leukemic cells treated with ^{S}G. Our results suggest that DNA ^{S}G, instead of its methylated derivative (S^{6}mG), may take the major role in invoking the post-replicative MMR pathway. In addition, as ^{S}G nucleotide metabolite, ^{S}GTP was quantified by LC-MS/MS.

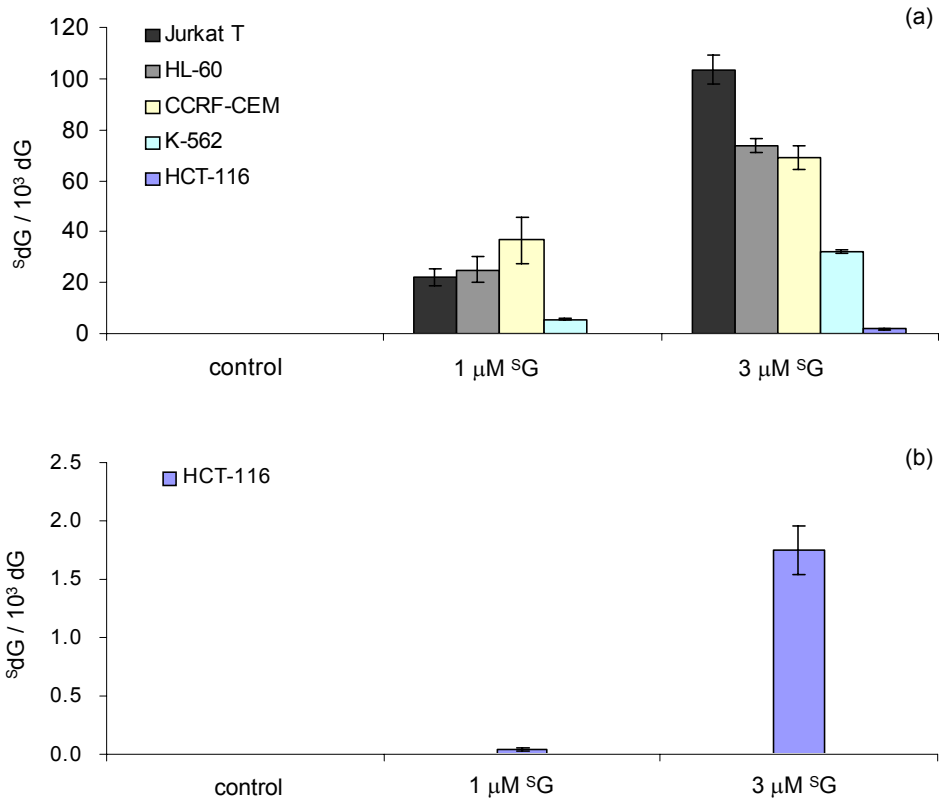

Figure 4.7 The incorporation of ^{S}dG in genomic DNA of human Jurkat T, HL-60, CCRF-CEM, K-562 and HCT-116 cells (a). In panel (b), the scale was enlarged to view better the incorporation of ^{S}dG in DNA of HCT-116 cells.

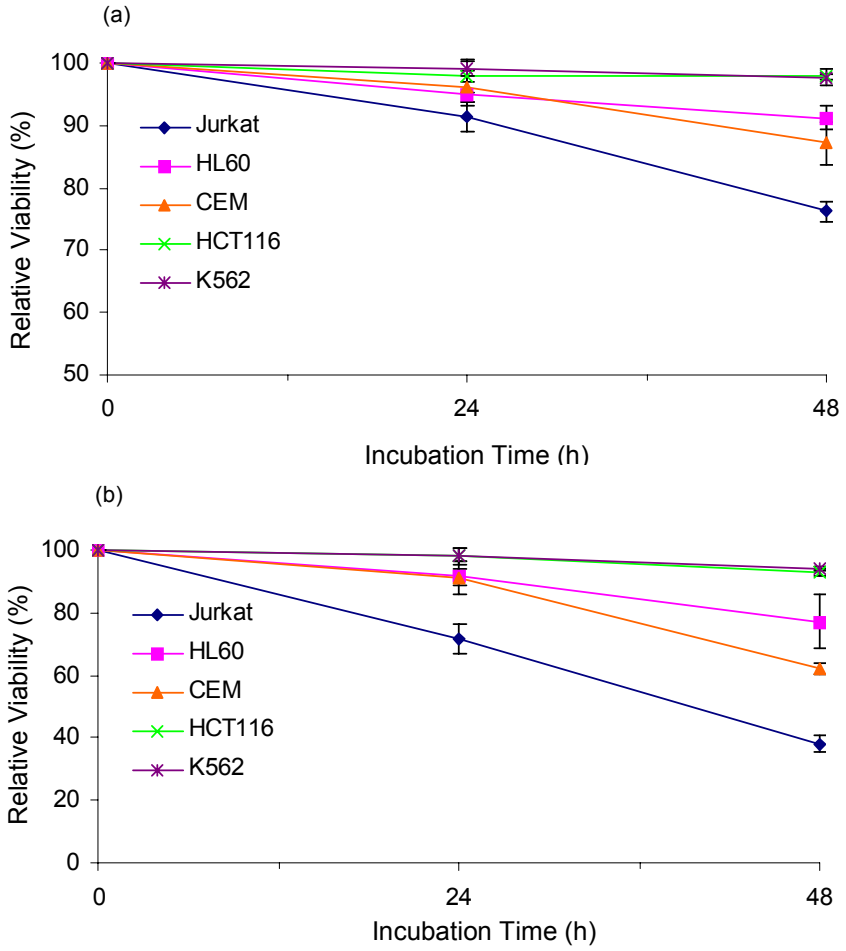

Figure 4.8 The relative viabilities of human cells after 24 and 48 hrs of treatment with 1 μM (a) and 3 μM (b) 6-thioguanine compared to untreated cells.

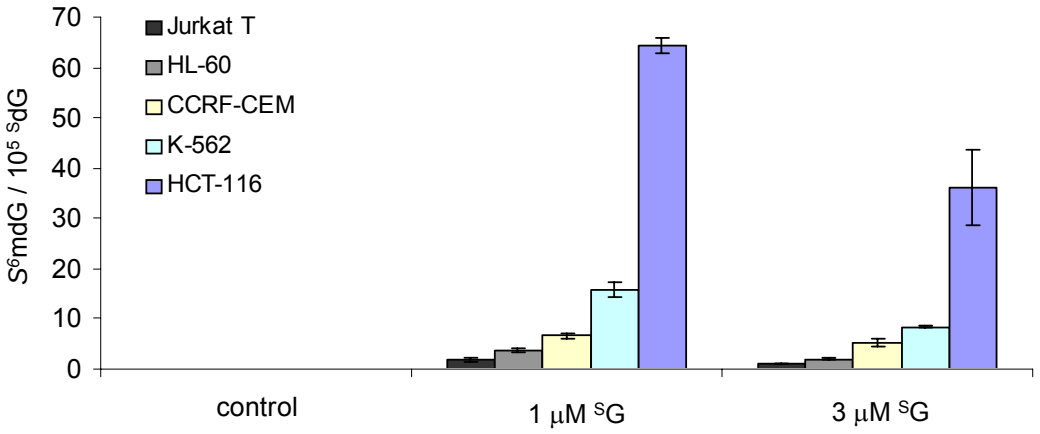

Figure 4.9 The formation of S^6mdG in genomic DNA of human Jurkat T, HL-60, CCRF-CEM, K-562 and HCT-116 cells.

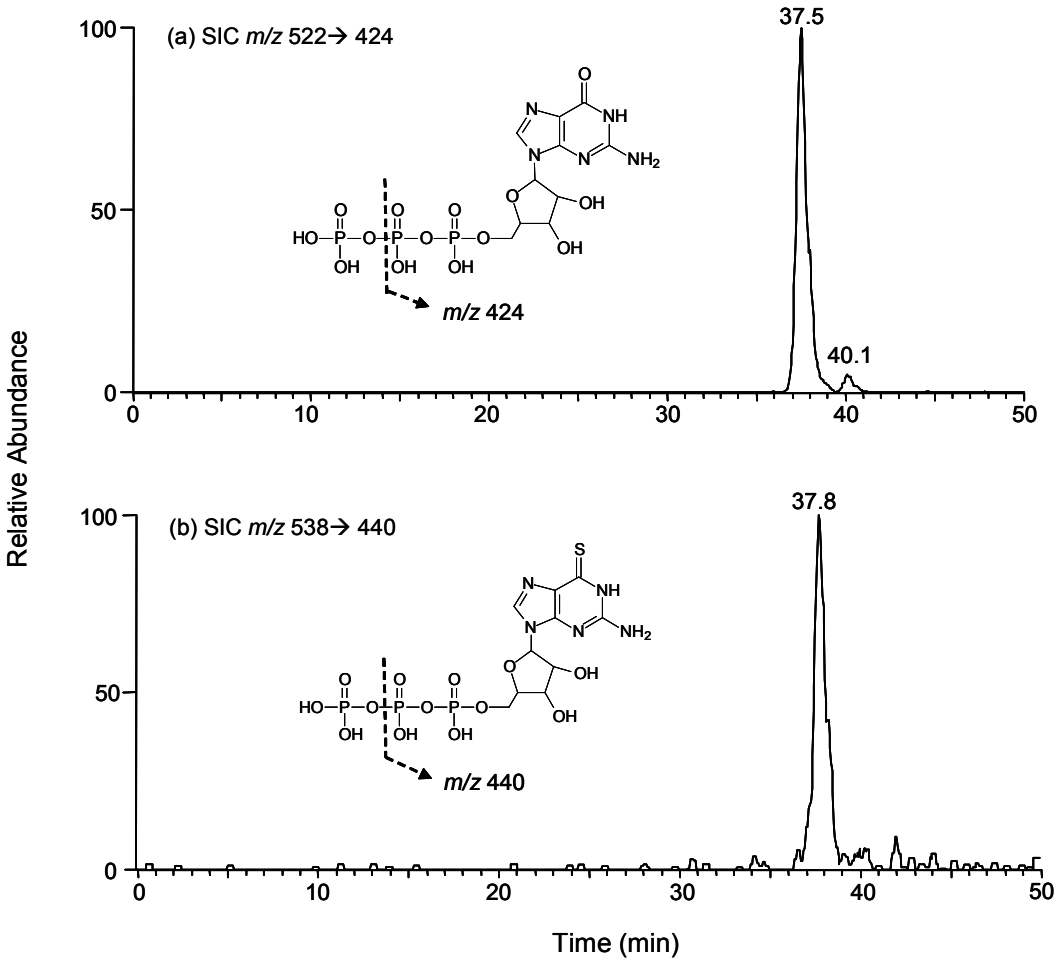

Figure 4.10 Selected-ion chromatograms (SICs) of GTP (a) and ^{S}GTP (b) in the ribonucleotide pool of extracted metabolites from human cancer cells upon treatment with 3 μM ^{S}G.

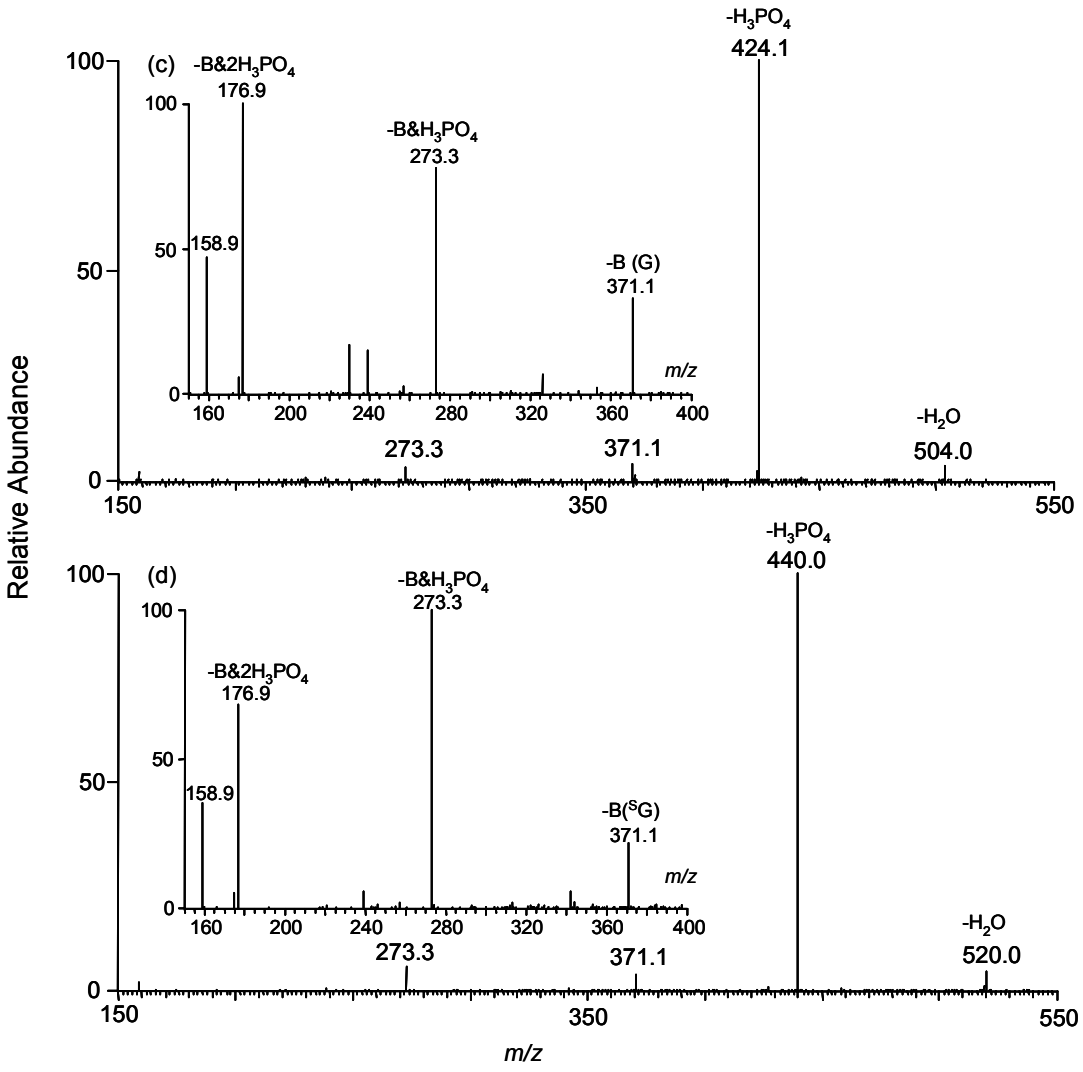

Figure 4.10 (c) and (d) are the MS/MS of the $[M - H]^-$ ions of GTP (*m/z* 522, top) and ^{S}GTP (*m/z* 538, bottom), respectively. Depicted in the two insets of (c) and (d) are the enlarged spectra from *m/z* 150 to 400.

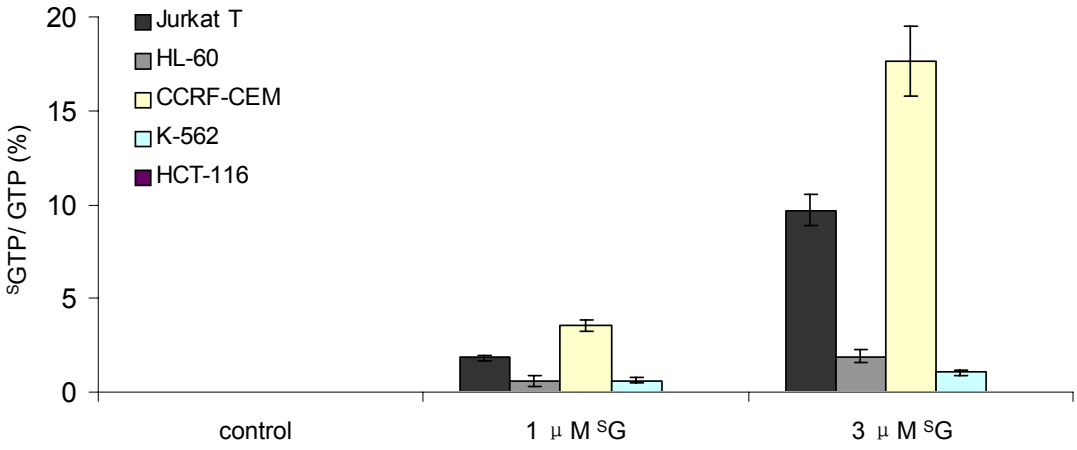

Figure 4.11 The levels of ^{S}GTP in five human cancer cell lines (Jurkat T, HL-60, CCRF-CEM, K-562 and HCT-116) that are untreated, or treated with 1 or 3 μM ^{S}G for 24 hrs.

References

(1) Pui, C. H. and Evans, W. E. (1998) Acute lymphoblastic leukemia. *N. Engl. J. Med. 339*, 605-615.

(2) Elion, G. B. (1989) The purine path to chemotherapy. *Science 244*, 41-47.

(3) Burchenal, J. H., Murphy, M. L., Ellison, R. R., Sykes, M. P., Tan, T. C., Leone, L. A., Karnofsky, D. A., Craver, L. F., Dargeon, H. W. and Rhoads, C. P. (1953) Clinical evaluation of a new antimetabolite, 6-mercaptopurine, in the treatment of leukemia and allied diseases. *Blood 8*, 965-999.

(4) Murray, J. E., Harrison, J. H., Dammin, G. J., Wilson, R. E. and Merrill, J. P. (1963) Prolonged survival of human-kidney homografts by immunosuppressive drug therapy. *N. Engl. J. Med. 268*, 1315-&.

(5) McLeod, H. L., Krynetski, E. Y., Relling, M. V. and Evans, W. E. (2000) Genetic polymorphism of thiopurine methyltransferase and its clinical relevance for childhood acute lymphoblastic leukemia. *Leukemia 14*, 567-572.

(6) Schutz, E., Gummert, J., Mohr, F. and Oellerich, M. (1993) Azathioprine-induced myelosuppression in thiopurine methyltransferase deficient heart-transplant recipient. *Lancet 341*, 436-436.

(7) Evans, W. E., Horner, M., Chu, Y. Q., Kalwinsky, D. and Roberts, W. M. (1991) Altered mercaptopurine metabolism, toxic effects, and dosage requirement in a thiopurine methyltransferase-deficient child with acute lymphocytic-leukemia. *J. Pediatr. 119*, 985-989.

(8) McLeod, H. L., Miller, D. R. and Evans, W. E. (1993) Azathioprine-induced

myelosuppression in thiopurine methyltransferase deficient heart-transplant recipient. *Lancet 341*, 1151-1151.

(9) Krynetski, E. Y., Tai, H. L., Yates, C. R., Fessing, M. Y., Loennechen, T., Schuetz, J. D., Relling, M. V. and Evans, W. E. (1996) Genetic polymorphism of thiopurine S-methyltransferase: Clinical importance and molecular mechanisms. *Pharmacogenetics 6*, 279-290.

(10) Tiede, I., Fritz, G., Strand, S., Poppe, D., Dvorsky, R., Strand, D., Lehr, H. A., Wirtz, S., Becker, C., Atreya, R., Mudter, J., Hildner, K., Bartsch, B., Holtmann, M., Blumberg, R., Walczak, H., Iven, H., Galle, P. R., Ahmadian, M. R. and Neurath, M. F. (2003) CD28-dependent Rac1 activation is the molecular target of azathioprine in primary human CD4(+) T lymphocytes. *J. Clin. Invest. 111*, 1133-1145.

(11) Wang, H. X. and Wang, Y. S. (2009) 6-Thioguanine perturbs cytosine methylation at the CpG dinucleotide site by DNA methyltransferases in vitro and acts as a DNA demethylating agent in Vivo. *Biochemistry 48*, 2290-2299.

(12) Christie, N. T., Drake, S., Meyn, R. E. and Nelson, J. A. (1984) 6-thioguanine-induced DNA damage as a determinant of cyto-toxicity in cultured Chinese-hamster ovary cells. *Cancer Res. 44*, 3665-3671.

(13) Pan, B. F. and Nelson, J. A. (1990) Characterization of the DNA damage in 6-thioguanine-treated cells. *Biochem. Pharmacol. 40*, 1063-1069.

(14) Maybaum, J. and Mandel, H. G. (1981) Differential chromatid damage induced by 6-thioguanine in cho-cells. *Exp. Cell Res. 135*, 465-468.

(15) Bodell, W. J. (1991) Molecular dosimetry of dister chromatid exchange induction in 9l cells treated with 6-thioguanine. *Mutagenesis 6*, 175-177.

(16) Swann, P. F., Waters, T. R., Moulton, D. C., Xu, Y. Z., Zheng, Q. G., Edwards, M. and Mace, R. (1996) Role of postreplicative DNA mismatch repair in the cytotoxic action of thioguanine. *Science 273*, 1109-1111.

(17) Yuan, B. F. and Wang, Y. S. (2008) Mutagenic and cytotoxic properties of 6-thioguanine, S-6-methylthioguanine, and guanine-S-6-sulfonic acid. *J. Biol. Chem. 283*, 23665-23670.

(18) Griffin, S., Branch, P., Xu, Y. Z. and Karran, P. (1994) Dna mismatch binding and incision at modified guanine bases by extracts of mammalian-cells - Implications for tolerance to DNA methylation damage. *Biochemistry 33*, 4787-4793.

(19) Waters, T. R. and Swann, P. F. (1997) Cytotoxic mechanism of 6-thioguanine: hMutS alpha, the human mismatch binding heterodimer, binds to DNA containing S-6-methylthioguanine. *Biochemistry 36*, 2501-2506.

(20) Dervieux, T., Chu, Y. Q., Su, Y., Pui, C. H., Evans, W. E. and Relling, M. V. (2002) HPLC determination of thiopurine nucleosides and nucleotides in vivo in lymphoblasts following mercaptopurine therapy. *Clin. Chem. 48*, 61-68.

(21) Keuzenkampjansen, C. W., Deabreu, R. A., Bokkerink, J. P. M. and Trijbels, J. M. F. (1995) Determination of extracellular and intracellular thiopurines and methylthiopurines by high-performance liquid-chromatography. *J. Chromatogr. B- Biomed. Appl. 672*, 53-61.

(22) Kroplin, T., Weyer, N., Gutsche, S. and Iven, H. (1998) Thiopurine

S-methyltransferase activity in human erythrocytes: a new HPLC method using 6-thioguanine as substrate. *European J. Clin. Pharmacol. 54*, 265-271.

(23) Rowland, K., Lennard, L. and Lilleyman, J. S. (1998) High-performance liquid chromatographic assay of methylthioguanine nucleotide. *J. Chromatogr. B 705*, 29-37.

(24) Dervieux, T., Meyer, G., Barham, R., Matsutani, M., Barry, M., Boulieu, R., Neri, B. and Seidman, E. (2005) Liquid chromatography-tandem mass spectrometry analysis of erythrocyte thiopurine nucleotides and effect of thiopurine methyltransferase gene variants on these metabolites in patients receiving azathioprine/6-mercaptopurine therapy. *Clin. Chem. 51*, 2074-2084.

(25) Kung, P. P. and Jones, R. A. (1991) One-flask syntheses of 6-thioguanosine and 2'-deoxy-6-thioguanosine. *Tetrahedron Lett. 32*, 3919-3922.

(26) Xu, Y. Z. (1996) Post-synthetic introduction of labile functionalities onto purine residues via 6-methylthiopurines in oligodeoxyribonucleotides. *Tetrahedron 52*, 10737-10750.

(27) Adamson, P. C., Poplack, D. G. and Balis, F. M. (1994) The cytotoxicity of thioguanine vs mercaptopurine in acute lymphoblastic-leukemia. *Leuk. Res. 18*, 805-810.

(28) Lowe, E. S., Kitchen, B. J., Erdmann, G., Stork, L. C., Bostrom, B. C., Hutchinson, R., Holcenberg, J., Reaman, G. H., Woods, W., Franklin, J., Widemann, B. C., Balis, F. M., Murphy, R. F. and Adamson, P. C. (2001) Plasma pharmacokinetics and cerebrospinal fluid penetration of thioguanine in children with acute

lymphoblastic leukemia: a collaborative pediatric oncology branch, NCI, and Children's Cancer Group study. *Cancer Chemother. Pharmacol. 47*, 199-205.

(29) O'Donovan, P., Perrett, C. M., Zhang, X. H., Montaner, B., Xu, Y. Z., Harwood, C. A., McGregor, J. M., Walker, S. L., Hanaoka, F. and Karran, P. (2005) Azathioprine and UVA light generate mutagenic oxidative DNA damage. *Science 309*, 1871-1874.

CHAPTER 5

Identification and Quantification of Cellular Proteins that Bind to 6-Thioguanine Containing Duplex DNA by SILAC, Affinity Purification and LC-MS/MS

Introduction

A common mechanism of cancer chemotherapy is to induce malignant cell apoptosis by damaging DNA (*195*). The treatment of cells with DNA-reactive compounds (e.g. cisplatin) or structural analogs of DNA precursors (e.g. gemcitabine, fludarabine and thiopurines) results in growth arrest and apoptosis (*196-198*). Previous studies demonstrated that distinct structure of damaged DNA provides the binding sites of damage-recognition proteins and subsequent assembly of multi-protein complex that are involved in maintaining the integrity and fidelity of genetic information (*199, 200*).

As a class of widely used antileukemic agents, thiopurines were shown to elicit their cytotoxicity by the conversion of these drugs into 6-thio-2'-deoxyguanosine triphosphate and its subsequent incorporation into DNA (*52*). This incorporation of 6-thioguanine results in local structural changes in DNA (*66*) and affects DNA-protein interactions, including the recognition of DNA by T4 ligase, RNase H and topoisomerase II (*57, 166*). Postreplicative mismatch repair proteins (MMR) proteins was proposed to induce thiopurine cytotoxicity through recognizing S^6mG:T mispair and inducing cell death through futile cycles of repair synthesis, where S^6mG arises from spontaneous methylation of 6-thioguanine by *S*-adenosyl-L-methionine and it is highly miscoding (*73*). Aside from the MMR system, recent studies suggested that other pathways may also

contribute to the cytotoxic effects of the thiopurine drugs. In this respect, thiopurines were found to be also cytotoxic to leukemia cell lines that are deficient in MMR pathway (*57, 201*). Given the importance of nucleic acid-binding proteins involved in gene regulation, DNA repair and oncogenesis, it is necessary to develop a general analytical technique to systematically identify proteins that can recognize 6-thioguanine in DNA.

Electrophoretic mobility shift assay (EMSA) is an extensively used assay for qualitative and quantitative characterization of protein-nucleic acid interactions (*202-204*). However, it is usually limited to *in vitro* interactions because the incubation of a purified protein or protein mixture with radio-labeled DNA probe is required. Chromatin immunoprecipitation (ChIP) is another common technique to identify DNA-binding proteins and their associated factors (*205, 206*) and it allows the characterization of *in vivo* interactions of specific proteins with DNA sequences through formaldehyde cross-linking in living cells(*207*). Due to their low-throughput, EMSA and ChIP are not suitable for studying the interaction between DNA sequences and many protein factors. In addition, these techniques are not amenable to the identification of unknown DNA-binding protein. Routine high-throughput identification of sequence-specific DNA-binding factors is mainly hampered by their low abundance, the degradation of their binding sites, and the non-specific binding of positively charged nuclear proteins to the negatively charged phosphate backbone of DNA (*142*).

Mass spectrometry (MS)-based proteomics allows for the identification and quantification of a large number of proteins in complex samples. Two-dimensional gel electrophoresis (2-D gel) coupled with MS has been reported to investigate DNA-binding

proteins isolated by using agarose immobilized with calf thymus DNA (*208*). However, 2-D gel is laborious which is not efficient in the proteome-wide identification of proteins. As a simple and efficient metabolic labeling method, SILAC-based LC-MS/MS analysis has been successfully developed to overcome the above-mentioned obstacles (*142*).

In this work, we employed SILAC, one-step affinity purification and LC-MS/MS to screen for cellular proteins in the nuclear proteome of Jurkat T human acute lymphoblastic leukemia cells that can recognize ^{S}G-bearing duplex DNA. We were able to quantify 39 proteins by using LC-MS/MS. Among these quantified proteins, 13 exhibited selective binding toward ^{S}G-bearing duplex DNA and 5 recognized more favorably to the control guanine-containing substrate over the ^{S}G-bearing counterpart. Identification of proteins capable of binding to ^{S}G-carrying duplex DNA may provide new insights into the determinants of drug sensitivity in cancer cells and other mechanisms by which thiopurines exert their cytotoxic effects.

Experimental Procedures

Materials

Heavy lysine and arginine ([$^{2}H_4$]-L-lysine and [$^{13}C_6$,$^{15}N_4$]-L-arginine) were purchased from Cambridge Isotope Laboratories (Andover, MA). All chemicals unless otherwise noted were from Sigma (St. Louis, MO). Jurkat T (Clone E6-1) acute lymphoblastic leukemia cells, penicillin, streptomycin, and Iscove's modified Dulbecoo's medium (IMDM) were purchased from ATCC (Manassas, VA, USA).

Preparation of Biotin-conjugated ODN Substrates Containing a Site-Specifically Inserted 6-Thioguanine

ODNs containing a 6-thioguanine were synthesized on a Beckman Oligo 1000S DNA synthesizer (Fullerton, CA) at 1-μmol scale. After solid-phase synthesis, the controlled pore glass support was treated with 1.0 M DBU (1,8-diazabicyclo[5.4.0]undec-7-ene) in anhydrous acetonitrile at room temperature for 5 hrs to remove the cyanoethyl protecting group on the thionucleoside. The solid support was subsequently treated with 50 mM NaSH in concentrated NH_4OH solution at room temperature for 24 hrs to complete the deprotection. The 15-mer ODN bearing biotin group at 5' end, 5'-Biotin-d(TGGCAGGTATCCATG), d(ACCCGGTGACACACC), 20-mer template DNA, d(GTCACCGGGTACTGGATACC), and a 30-mer complementary strand, d(GGTGTGTCACCGGGTACTGGATACCTGCCA) were purchased from Integrated DNA Technology Inc. (IDT, San Diego, CA). The synthesized 15-mer ODN, d(ACCC^{S}GGTGACACACC) together with above four substrates were purified by HPLC and their identities were confirmed by electrospray ionization-mass spectrometry (ESI-MS) and tandem MS (MS/MS) measurements.

The above 15-mer ^{S}G-bearing and unmodified guanine-bearing ODNs were ligated with 5'-Biotin-d(TGGCAGGTATCCATG) in the presence of template DNA to afford the 5'-Biotin-d(TGGCAGGTATCCAGTACCC^{S}GGTGACACACC) and 5'-Biotin-d (TGGCAGGTATCCAGTACCCGGTGACACACC), respectively (Table 5.1). The ligation reaction was performed at 16°C overnight with 5 nmol each of the two short ODNs along with template DNA and 1200 units of T4 DNA ligase in a buffer containing

50 mM Tris-HCl (pH 7.5), 10 mM $MgCl_2$, 10 mM DTT, 1 mM ATP and 25 μg/mL BSA. The ligation products were purified by employing 15%, 1:19 cross-linked polyacrylamide gels containing 8 M urea. The substrates were then isolated from the gel and desalted by ethanol precipitation. The purity of the resulting ODNs was confirmed by polyacrylamide gel electrophoresis (PAGE) analysis and their identities were verified by ESI-MS and MS/MS.

HPLC

The ODNs were purified on a Beckman HPLC system with pump module 125 and a UV detector (module 126). A 4.6 × 250 mm Apollo C18 column (5 μm in particle size and 300 Å in pore size, Alltech Associate Inc., Deerfield, IL) was used. Triethylammonium acetate (TEAA, 50 mM, pH 6.6, Solution A) and a mixture of 50 mM TEAA and acetonitrile (70/30, v/v, Solution B) were employed as mobile phases. The flow rate was 0.8 mL/min. A gradient of 0-20% B in 5 min, 20-45% B in 40 min, and 45-100% B in 5 min was employed for the separation. The purified ODNs were desalted on the same HPLC system using H_2O and acetonitrile as mobile phases A and B, respectively, and a gradient of 0% B in 20 min, 0-50% B in 5 min, and 50% B in 25 min was used.

Cell Culture

Jurkat T cells were cultured in ATCC-recommended IMDM medium with 10% (v/v) fetal bovine serum (FBS), 100 IU/mL of penicillin, and 100 μg/mL of streptomycin at

37°C in a 5% CO_2 atmosphere, with medium renewal at every 2 or 3 days depending on cell density. For SILAC experiments, the IMDM medium without L-lysine or L-arginine was custom-prepared according to the ATCC formulation. The complete light and heavy IMDM media were prepared by the addition of light or heavy lysine and arginine, along with dialyzed FBS (Invitrogen, Carlsbad, CA), to the above lysine, arginine-depleted medium. The Jurkat T cells were cultured in heavy IMDM medium for at least 5 cell doublings to achieve complete isotope incorporation.

Isolation of Nuclear Extract

Nuclei extract was prepared using a protocol adapted from that reported by Dignam et al. (*209*). Cell pellets were harvested separately from light and heavy media by centrifugation at 2000 rpm at 4°C for 10 min and then suspended in five volumes of phosphate buffered saline (PBS), which was pre-chilled at 4°C, and collected by centrifugation as detailed above. Cell pellets were suspended in five volumes of buffer A containing 10 mM HEPES (pH 7.9), 1.5 mM $MgCl_2$, 10 mM KCl, and 0.5 mM DTT, allowed to stand at 4°C for 10 min and collected again by centrifugation. Next, cell pellets were resuspended in two volume of Buffer A and the mixture was incubate on ice for 30 min. Cells were lysed with Dounce Homogenizer with B type pestle for 30 strokes on ice. The homogenate was checked microscopically and centrifuged at 2000 rpm at 4°C for 10 min to pellet the nuclei. The supernatant was carefully decanted and centrifuged at 13,200 rpm at 4°C for 30 min to remove residual cytoplasmic material. The crude nuclei were suspended in Buffer B, which contained 20 mM HEPES (pH 7.9), 0.42 M NaCl, 1.5

mM $MgCl_2$, 0.2 mM EDTA, 0.5 mM PMSF, 0.5 mM DTT and 25% (v/v) glycerol, and was further lysed by using a Dounce homogenizer for 10 strokes on ice. The nuclear fraction was vortexed at 4°C for 30 min and collected as supernatant after centrifugation at 13,200 rpm for 30 min. To the supernatant was subsequently added a protease inhibitor cocktail (Sigma, St. Louis, MO), and the protein concentrations were determined by using Quick Start Bradford Protein Assay kit (Bio-Rad, Hercules, CA).

Binding Assay and Affinity Purification of DNA-Binding Proteins

The 30-mer biotinylated ODNs containing 6-thioguanine (target DNA probe) or unmodified guanine (normal DNA probe) were annealed with slight excess amount of complementary strand in buffer A, which contained 20 mM Tris-HCl, 0.1 M KCl, 0.5 mM EDTA and 10mM $MgCl_2$. The resulting biotin-conjugated duplex DNA probes (~250 pmol) were incubated with 300 μL of streptavidin resin (50%, v/v) equilibrated with buffer A in a final volume of 400 μL at room temperature for 3 hrs with gentle vortexing. The streptavidin resins harboring immobilized duplex DNA probes were collected after centrifugation at 13,200 rpm for 10 min and stored at -20°C.

Prior to the DNA affinity pull-down experiment, 400 μL of streptavidin resins (50%, v/v) were equilibrated with buffer B containing 2 mM DTT, 10 % (v/v) glycerol, 104 mM 4-(2-aminoethyl)-benzenesulfonyl fluoride, 80 μM aprotinin, 2 mM leupeptin, 4 mM bestatin, 1.5 mM pepstatin A, 1.4 mM E-64 and 0.4 mM PMSF. Light and heavy labeled nuclear extracts (1 mg each) were incubated with 200 μL of above streptavidin resins at 4°C for 3 hrs with gentle vortexing and centrifuged at 1000 g to remove

non-specific binding proteins. In forward SILAC experiment, the precleaned heavy isotope-labeled nuclear extract was incubated with the ^{S}G-containing target DNA probe, whereas unlabeled light nuclear extract mixed with normal DNA probe at 4°C for 3 hrs. Reverse SILAC experiments were performed where labeled and unlabeled nuclear extracts were incubated with normal and target DNA probes, respectively (Figure 5.1). After binding, streptavidin resins harboring heavy and light labeled protein-DNA complex was collected by centrifugation at 1000 g for 10 min and combined at 1:1 ratio. DNA-binding proteins were eluted from the mixture by adding half of the resin volume of 8 M urea in 100 mM NH_4HCO_3 and vortexing at room temperature for 1 h and recovered from high-speed centrifugation.

Enzymatic Digestion and Desalting

The obtained protein mixture was reduced with dithiothreitol (DTT) at a final concentration of 10 mM and alkylated in dark with iodoacetamide (IAA) at a final concentration of 50 mM for 30 min. The resulting protein solutions were diluted 4 times with 100 mM NH_4HCO_3 (pH 8.0) and digested with mass spectrometry-grade trypsin (Promega, Madison, WI) at an enzyme-to-substrate ratio of 1/20 (w/w) at 37°C overnight. The peptide mixtures were dried in a Speed-Vac. The digested peptides were reconstituted in 0.1% formic acid (FA) and salts were removed by C18 Ziptip (Millipore, Billerica, MA). The peptides were dried and redissolved in 0.1% FA for LC-MS/MS analysis.

Nanoflow LC-MS/MS Analysis

On-line LC-MS/MS analysis was performed on an Agilent 6510 Q-TOF system coupled with an Agilent HPLC-Chip Cube MS interface (Agilent Technologies, Santa Clara, CA). The sample injection, enrichment, desalting, and HPLC separation were carried out automatically on the Agilent HPLC Chip with an integrated trapping column (160 nL) and a separation column (Zorbax 300SB-C18, 75 μm×150 mm, 5 μm in particle size). The peptide mixture was first loaded onto the trapping column with a solvent mixture of 0.1% formic acid in CH_3CN/H_2O (2:98, v/v) at a flow rate of 4 μL/min, which was delivered by an Agilent 1200 capillary pump. The peptides were then separated with a 98-min linear gradient of 2-35% acetonitrile in 0.1% formic acid and at a flow rate of 300 nL/min, which was delivered by an Agilent 1200 Nano pump.

The Chip spray voltage (VCap) was set as 1950 V and varied depending on the chip conditions. The temperature and flow rate of the drying gas were set at 325ºC and 4 L/min, respectively. Nitrogen was used as the collision gas; the collision energy followed an equation with a slope of 3 V/100 Da and an offset of 2.5 V. MS/MS experiments were carried out in the data-dependent scan mode with a maximum of five MS/MS scans following each MS scan. The m/z ranges for MS and MS/MS were 300-2000 and 60-2000, and the acquisition rates were 6 and 3 spectra/s, respectively.

Data Processing

Agilent MassHunter workstation software (Version B.01.03) was used to extract the MS and MS/MS data. The data were converted to *m*/*z* Data files with MassHunter

Qualitative Analysis. Bioworks 3.2 was used for protein identification by searching the m/z Data files against the human IPI protein database (version 3.21) and its reversed complement. The maximum number of miss-cleavages for trypsin was set as two per peptide. Cysteine carbamidomethylation was set as a fixed modification. Methionine oxidation (+16 Da) as well as lysine (+4 Da) and arginine (+10 Da) mass shifts introduced by heavy isotope labeling were considered as variable modifications. The mass tolerances for MS and MS/MS were 100 ppm and 0.6 Da, respectively. The searching results were then filtered with DTASelect software, developed by Yates and coworkers (*210*), to achieve a protein false discovery rate of <1%.

Protein quantification was carried out using Census (*211*). The ratio obtained for each individual protein was then normalized against the average ratio for all quantified proteins. This "multi-point" normalization strategy assumes that the ratios for the majority of proteins are not affected by the drug treatment, facilitating the use of the average ratio of all quantified proteins to re-scale the data. This has been widely employed to eliminate the inaccuracy during sample mixing introduced by protein quantification with the Bradford assay (*212, 213*). Reverse SILAC labeling and binding assay was performed in addition to two forward SILAC experiments. Due to sensitivity drop of the mass spectrometer while analyzing the reverse-SILAC sample, the quantification (listed in Table 5.2) was based on two independent forward SILAC, DNA protein binding experiments and LC-MS/MS analyses. Some peptides identified in only 1 trial of QTOF analysis could be quantified in two trials, where the accurate mass of peptide ions, retention time, and the numbers of isotope-labeled lysine and/or arginine in

the peptide were employed as criteria to locate the light/heavy peptide pairs for the quantification.

Results and Discussion

Nucleic acid binding proteins are involved in chromatin organization, transcription, DNA replication, recombination and repair (*214, 215*). Due to their low abundance, and their highly dynamic and weak interactions with DNA sequence, many DNA-binding proteins are still unknown. SILAC approach has been extended to an unbiased proteome-wide screening for the quantitative identification of proteins that can bind specifically to baits containing peptides (*140*), proteins (*141*), DNA (*142*) and RNA (*143*). Recently, SILAC coupled with affinity purification and highly sensitive LC-MS/MS has been successfully employed to screen transcription factors binding to the mutated and nonmethylated control ODNs (*142*). Previous studies demonstrated that MMR system was involved in the modulation of thiopurine cytotoxicity (*73*) and MMR-deficient human leukemia cells were highly sensitive to thiopurine treatment (*57, 201*). Krynetski and co-workers (*216*) revealed that high mobility group proteins B1 and B2, heat shock protein 70, ERp60 and glyceraldehydes-3-phosphate dehydrogenase were associated with the incorporation of 6-thioguanine into DNA sequence, illustrating that other pathways may also contribute to the cytotoxic effects of thiopurine drugs. Therefore, we employed an approach encompassing SILAC, one-step affinity purification and LC-MS/MS to identify systematically cellular proteins recognizing ^{S}G-bearing duplex DNA from the nuclei of Jurkat T cells, which are acute lymphoblastic leukemia cells deficient in MMR.

Preparation of Biotin-Conjugated ODN Substrates Containing 6-Thioguanine

We first obtained two DNA substrates (Table 5.1) by using enzymatic ligation (see Experimental Procedures) and confirmed the identities of these substrates by ESI-MS (Figure 5.1).

Strategy for the Indentification of DNA-Binding Proteins

Two populations of cells were cultured in the light (unlabeled Lys and Arg) and heavy ($^{13}C_6$, $^{15}N_4$-Arg and 2H4-Lys) media (Figure 5.2). The amount of extracted nuclear proteins was quantified and equal amount of heavy and light nuclear extracts were then incubated with streptavidin resins that were immobilized with biotin-conjugated duplex DNA harboring normal G:C (control bait) and ^{S}G:C (target bait) base pairs, respectively. DNA-binding proteins were pulled down by combining resins from two different states and eluted out from the mixture. The resulting proteins were digested into peptides and subjected to LC-MS/MS analysis. Background proteins occur equally in control and bait elutes, and the SILAC peptide pairs in the mass spectrum show a 1:1 intensity ratio. By contrast, proteins with specific binding to the bait exhibits heavy/light ratio substantially greater than 1.

Identification of Nuclear Proteins that can Bind to 6-Thioguanine-containing Duplex DNA

To obtain reliable results, we carried out the SILAC experiments in triplicate and both forward and reverse SILAC labeling were performed. Figure 5.3 shows example

results for the quantification of the peptide EGDVLTLLESER from 40S ribosomal protein S28, which clearly reveals the selective pull-down of this protein with the 6-thioguanine-containing bait (Figure 5.3a). The peptide sequence was confirmed by MS/MS analysis (Figure 5.3b&c). Totally 39 proteins were identified and quantified. Among these quantified proteins, 18 displayed significant differences towards binding to the two DNA substrate sequences (the ratio of ^{S}G/G was greater than 1.5 or less than 0.67), with 13 and 5 being able to bind favorably to the ^{S}G- and G-containing substrates, respectively. The quantification results for the proteins with significant changes are summarized in Table 5.2.

The proteins binding to modified DNA may recruit other protein factors and the assembly of protein complex to modified DNA may be considered as the initial step toward activation of DNA repair or apoptosis (*217, 218*). Our recent quantification results revealed a positive correlation between the level of 6-thioguanine incorporation and the extent of cell death in human leukemia cells that are repair-proficient and MMR-deficient (*115*). In line with previous studies by Krynetski (*216*), we found that HMGB1 and HMGB2 proteins bear specific binding to DNA sequence with ^{S}G. It has been reported that when cells undergo apoptosis, the dynamic behavior of HMGB1 changes dramatically and its movement within the cell is blocked (*219*), which facilitates its binding to damaged DNA.

Heterogeneous nuclear ribonucleoprotein A/B (hnRNP A) and D0 (hnRNP D0) were among the identified proteins capable of binding favorably toward the ^{S}G-bearing DNA. hnRNP A is a nuclear DNA helix-destabilizing protein (*220*) and hnRNP D0

protein appears to enhance target mRNA decay and is involved in processes of apoptosis by its interactions with adenylate/uridylate-rich element (ARE)-bearing mRNAs (*221*). The incorporation of ^{S}G into duplex DNA was reported to induce local changes in the geometry and dynamics of the double helix around ^{S}G site (*66*), while keeping the structure integrity of DNA. It raises the possibility that during transcription, the binding of hnRNP A to ^{S}G-containing DNA will destabilize duplex structure and the subsequent interaction between hnRNP D0 and distorted DNA structure will initiate cell apoptosis by decay mRNAs on ARE. Recent study showed that nucleolin served as MGT-40 cell surface receptor for tumor necrosis factor-alpha (TNF-α) inducing protein, which specifically binds to cells and is incorporated into cytosol and nucleus, where it strongly induces expression of TNF-α and chemokine genes mediated through NF-κB activation, resulting in tumor development (*222*). We found a CDNA FLJ45706 fis, clone FEBRA2028457, highly similar to nucleolin, and this protein might have similar function in inhibiting cancer development.

In the near future, reverse SILAC experiment will be performed to confirm the results obtained from forward SILAC screening. Since the above-described SILAC screening may also lead to the identification of proteins that can bind to the ^{S}G-bearing DNA indirectly, i.e., through protein-protein interactions. Therefore, it is important to assess whether the identified proteins can bind directly to the ^{S}G-bearing DNA. To this end, future EMSA experiments are needed to evaluate the binding of the some of the identified proteins to ^{S}G-containing DNA.

Table 5.1 Substrates employed for binding assay.

^{S}G-DNA probe	5′-Biotin-TGG CAG GTA TCC AGT ACC C^{S}GG TGA CAC ACC-3′ 3′-ACC GTC CAT AGG TCA TGG G CC ACT GTG TGG-5′
G-DNA probe	5′-Biotin-TGG CAG GTA TCC AGT ACC CGG TGA CAC ACC-3′ 3′-ACC GTC CAT AGG TCA TGG GCC ACT GTG TGG-5′

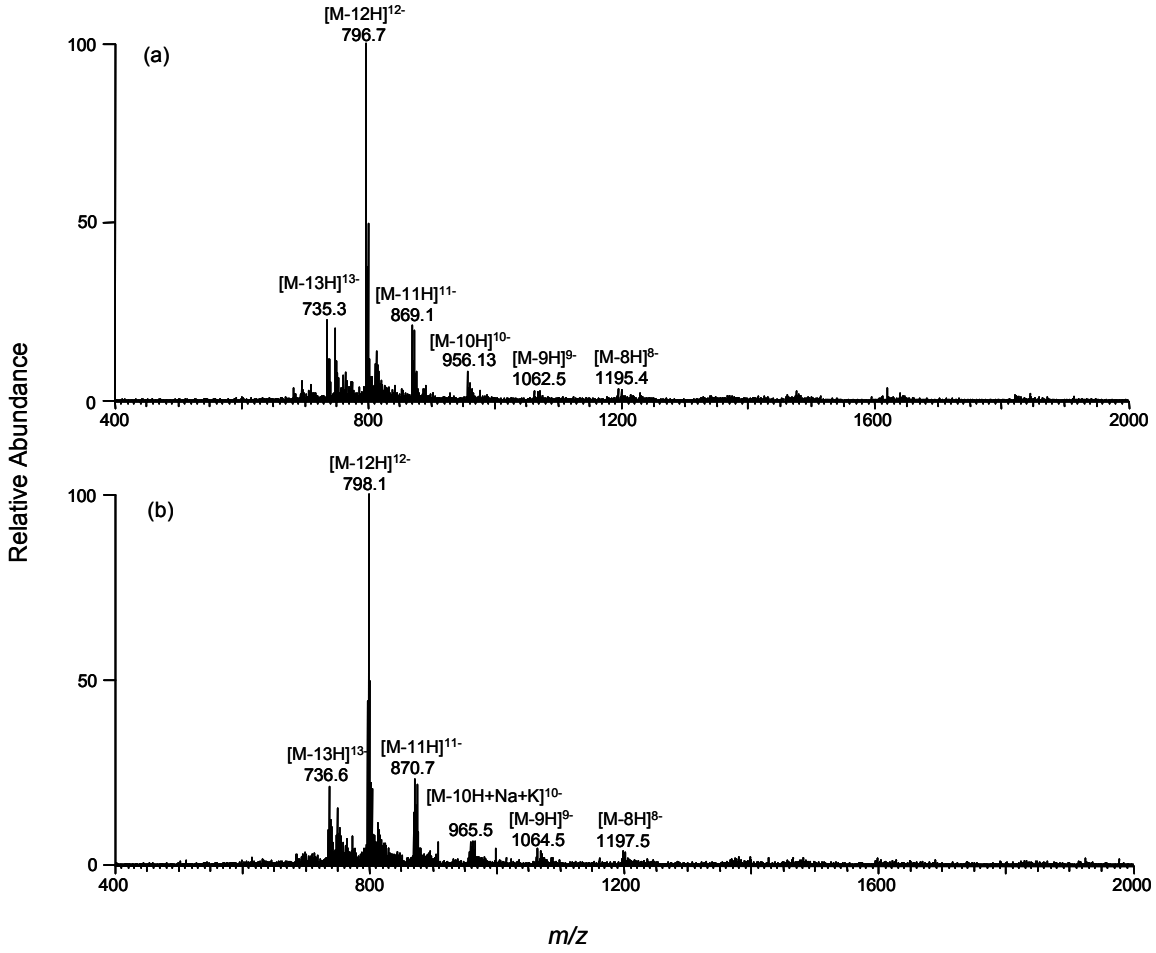

Figure 5.1 Negative-ion ESI-MS of 30-mer biotin conjugated ligation products, i.e. 5'-Biotin-d(TGGCAGGTATCCAGTACCCGGTGACACACC) (a) and 5'-Biotin-d(TGGCAGGTATCCAGTACCC^{S}GGTGACACACC) (b).

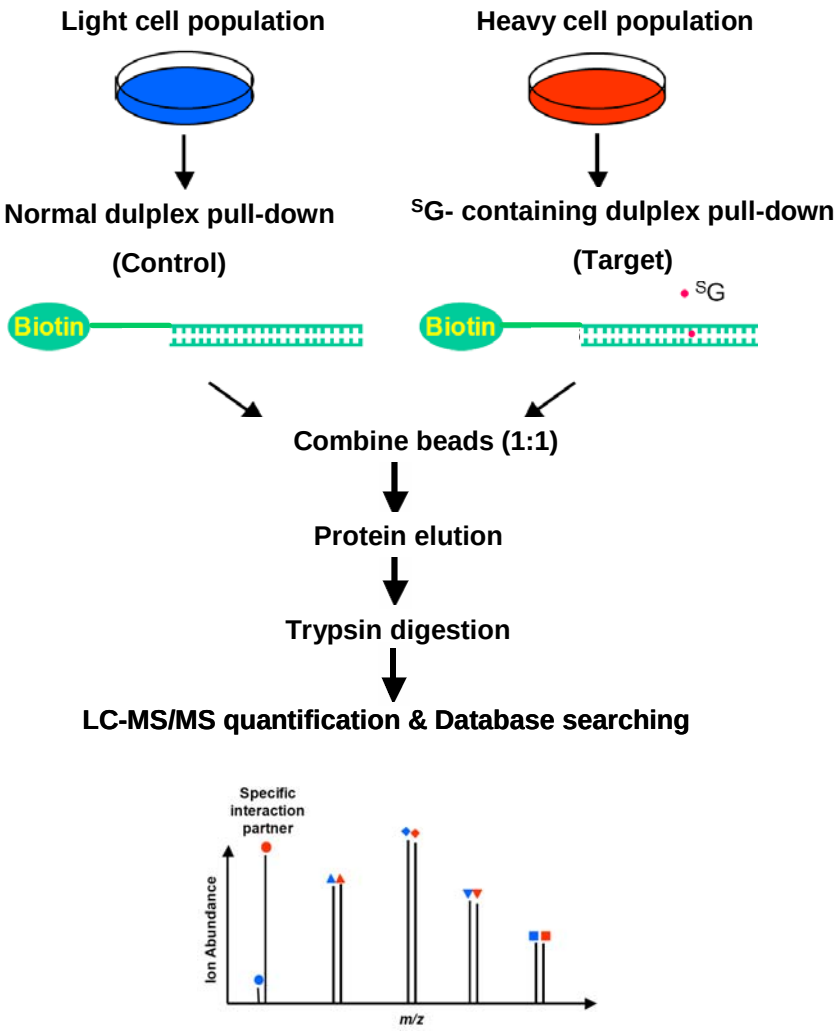

Figure 5.2 A SILAC, affinity purification, and LC-MS/MS strategy for the quantitative identification of proteins capable of binding to ^{S}G-containing ds-DNA.

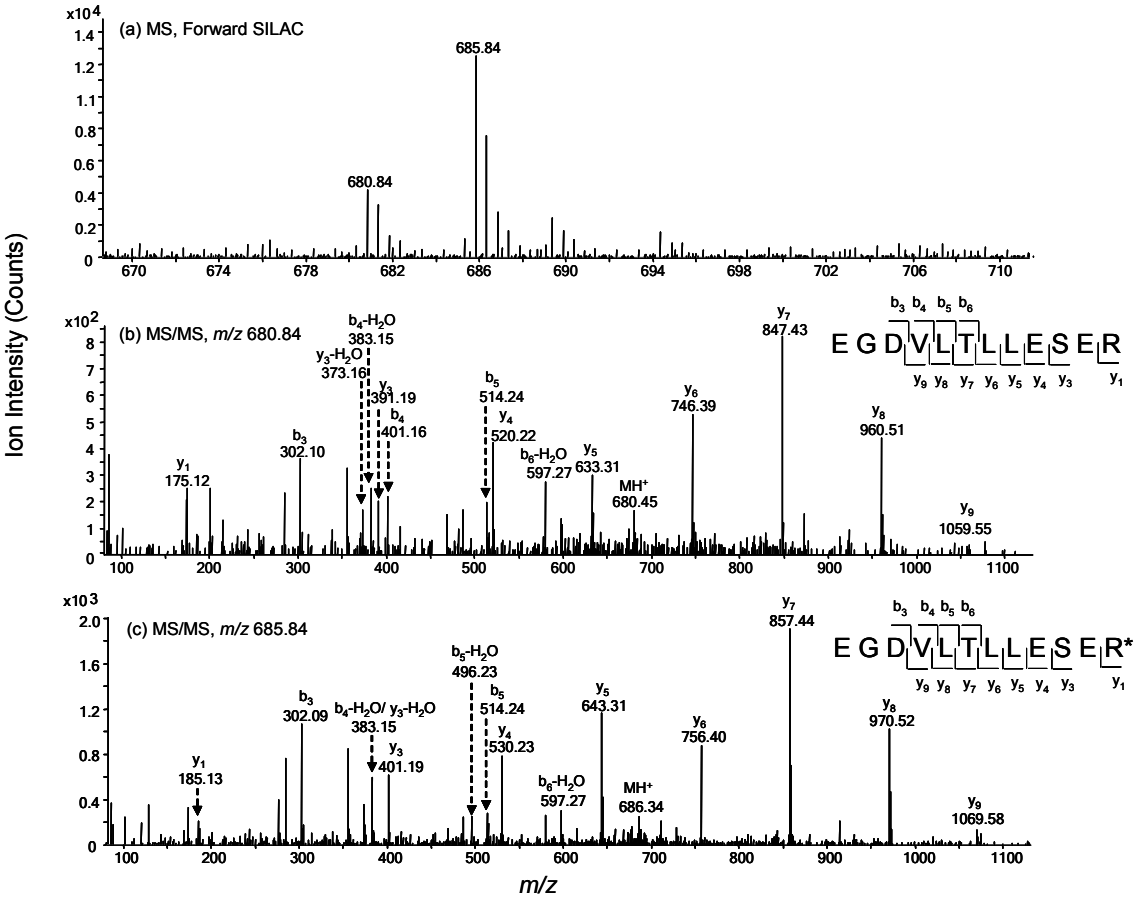

Figure 5.3 Example ESI-MS and MS/MS data revealed the preferential binding of 40S ribosomal protein S28 (40SR-S28) towards ^{S}G-containing duplex DNA over the corresponding G-carrying duplex DNA. Shown in (a) is the MS for the $[M + 2H]^{2+}$ ions of 40SR-S28 peptide EGDVLTLLESER and EGDVLTLLESER* ('R*' represents the heavy arginine) from the forward SILAC sample. Depicted in (b) and (c) are the MS/MS for the $[M + 2H]^{2+}$ ions of EGDVLTLLESER and EGDVLTLLESER*, respectively.

Table 5.2 Proteins quantified with more than 1.5-fold changes, with IPI number, protein name and ratio listed.

IPI number	protein name	ratio (^{S}G/G)		
	Up-regulated proteins	Trial 1	Trial 2	Ave
00556589.2	PREDICTED: similar to 40S ribosomal protein S28	2.94	2.94	2.94
00027569.1	Heterogeneous nuclear ribonucleoprotein C-like 1	1.89	1.83	1.86
00140827.2	PREDICTED: similar to SMT3 suppressor of mif two 3 homolog 2	1.56	1.61	1.59
00183526.5	NCL protein	1.49	1.52	1.51
00444262.1	CDNA FLJ45706 fis, clone FEBRA2028457, highly similar to Nucleolin	1.82	1.77	1.80
00334587.1	Heterogeneous nuclear ribonucleoprotein A/B, splice Isoform 2	1.59	1.48	1.54
00028888.1	Heterogeneous nuclear ribonucleoprotein D0, splice Isoform 1	1.64	1.56	1.60
00216592.1	Heterogeneous nuclear ribonucleoproteins C1/C2, splice Isoform C1	1.61	1.53	1.57
00219097.3	High mobility group protein B2	1.45	1.53	1.49
00018755.1	High mobility group protein 1-like 10	2.27	2.10	2.40
00419258.3	High mobility group protein B1	1.49	1.51	1.50
00013881.5	Heterogeneous nuclear ribonucleoprotein H1	1.49	1.58	1.54
00020928.1	Transcription factor A, mitochondrial precursor	1.45	1.48	1.47
	Down-regulated proteins			
00216049.1	Heterogeneous nuclear ribonucleoprotein K, splice Isoform 1	0.68	0.71	0.70
00298363.2	Far upstream element-binding protein 2	0.55	0.53	0.54
00014424.1	Elongation factor 1-alpha 2	0.56	0.55	0.56
00000015.2	Splicing factor, arginine/serine-rich 4	0.65	0.57	0.61
00010740.1	Splice Isoform Long of Splicing factor, proline- and glutamine-rich	0.24	N/A	N/A

References

(1) Johnstone, R. W., Ruefli, A. A. and Lowe, S. W. (2002) Apoptosis: A link between cancer genetics and chemotherapy. *Cell 108*, 153-164.

(2) Huang, P. and Plunkett, W. (1995) Fludarabine-induced and gemcitabine-induced apoptosis - Incorporation of analogs into DNA is a critical event. *Cancer Chemother. Pharmacol. 36*, 181-188.

(3) Jacobson, M. D., Burne, J. F., King, M. P., Miyashita, T., Reed, J. C. and Raff, M. C. (1993) Bcl-2 blocks apoptosis in cells lacking mitochondrial-DNA. *Nature 361*, 365-369.

(4) Kaufmann, S. H. and Earnshaw, W. C. (2000) Induction of apoptosis by cancer chemotherapy. *Exp. Cell Res. 256*, 42-49.

(5) Nelms, B. E., Maser, R. S., MacKay, J. F., Lagally, M. G. and Petrini, J. H. J. (1998) In situ visualization of DNA double-strand break repair in human fibroblasts. *Science 280*, 590-592.

(6) Paull, T. T., Cortez, D., Bowers, B., Elledge, S. J. and Gellert, M. (2001) Direct DNA binding by Brca1. *Proc. Natl. Acad. Sci. USA 98*, 6086-6091.

(7) Elion, G. B. (1989) The purine path to chemotherapy. *Science 244*, 41-47.

(8) Somerville, L., Krynetski, E. Y., Krynetskaia, N. F., Beger, R. D., Zhang, W. X., Marhefka, C. A., Evans, W. E. and Kriwacki, R. W. (2003) Structure and dynamics of thioguanine-modified duplex DNA. *J. Biol. Chem. 278*, 1005-1011.

(9) Krynetskaia, N. F., Krynetski, E. Y. and Evans, W. E. (1999) Human RNase H-mediated RNA cleavage from DNA-RNA duplexes is inhibited by

6-deoxythioguanosine incorporation into DNA. *Mol. Pharmacol. 56*, 841-848.

(10) Krynetskaia, N. F., Cai, X. J., Nitiss, J. L., Krynetski, E. Y. and Relling, M. V. (2000) Thioguanine substitution alters DNA cleavage mediated by topoisomerase II. *FASEB J. 14*, 2339-2344.

(11) Swann, P. F., Waters, T. R., Moulton, D. C., Xu, Y. Z., Zheng, Q. G., Edwards, M. and Mace, R. (1996) Role of postreplicative DNA mismatch repair in the cytotoxic action of thioguanine. *Science 273*, 1109-1111.

(12) Krynetski, E. Y., Krynetskaia, N. F., Gallo, A. E., Murti, K. G. and Evans, W. E. (2001) A novel protein complex distinct from mismatch repair binds thioguanylated DNA. *Mol. Pharmacol. 59*, 367-374.

(13) Garner, M. M. and Revzin, A. (1986) The use of gel-electrophoresis to detect and study nucleic-acid protein interactions. *Trends Biochem. Sci. 11*, 395-396.

(14) Fried, M. G. (1989) Measurement of protein-DNA interaction parameters by electrophoresis mobility shift assay. *Electrophoresis 10*, 366-376.

(15) Hellman, L. M. and Fried, M. G. (2007) Electrophoretic mobility shift assay (EMSA) for detecting protein-nucleic acid interactions. *Nat. Protoc. 2*, 1849-1861.

(16) Chen, H. W., Lin, R. J., Xie, W., Wilpitz, D. and Evans, R. M. (1999) Regulation of hormone-induced histone hyperacetylation and gene activation via acetylation of an acetylase. *Cell 98*, 675-686.

(17) Spencer, V. A., Sun, J. M., Li, L. and Davie, J. R. (2003) Chromatin immunoprecipitation: a tool for studying histone acetylation and transcription

factor binding. *Methods 31*, 67-75.

(18) Orlando, V. (2000) Mapping chromosomal proteins in vivo by formaldehyde-crosslinked-chromatin immunoprecipitation. *Trends Biochem. Sci. 25*, 99-104.

(19) Mittler, G., Butter, F. and Mann, M. (2009) A SILAC-based DNA protein interaction screen that identifies candidate binding proteins to functional DNA elements. *Genome Res. 19*, 284-293.

(20) Henrich, S., Cordwell, S. J., Crossett, B., Baker, M. S. and Christopherson, R. I. (2007) The nuclear proteome and DNA-binding fraction of human Raji lymphoma cells. *Biochim. Biophys. Acta, Proteins Proteomics 1774*, 413-432.

(21) Dignam, J. D., Lebovitz, R. M. and Roeder, R. G. (1983) Accurate transcription initiation by RNA polymerase-II in a soluble extract from isolated mammalian nuclei. *Nucleic Acids Res. 11*, 1475-1489.

(22) Tabb, D. L., McDonald, W. H. and Yates, J. R. (2002) DTASelect and contrast: Tools for assembling and comparing protein identifications from shotgun proteomics. *J. Proteome Res. 1*, 21-26.

(23) Park, S. K., Venable, J. D., Xu, T. and Yates, J. R. (2008) A quantitative analysis software tool for mass spectrometry–based proteomics. *Nat. Methods 5*, 319-322.

(24) Romijn, E. P., Christis, C., Wieffer, M., Gouw, J. W., Fullaondo, A., van der Sluijs, P., Braakman, I. and Heck, A. J. R. (2005) Expression clustering reveals detailed coexpression patterns of functionally related proteins during B cell differentiation - A proteomic study using a combination of one-dimensional gel

electrophoresis, LC-MS/MS, and stable isotope labeling by amino acids in cell culture (SILAC). *Mol. Cell. Proteomics 4*, 1297-1310.

(25) Uitto, P. M., Lance, B. K., Wood, G. R., Sherman, J., Baker, M. S. and Molloy, M. P. (2007) Comparing SILAC and two-dimensional gel electrophoresis image analysis for profiling urokinase plasminogen activator signaling in ovarian cancer cells. *J. Proteome Res. 6*, 2105-2112.

(26) Levine, M. and Tjian, R. (2003) Transcription regulation and animal diversity. *Nature 424*, 147-151.

(27) Naar, A. M., Lemon, B. D. and Tjian, R. (2001) Transcriptional coactivator complexes. *Annu. Rev. Biochem. 70*, 475-501.

(28) Schulze, W. X. and Mann, M. (2004) A novel proteomic screen for peptide-protein interactions. *J. Biol. Chem. 279*, 10756-10764.

(29) Vermeulen, M., Hubner, N. C. and Mann, M. (2008) High confidence determination of specific protein-protein interactions using quantitative mass spectrometry. *Curr. Opin. Biotechnol. 19*, 331-337.

(30) Butter, F., Scheibe, M., Morl, M. and Mann, M. (2009) Unbiased RNA-protein interaction screen by quantitative proteomics. *Proc. Natl. Acad. Sci. USA 106*, 10626-10631.

(31) Krynetski, E. Y., Krynetskaia, N. F., Bianchi, M. E. and Evans, W. E. (2003) A nuclear protein complex containing high mobility group proteins B1 and B2, heat shock cognate protein 70, ERp60, and glyceraldehyde-3-phosphate dehydrogenase is involved in the cytotoxic response to DNA modified by

incorporation of anticancer nucleoside analogues. *Cancer Res. 63*, 100-106.

(32) daSilva, C. P., deOliveira, C. R. and deLima, M. C. P. (1996) Apoptosis as a mechanism of cell death induced by different chemotherapeutic drugs in human leukemic T-lymphocytes. *Biochem. Pharmacol. 51*, 1331-1340.

(33) Tsurusawa, M., Saeki, K. and Fujimoto, T. (1997) Differential induction of apoptosis on human lymphoblastic leukemia Nalm-6 and Molt-4 cells by various antitumor drugs. *Int. J. Hematol. 66*, 79-88.

(34) Wang, H. X. and Wang, Y. S. (2010) LC-MS/MS coupled with stable isotope dilution method for the quantification of 6-thioguanine and S-6-methylthioguanine in genomic DNA of human cancer cells treated with 6-thioguanine. *Anal. Chem. 82*, 5797-5803.

(35) Scaffidi, P., Misteli, T. and Bianchi, M. E. (2002) Release of chromatin protein HMGB1 by necrotic cells triggers inflammation. *Nature 418*, 191-195.

(36) Kumar, A., Williams, K. R. and Szer, W. (1986) Purification And Domain-Structure Of Core Hnrnp Proteins-A1 And Protein-A2 And Their Relationship To Single-Stranded Dna-Binding Proteins. *J. Biol. Chem. 261*, 1266-1273.

(37) Loflin, P., Chen, C. Y. A. and Shyu, A. B. (1999) Unraveling a cytoplasmic role for hnRNP D in the in vivo mRNA destabilization directed by the AU-rich element. *Genes Dev. 13*, 1884-1897.

(38) Watanabe, T., Tsuge, H., Imagawa, T., Kise, D., Hirano, K., Beppu, M., Takahashi, A., Yamaguchi, K., Fujiki, H. and Suganuma, M. Nucleolin as cell

surface receptor for tumor necrosis factor-alpha inducing protein: a carcinogenic factor of Helicobacter pylori. *J. Cancer Res. Clin. Oncol. 136*, 911-921.

CHAPTER 6

Summary and Future Directions

In this dissertation, I focus on the development of novel MS-based strategies to identify and quantify DNA lesions formed in isolated DNA and in cells to monitor the progression of enzymatic reactions *in vitro* and glyoxal or methylglyoxal exposure *in vivo*. In addition, a combined SILAC, one-step affinity purification and LC-MS/MS approach was employed for identifying systematically cellular proteins capable of binding to 6-thioguanine (^{S}G)-containing duplex DNA.

In Chapter 2, I developed a stable isotope dilution coupled with LC-MS/MS/MS method to quantify accurately DNA advance glycation end products (AGEs) including N^2-carboxymethyl-2'-deoxyguanosine (N^2-CMdG), and two diastereomers of N^2-(1-carboxyethyl)-2'-deoxyguanosine (N^2-CEdG) induced by hyperglycemia in calf thymus DNA, cellular DNA, rat and mouse tissues and human blood samples. In this study, I first assessed the stabilities of N^2-CMdG and 3-(2'-deoxy-β-D-*erythro*-pentofuranosyl)-5,6,7-trihydro-6,7-dihydroxyimidazo[1,2-*a*]purine-9-one (1,N^2-glyoxal-dG). It turned out that 1,N^2-glyoxal-dG was very unstable, with more than 70% of the adduct being decomposed to 2'-deoxyguanosine (dG) upon a 24 h incubation at 37°C in phosphate-buffered saline. However, N^2-CMdG was very stable; less than 0.5% of the lesion was degraded to dG after a 7-day incubation under the same conditions. The formation of N^2-CMdG in calf thymus DNA was dose-responsive to the concentration of glyoxal and D-glucose. N^2-CMdG was also induced endogenously in

293T human kidney epithelial cells and exposure to glyoxal further stimulated the formation of this lesion; the level of this adduct ranged from 7 to 15 lesions per 10^8 nucleosides, while the glyoxal concentration increased from 10 μM to 1.25 mM. Furthermore, I demonstrated that as stable AGEs, the levels of N^2-CMdG and N^2-CEdG were higher in the liver tissues of diabetic mice than those of the healthy control. This work shows that N^2-CMdG and N^2-CEdG might serve as molecular biomarkers for monitoring glyoxal and methylglyoxal exposure.

In Chapter 3, I established a novel restriction enzyme digestion coupled with LC-MS/MS method to investigate the effect of 6-thioguanine on the *Hpa*II- and DNMT1-mediated methylation of cytosine in synthetic duplex DNA. Moreover, the global cytosine methylation level in different leukemia cell lines upon ^{S}G treatment was evaluated by an offline HPLC method. LC-MS/MS results revealed that the presence of ^{S}G at the methylated CpG site enhanced the DNMT1-mediated methylation of the opposing cytosine in the complementary strand, whereas the presence of ^{S}G at the unmethylated CpG site abolished almost completely the methylation of its 5′ adjacent cytosine by both *Hpa*II and DNMT1. I further demonstrated that the treatment of human lymphoblastic leukemia cells with ^{S}G could result in an appreciable drop in the level of global cytosine methylation. These results showed that 6-thioguanine, after being incorporated into DNA, may perturb the epigenetic pathway of gene regulation. These results provide us important insights about the relationship between aberrant cytosine methylation and cancer development.

In Chapter 4, I reported for the first time the simultaneous and accurate quantification of DNA 6-thioguanine (^{S}dG) and its metabolite, S^{6}-methylthio-2'-deoxyguanosine (S^{6}mdG) in five human cultured cancer cells treated with ^{S}G. The LC-MS/MS results revealed that, upon treatment with 3 μM ^{S}G for 24 h, approximately 10, 7.4, 7, and 3% of guanine (G) was replaced with ^{S}G in human leukemia cell lines, Jurkat T, HL-60, CCRF-CEM and K-562, respectively. However, only less than 0.02% of ^{S}dG was converted to S^{6}mdG in the above cell lines. HCT-116, human colon cancer cells, had the lowest level (0.2%) of G being replaced with ^{S}G in DNA, and approximately 5 out of 10^{4} ^{S}G was converted to its methylated counterpart. This data support our hypothesis that, after being incorporated into DNA, 6-thioguanine instead of S^{6}-methylthioguanine plays the major role to exert the cytotoxic effects of thiopurines. In addition, another nucleotide metabolite, 6-thioguanosine triphosphate was extracted and quantified by LC-MS/MS.

In Chapter 5, a strategy, including SILAC, affinity purification and LC-MS/MS, was employed to identify nuclear proteins that are capable of binding to ^{S}G-containing duplex DNA. The initial quantification results based on two independent forward SILAC, DNA protein binding experiments and LC-MS/MS analysis showed that totally 39 proteins were identified and quantified. Among these quantified proteins, 18 displayed significant differences towards binding to the two duplex DNA substrate sequences, with 13 and 5 being able to bind favorably to the ^{S}G- and G-containing substrates, respectively.

Future studies can focus on the identification and quantification of proteins that are capable of binding to ^{S}G-containing duplex DNA in human acute lymphoblastic leukemia cells. The identified proteins with specific binding affinity to ^{S}G-containing DNA will be chosen and EMSA will be employed to assess whether these proteins can bind directly to ^{S}G-bearing duplex DNA. The outcome of the study will facilitate the exploration of other mechanisms involved in the cytotoxicity of the thiopurine drugs.